The Interplay Between Spontaneous and Evoked Brain Activity During Visual Perception

Marieke Louise Schölvinck

Dissertation submitted for the degree of

Doctor of Philosophy of University College London

Institute of Cognitive Neuroscience
Wellcome Trust Centre for Neuroimaging
Institute of Neurology

Declaration

I, Marieke Louise Schölvinck, confirm that the work presented in this thesis is my own. Where information has been derived from other sources, I confirm that this has been indicated in the thesis.

The study described in Chapter 3 of this thesis was carried out in collaboration with David Attwell and Clare Howarth in the Department of Physiology, University College London. The study described in Chapter 4 was carried out at the National Institute of Mental Health, Bethesda, USA, in collaboration with David Leopold, Alexander Maier, Frank Yeh, and Jeff Duyn. The work presented in Chapters 3, 4, 6, and 7 has been published as the following papers:

Schölvinck ML, Howarth C, Attwell D (2008) The cortical energy needed for conscious perception. NeuroImage 40(4): 1460-1468

Schölvinck ML, Maier AV, Yeh FQ, Duyn JH, Leopold DA (2010) Neural basis of widespread resting state fMRI activity. Proceedings of the National Academy of Sciences of the USA 107(22): 10238-10243

Schölvinck ML, Rees G (2010) Neural correlates of motion-induced blindness in the human brain. Journal of Cognitive Neuroscience 22(6): 1235-1243

Schölvinck ML, Rees G (2009) Attentional influences on the dynamics of motion-induced blindness. Journal of Vision 9(1): 38, 1-9

Acknowledgements

Completing a PhD is not a solo act. Over the past four years, I've had support, advice, and a listening ear from countless people on the way. First of all, I want to most deeply thank my two supervisors: Geraint, for being invariably enthusiastic and supportive of my work, and for giving me the freedom to pursue what really interested me; and David, for generously sharing his enthusiasm for research and for giving me scientific direction. Thanks also to Karl, my 'third' supervisor, for giving helpful advice when needed.

Then I want to thank the Rees lab – Claire, Bahador, David, Christian, Lauri, Rimona, Elaine, Sam, Frank, Ayse, and Sharon, for being an tremendously friendly bunch who made VSS, lab meetings, and many evenings in the pub a lot of fun; and my NIH lab – Sylwia, Melanie, Alex, Michael, David, Frank, Charles, Neil, Katie, Geoff, Eric, and not to forget, Yolanda, for kindly adopting me for almost a year and making me feel at home in Bethesda.

There are more people at the ICN that I want to thank. Thank you Klaartje, Margarita, Eva, Markus, Petra, Elisa, Lucia, Cat, Stephanie, and of course Iroise, for all the lunches in the park, the coffee breaks, walks, exhibitions, evenings in the pub, and generally for making my time at the ICN an extremely enjoyable and memorable one.

Thanks also to the 4 year PhD committee, especially David Attwell; the radiographers for assistance during many hours of scanning, and the Wellcome Trust for funding me.

There are many good friends who have all contributed to my PhD years in some way or another and who I don't want to leave unmentioned here, including Indraneel, Che, Frank, Jovanka, Piet, Jasper, Andrew, Adam, Nikos, Jasminka, Roel, Misha, and Ingrid. Special thanks to Hanneke and Nienke, for being such wonderful housemates, adventurous travel companions, dear 'replacement' sisters in London, and very good friends.

Doing research has given me profound joy and satisfaction, and I feel privileged to having been given the opportunity to do the work described in this thesis. However, I feel even more fortunate to be surrounded and supported by such a fantastic family. I want to thank my parents, Eduard en Annet, for always making me still feel very much part of the family; my sisters, Willemijn, Brechje en Anne-Floor, for coming to visit me in London so many times, whether by plane, boat, or even bicycle; and - of course and most dearly – Hermann, for making thesis-writing sound more scary than it turned out to be, and for his cheerfulness, support, and love.

Abstract

The vast majority of studies in cognitive neuroscience have focused on the brain's response to a task or stimulus. However, the brain is very active even in the absence of explicit input or output, as its enormous energy consumption at rest suggests. This ongoing brain activity is present at all timescales; as spontaneous neuronal firing measured by electrophysiology, and as slow fluctuations in the BOLD signal measured by functional magnetic resonance imaging (fMRI). Its significance for behaviour is still unclear. This thesis explores the nature of the brain's spontaneous activity, with an emphasis on its interaction with brain activity devoted to visual perception. Using a theoretical approach, I first show that the amount of energy expended on evoked brain activity related to a perceptual decision is minute compared to the energy expenditure associated with spontaneous activity. I then focus on spontaneous brain activity measured in the fMRI signal, the so-called resting-state fluctuations. Using simultaneous fMRI-electrophysiology in awake monkeys, I demonstrate that these fMRI resting-state fluctuations are strongly correlated to underlying fluctuations in neural activity, and are therefore likely to be neural in origin. A further fMRI study in humans shows that resting-state fluctuations in visual cortex can account for a significant degree to the variability in cortical, and to a lesser degree to the variability in behavioural responses to a visual stimulus at perceptual threshold. Lastly, I use a visual illusion called motion-induced blindness as a model system for studying the effect of spontaneous fluctuations in internal brain state on bistable perception. Using fMRI in humans, I show that while the retinal input remains constant, activity in early visual cortex reflects awareness of the stimulus. In the final, behavioural experiments, I manipulate the brain's internal state by examining the influence of endogenous attention on the temporal dynamics of motion-induced blindness. Taken together, these studies show that spontaneous brain activity plays an important role in visual perception, and argue that understanding the brain's internal dynamics is essential to understanding the brain as a whole.

Contents

List of Figures

List of Tables

Chapter 1 General Introduction

1.1 Spontaneous and evoked activity

The activity of the brain can be thought of as an iceberg; some of it is devoted to various cognitive functions, such as the processing of sensory stimuli, memory, and the execution of movements, yet surprisingly, most of the brain's activity is present spontaneously. This ongoing activity cannot be attributed to a particular task or stimulus and therefore stays beneath the surface in most cognitive neuroscience studies. The only way in which its existence becomes apparent in conventional task designs, is in the large variability in cortical responses to the repeated presentation of a stimulus. This variability is often as large as the response itself (Snowden et al., 1992;Vogels et al., 1989). The standard approach to this variability has been to recover the response of the brain to the stimulus by averaging over repeated trials (Gerstein, 1960). This approach tacitly assumes that the variability reflects noise. There is an increasing awareness, however, that spontaneous brain activity does not just reflect noise and instead might play an important role in sensory processing (Arieli et al., 1996;Tsodyks et al., 1999). This thesis explores the nature of this spontaneous brain activity, with an emphasis on its interaction with the brain activity devoted to visual perception.

1.2 Cortical energy expenditure

In the awake resting state, the brain receives 11% of the cardiac output and accounts for 20% of the total oxygen consumption of the body (Clark and Sokoloff, 1999), despite the fact that it represents only 2% of body weight. Task-related increases in neuronal metabolism are usually small (<5%) when compared with this large resting energy consumption (Raichle and Mintun, 2006). Therefore, most of our knowledge about brain

function comes from studying a minor component of total brain activity. This fact alone should be a motivation for studying the component that consumes most of the brain's energy: spontaneous neuronal activity.

So what is cortical energy spent on? Answering this question requires a quick review of the cellular processes underlying neuronal signalling (Fig 1.1). Signals travel within neurons as local depolarisations of the membrane potential; this is called an action potential. When an action potential in the presynaptic cell reaches the synapse, the depolarisation of the membrane causes voltage-dependent membrane channels to open that are permeable to calcium ions. Calcium ions enter the presynaptic neuron, rapidly increasing the internal calcium concentration. This in turn activates a set of calcium-sensitive proteins attached to vesicles that contain neurotransmitters (typically glutamate). These vesicles fuse with the presynaptic membrane, releasing their neurotransmitters into the synaptic cleft. The neurotransmitters bind to receptors located on the membrane of the postsynaptic neuron and either trigger a postsynaptic depolarisation (excitatory synapse) or a hyperpolarisation (inhibitory synapse) of the membrane. In order to clear the stage for the next synaptic transmission, ion fluxes related to the opening of membrane channels pre- and postsynaptically are reversed, and excess neurotransmitter in the synaptic cleft is taken up by astrocytes surrounding the neurons and recycled to the presynaptic neuron.

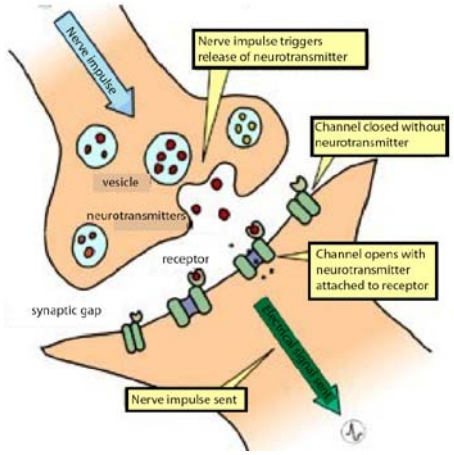

Figure 1.1 Schematic of synaptic transmission. *Arriving presynaptic action potentials trigger the release of neurotransmitters, which then bind to postsynaptic receptors and trigger a postsynaptic action potential. Adapted from http://universe-review.ca/R10-16-ANS.htm.*

Based on the measured properties of the individual ion channels and synapses, the amount of expended energy has been estimated for all these steps separately (Attwell and Laughlin, 2001). This analysis concluded that most of the energy is in fact expended on reversing the ion fluxes underlying postsynaptic events such as neurotransmitter binding and action potential generation; this accounts for ~75% of the total energy used on signalling (Attwell and Iadecola, 2002). However, not all energy consumed by neurons is expended on signalling. Action potential driven signalling energy accounts for ~50-75% of the total energy consumption; the remaining 25-50% of brain energy is expended on the resting potentials of neurons and glia, and on non-signalling housekeeping tasks (Attwell and Laughlin, 2001). This large amount of energy spent on housekeeping tasks, together with a certain baseline firing rate, suggest that spontaneous brain activity consumes a large fraction of the total energy available. Only a robust task-related increase in firing rate will alter energy consumption substantially, a hypothesis which will be explored later in this thesis.

Brain metabolism has also been studied globally in the brain, primarily with the use of positron emission tomography (PET). Increases in brain metabolism induced by a task are small; in fact, local task-induced increases in functional activity, although associated with *regionally* increased blood flow, are too small to induce perceptible changes in *global* blood flow or metabolism (Sokoloff et al., 1955). Quantitative measurements of brain glucose uptake, oxygen metabolism, and blood flow in humans revealed that during rest, oxygen consumption was much higher than glucose consumption (4.1:1 ratio) (Fox et al., 1988). However, during presentation of a strong visual stimulus, oxygen consumption in visual cortex increased only relatively little (5%) compared to glucose consumption (51%) (Fig 1.2). Since the conversion of glucose to energy in the form of adenosine triphosphate (ATP) requires oxygen, this small increase in oxygen consumption implies that much of the glucose taken up is not converted to energy directly. Therefore the increase in energy consumption during perceptual processing is very small compared to the resting energy consumption (Fox et al., 1988).

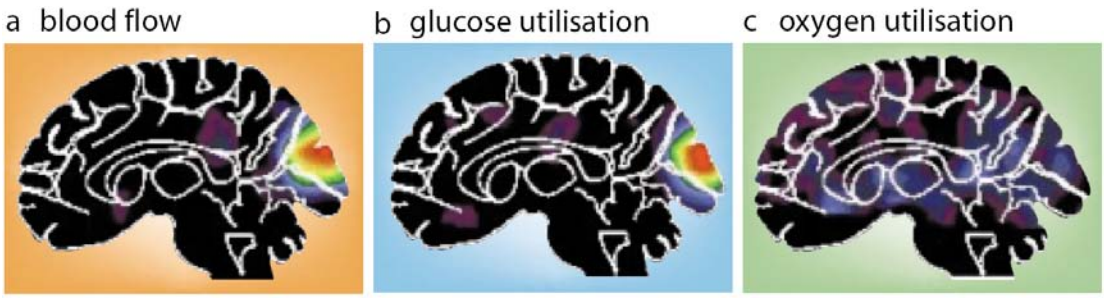

Figure 1.2 Energy consumption during visual stimulation. *PET images showing a robust increase in blood flow and glucose consumption, and a minute increase in oxygen consumption, in visual cortex during presentation of a strong visual stimulus. Adapted from Gusnard and Raichle, 2001.*

Taken together, these studies suggest that the brain's energy consumption is dominated by spontaneous cortical activity and only slightly altered by evoked activity. To examine whether neuronal processing, similarly, is dominated by spontaneous activity, electrophysiological measurements are needed.

1.3 Electrophysiological evidence of spontaneous activity

1.3.1 Response variability

One of the pioneering studies to investigate the relationship between spontaneous neural activity and activity evoked by a stimulus, was performed by Arieli and colleagues (1996). Using optical imaging and electrophysiological (local field potential) recordings in the visual cortex of anaesthetised cats, these researchers determined the separate contribution of evoked and spontaneous activity to the cortical response to a moving grating. Specifically, they tested the hypothesis that the response to the stimulus on a single trial could be approximated by a linear combination of the average response to the stimulus (the evoked activity) and the ongoing activity present already at that particular trial (the spontaneous activity). They found that this model predicted the cortical response very well on a trial by trial basis (Fig 1.3). This important finding implies that the amount of cortical activity

evoked by a stimulus is fixed; inter-trial variability is entirely due to variations in spontaneous activity. Subsequent intracellular recordings, also in cat striate cortex, confirmed this finding (Azouz and Gray, 1999). This study measured the membrane potential fluctuations and spiking activity immediately before and after the onset of an evoked response and found that the response magnitude in the postsynaptic cell was linearly correlated with the spontaneous membrane potential preceding the evoked response. This demonstrates that inter-trial variability is attributable partly to variations in preceding membrane potential (Azouz and Gray, 1999).

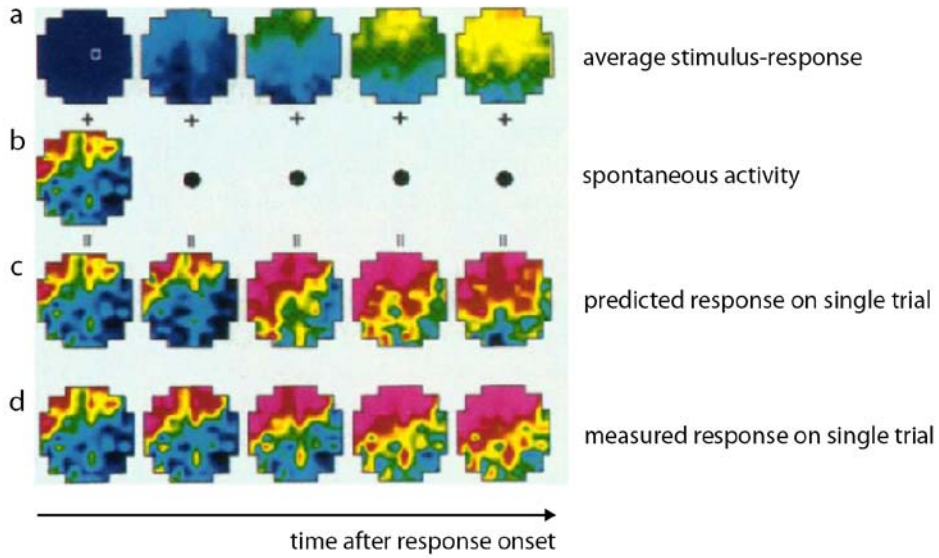

Figure 1.3 Inter-trial variability and spontaneous activity. (a) *Average activity pattern evoked by a stimulus, shown in optical imaging windows at 5 different times after response onset (from left to right).* ***(b)*** *Initial state on a single trial, approximating the spontaneous activity during the response. Black dots represent an identical frame to the one on the left.* ***(c)*** *Predicted response on the same trial, obtained by adding the frames in* ***a*** *and* ***b****.* ***(d)*** *Measured response. Note the large degree of similarity between the predicted and the measured response. Adapted from Arieli et al., 1996.*

1.3.2 Cortical states

The activity of single neurons, therefore, is a combination of their spontaneous and evoked activity. The relation of the spontaneous activity of single neurons to their

neighbouring neurons has been extensively investigated (Fiser et al., 2004;Kenet et al., 2003;Tsodyks et al., 1999). Using a combination of optical imaging and single-unit recordings in cat visual cortex, it was shown that the firing rate of a spontaneously active single neuron strongly depends on the instantaneous spatial pattern of ongoing population activity in its neighbours (Tsodyks et al., 1999). In other words, a neuron is mostly silent during certain patterns of spontaneous activity in its neighbours, and fires maximally during other patterns of activity. Ongoing activity of a whole network of neurons is therefore strongly correlated. Furthermore, spontaneous firing of the neuron and firing driven by its optimal stimulus coincide with very similar spatial patterns in the network (Tsodyks et al., 1999). The fact that the same states appear in the network during both spontaneous and evoked activity of the neuron suggest that even in the presence of sensory input, the response of cortical neurons is affected to a large degree by these 'cortical states' and is not only a direct reflection of the input. Indeed, spontaneous population activity in visual cortex seems to be continually switching between these cortical states, many of which correspond closely to orientation maps (Kenet et al., 2003) (Fig 1.4). This suggests that orientation maps are largely determined by intra-cortical connectivity, and that spontaneous cortical states could represent the brain's 'internal context' for memory or perception. Even under free viewing conditions of natural scenes rather than moving gratings, activity in visual cortical neurons reflects ongoing circuit dynamics more than the structure of the input itself (Fiser et al., 2004). Importantly, this work was done in awake rather than anaesthetised animals. This implies that spontaneous activity is an integral component of sensory processing, which would seem sensible given the high metabolic cost of maintaining baseline neural activity in the brain (Attwell and Laughlin, 2001). Taken together, these studies show that spontaneous activity has a highly coherent spatio-temporal structure and that correlations in spontaneous neural firing are only slightly modified by visual stimulation, irrespective of the specifics of the sensory input.

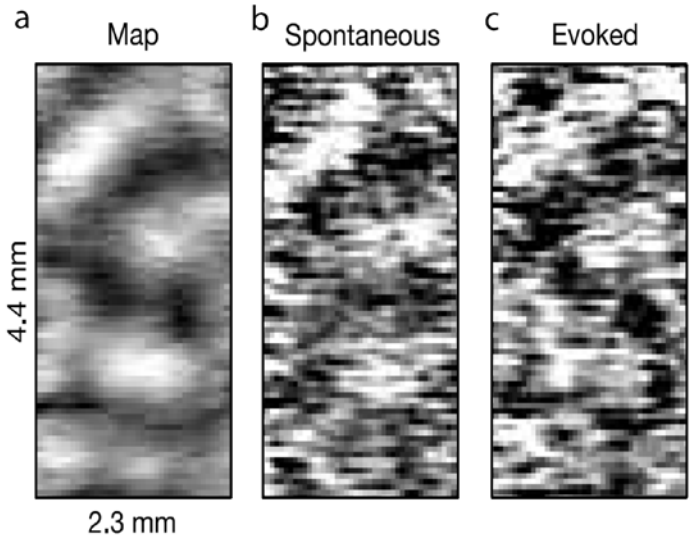

Figure 1.4 Spontaneously emerging orientation maps. (a) *Orientation map in visual cortex obtained by averaging over repeated presentations of full-field gratings.* ***(b)*** *Map obtained in a single instance from a spontaneous recording session.* ***(c)*** *Map obtained on a single presentation of the full-field grating. Note the large degree of similarity between the three maps. Adapted from Kenet et al., 2003.*

1.3.3 Predictive coding

The fact that spontaneous activity has a much more pronounced influence on the firing of single sensory neurons than does sensory input itself, begs the question whether spontaneous activity contains any functional significance for the brain. In other words, why is it there? One possible role for spontaneous activity might be found in the framework of predictive coding (Engel et al., 2001). Sensory input, while highly diverse and variable itself, needs to be processed fast and reliably. Predictive coding proposes that the brain does this by anticipating the forthcoming sensory environment, having ready a template against which to match the observed sensory evidence (Summerfield et al., 2006). A mismatch between the template and the sensory input leads to a modification of the template, while a match between the two strengthens the template. These templates, or predictions, might be embodied in the temporal structure of spontaneous activity. There are several lines of evidence that support such an account. For instance, the emergence of orientation maps in spontaneous population activity (Kenet et al., 2003) suggests that this is the cortical way to prepare 'default' network activity, which might reflect expectations about the sensory input.

If spontaneous activity carries predictions about the sensory environment, it is reasonable to assume that these predictions are expressed just before stimulus onset. Specific patterns of coherence in spontaneous activity prior to a stimulus have indeed been shown, and behavioural evidence indicates that these patterns are related to states of expectancy about task-relevant events (Fries et al., 2001a;Fries et al., 2001b;Von Stein et al., 2000). For instance, the local field potential (LFP) in the gamma band (>30 Hz) recorded from different sensory areas in awake cats exhibits strong synchrony between areas just before the onset of a behaviourally relevant stimulus (Fries et al., 2001b). These synchronisations are spatially specific and cannot therefore be attributed to an increased arousal state. Anticipation-related increases just before trial onset have also been shown in the haemodynamic signal in the sensory cortex of awake monkeys, which, intriguingly, did not correspond to any increases in neuronal activity (Sirotin and Das, 2009).

A more stringent method of assessing the presence of predictions about a forthcoming stimulus in spontaneous activity is to examine whether spontaneous activity has any predictive power for the subsequent neural response to that stimulus. This is indeed the case in visual cortex (Fries et al., 2001a). Pairs of neurons show correlated fluctuations in response latency in response to a stimulus flashed in their receptive field, but only when they fluctuate synchronously in the gamma frequency band before stimulus onset (Fig 1.5). The phase of these gamma oscillations at stimulus onset predicts the absolute latency of the neuronal spike response. The neuronal pairs can even be interhemispheric, and they are most strongly synchronised in their gamma band activity when they have overlapping receptive fields or similar orientation preferences.

Predictions are, by necessity, reflected in the spontaneous activity before stimulus onset. However, also after the stimulus has ended, spontaneous activity and the stimulus seem to interact. Optical imaging in rat visual cortex shows that visually evoked activity reverberates in subsequent waves of spontaneous activity (Han et al., 2008). Such reverberation could contribute to short-term memory by helping to consolidate recent sensory experiences into stable cortical modifications.

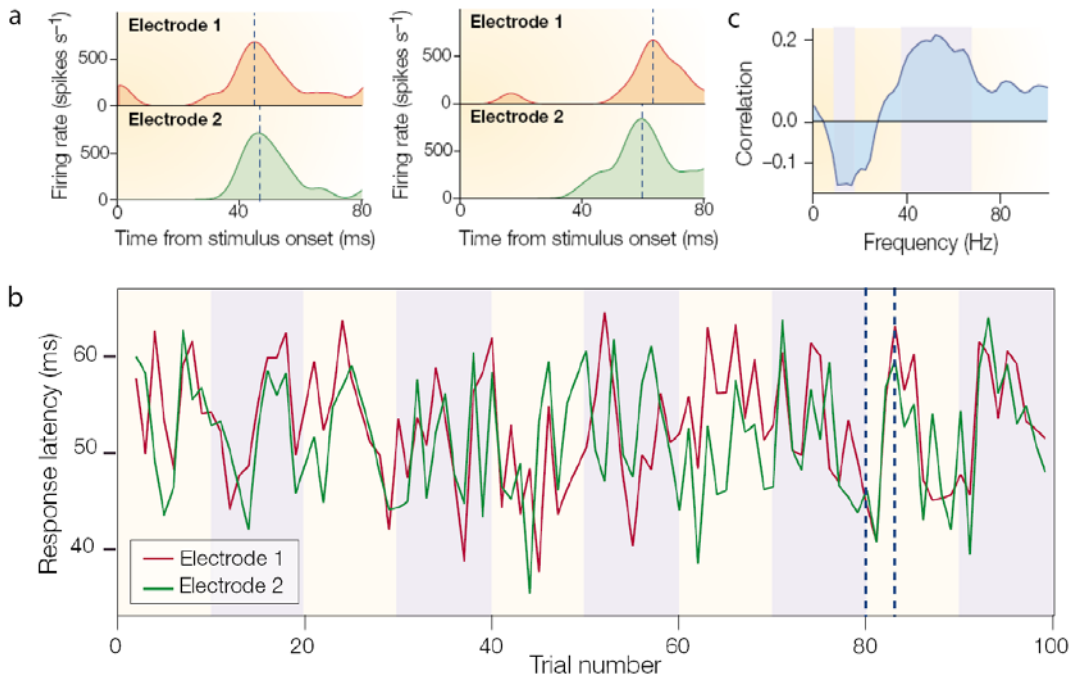

Figure 1.5 Prestimulus gamma oscillations predict response latency. ***(a)*** *Electrode pair (1 and 2) showing correlated short (left panel) or long (right panel) response latencies on single trials.* ***(b)*** *Covariation of latencies across 100 successive trials for the same electrode pair. Vertical lines refer to the single trials in* ***a****.* ***(c)*** *Prediction strength of correlation between neuron pairs as a function of prestimulus frequency. Prestimulus gamma band (>30 Hz) synchrony positively predicts a neuronal pair to be correlated in their response latencies, while alpha band synchrony predicts a negative correlation. Adapted from Engel et al., 2001.*

1.3.4 Summary

To conclude, electrophysiological studies have shown that variability in the response to a repeated stimulus is due to fluctuations in ongoing activity. The spontaneous activity of single neurons is embedded in a highly coherent network of ongoing fluctuations, that switches spontaneously between several dynamic states and is only slightly altered by sensory input. These dynamic states might reflect predictions about forthcoming sensory events.

1.4 Neuroimaging evidence of spontaneous activity

1.4.1 Resting-state fluctuations

The basic properties of spontaneous neuronal activity as measured by electrophysiological methods, such as the dynamically switching cortical states, have been inaccessible to functional MRI due to its low temporal resolution. However, spontaneous brain activity also leaves its footprint at a much slower timescale. This was recognised first in a pioneering study by Biswal and colleagues (1995). Instructing participants to engage in a simple finger tapping task, they observed activations in the familiar network of bilateral motor areas. They then instructed their participants to rest and not engage in any particular task, and again observed a high degree of temporal correlation between the areas activated by the motor task (Fig 1.6). They concluded that these correlated fluctuations in the resting state are a manifestation of functional connectivity between related brain areas (Biswal et al., 1995). These slow, global fluctuations observed in the fMRI signal measured in the brain at rest, which can be of the same magnitude as signal changes found in task-related experiments (Damoiseaux et al., 2006), have since been termed resting-state fluctuations (Fox and Raichle, 2007).

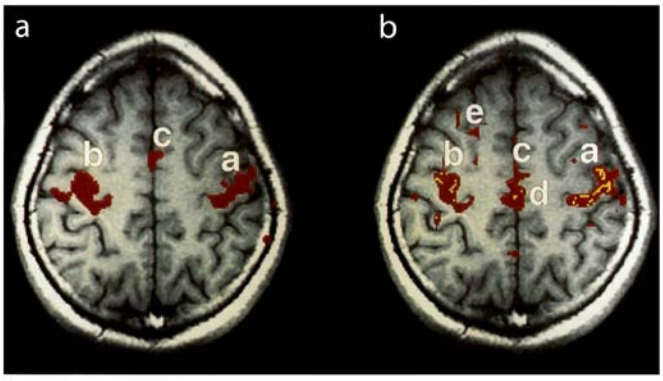

Figure 1.6 Correlated fluctuations in the fMRI signal at rest. (a) *fMRI activations induced by finger tapping.* ***(b)*** *Correlated fluctuations in the same regions, observed while the participants were at rest. Red is positive correlation, yellow is negative. Letters refer to various brain regions. Adapted from Biswal et al., 1995.*

1.4.2 Functional networks

The original observation by Biswal et al. (1995) that the somatomotor system is coherent in its spontaneous activity has since been replicated many times (Cordes et al., 2000;Lowe et al., 1998;Xiong et al., 1998). Much research has focused on partitioning these global resting-state fluctuations into several functional networks (Fox and Raichle, 2007;Moeller et al., 2009), and many neuroanatomical systems have now been shown to be coherent in their spontaneous activity, including the visual (Wang et al., 2008), auditory (Cordes et al., 2000), and somatomotor (Xiong et al., 1998) systems. These resting-state networks are highly consistent across subjects (Damoiseaux et al., 2006). A common finding seems to be that regions that are co-activated during certain tasks, tend to be correlated in their resting-state activity.

Interestingly, regions that are activated by apparently opposite tasks have been found to be anticorrelated in their spontaneous activity (Fox et al., 2005;Fox et al., 2006a;Greicius et al., 2003). An example of this is the dorsal and ventral attention systems in the human brain that are differentially active in the context of a task, and that also anticorrelate in their resting-state activity (Fox et al., 2006a). These anticorrelations in rest have been taken as evidence that differences between certain brain regions in a task-context are an intrinsic feature of the brain's organisation.

A certain subset of brain regions routinely decreases its activity during almost any task compared to rest. The fact that these brain regions are less active during task performance than during rest led to the hypothesis that the brain remains active in an organised fashion during the resting state, and these regions have been collectively termed as the 'default mode network' (Buckner et al., 2008;Raichle et al., 2001). The default mode network includes the ventral and dorsal medial prefrontal cortex, the posterior cingulate, the superior and inferior parietal lobule, and the lateral temporal cortex (Buckner et al., 2008). Activations in the default mode network have been associated with stimulus independent thought and mind

wandering (Mason et al., 2007), and these regions are highly correlated in their resting-state activity (Greicius et al., 2003).

1.4.3 Behavioural states

The emergence of functional networks such as the default mode network in the resting state, suggests that resting-state fluctuations, despite being present at rest, are very dependent on cognitive functioning. The same functional networks, however, are present in anaesthetised monkeys even at anaesthetic levels known to induce profound loss of consciousness (Vincent et al., 2007). Correlated spontaneous fluctuations were present in the oculomotor, the somatomotor, the visual, and even the default mode system (Fig 1.7).

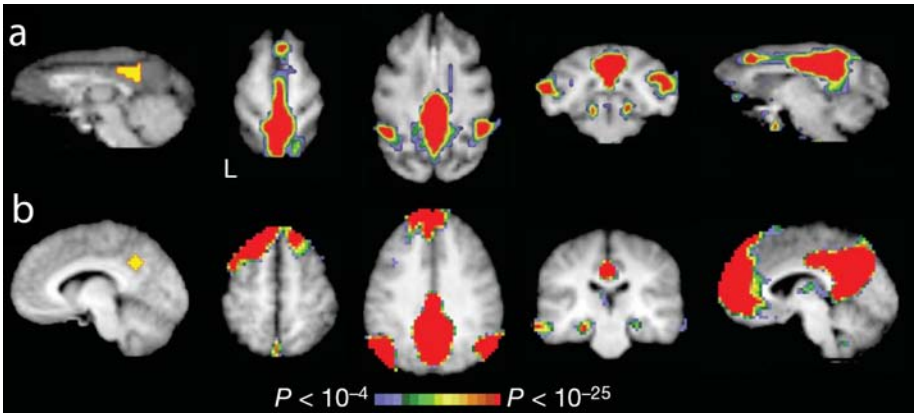

Figure 1.7 Default mode network in spontaneous activity. (a) *Data from 8 anaesthetised monkeys.* ***(b)*** *Data from 10 resting humans. Adapted from Vincent et al., 2007.*

These findings suggest that coherent fluctuations within cortical systems are not critically dependent on cognitive functioning, but probably reflect an intrinsic property of functional brain organisation that transcends levels of consciousness (Vincent et al., 2007). Consistent with this, resting-state functional networks have been observed in premature babies (Doria et al., 2008). Subsequent studies have shown that also in humans, functional networks persist across several behavioural states such as sleep (Horovitz et al., 2008), anaesthesia, and coma (Boly et al., 2008). Recent findings in the monkey brain, however,

suggest that anaesthesia does have an effect on the spatial structure of these functional networks (Moeller et al., 2009). The persistence of these networks under anaesthesia suggests that their coherence is mediated by known anatomical connections, and substantial correspondence between structural connectivity and resting-state correlated networks measured in the same participants has indeed been found (Hagmann et al., 2008;Honey et al., 2009).

1.4.4 Functional connectivity

Resting-state networks are often described in terms of functional connectivity, which may refer to any result reporting inter-regional correlations in neuronal variability (Friston et al., 1993;Horwitz, 2003). Both resting-state and task-state data have been defined in the framework of functional connectivity, and an important question is whether the term 'functional connectivity' in these contexts refers to the same or to different phenomena. Since spontaneous activity persists under task conditions, it is likely that functional connectivity measured during a task reflects some combination of resting-state connectivity and task-related connectivity. Another important question concerns the relationship of functional connectivity to structural connectivity. Monkey data are helpful in this respect because of the possibility of obtaining data on structural pathways with histological tracer methods. Using these methods, the correspondence between the oculomotor system as revealed in resting-state data and anatomical data could be visualised (Vincent et al., 2007) (Fig 1.8). Interestingly, the same resting-state data revealed regions in bilateral primary visual cortex that retinotopically represented the periphery of the visual field, and that were strongly correlated in their spontaneous activity, despite the absence of a direct interhemispheric connection (Vincent et al., 2007). Such strong functional correlations must therefore be supported by polysynaptic pathways. Also in humans, it has been shown that strong functional connections in resting-state data commonly exist between regions with no direct structural connection (Honey et al., 2009). However, some structural connections are

essential, as was shown by a striking loss of interhemispheric functional connectivity in a patient after complete section of the corpus callosum (Johnston et al., 2008). On overall, therefore, functional connectivity roughly follows structural connectivity.

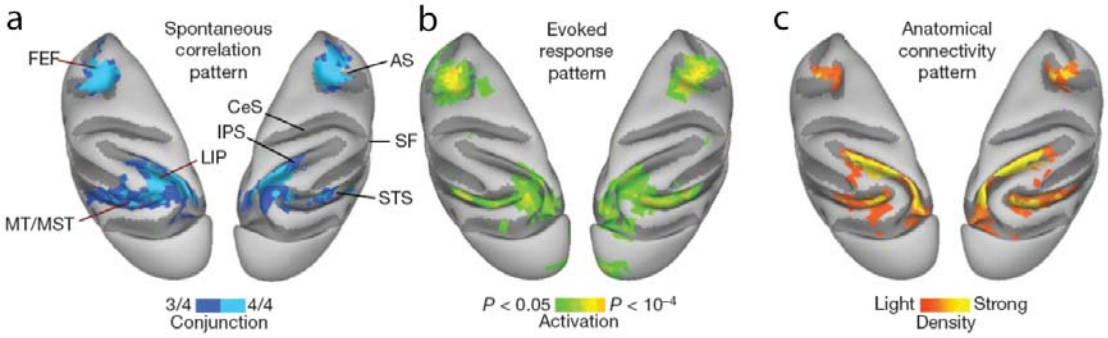

Figure 1.8 Similarity between functional and structural connectivity. ***(a)*** *Oculomotor system as revealed in spontaneous BOLD fluctuations in anaesthetised monkey.* ***(b)*** *The oculomotor network in the resting state is similar to the activation pattern evoked by performance of a saccadic eye movement task.* ***(c)*** *Anatomical connections within the oculomotor system as revealed by retrograde tracer injections into LIP. Adapted from Vincent et al., 2007.*

1.4.5 Vascular basis

Spontaneous fMRI fluctuations thus exhibit strong coherence in functional networks. In addition, a global level of coherence is present between all voxels in the brain. The presence of this 'global network' suggests that the origin of these spontaneous fluctuations might lie in global blood flow changes; if blood flow to the entire brain fluctuates on a slow timescale, this will certainly induce temporal correlations between all regions of the brain. Changes in heart rate and respiration, which influence blood flow and blood oxygenation in the brain, indeed contribute to fMRI resting-state fluctuations (Birn et al., 2006;Wise et al., 2004). Spontaneous fluctuations have highest power below 0.1 Hz (Cordes et al., 2001); this is well below normal breathing frequency, though *variations* in breathing rate or depth do occur at very low frequencies (Birn et al., 2006). These variations correlate well with the BOLD

signal acquired at rest in blood vessels and regions with high blood volume (grey matter). In addition, these correlations coincide with many of the areas identified as part of the default mode network (Birn et al., 2006). Sophisticated methods have been developed to deal with cardiac and respiratory confounds in resting-state data (Birn et al., 2008;Glover et al., 2000); some of these methods will be described in Chapter 2, Measuring Spontaneous Activity.

1.4.6 Neural basis

FMRI resting-state fluctuations thus partly depend on physiological (non-neuronal) factors. However, the existence of functional networks such as the oculomotor system in resting-state data suggests that these fluctuations might also be underlied by coherent neuronal fluctuations. A first indication for this comes from the observation that the power of local field potentials (LFP) recorded in monkey visual cortex fluctuates at a timescale similar to that of the resting-state fluctuations measured by fMRI, i.e. <0.1 Hz (Leopold et al., 2003). Furthermore, these fluctuations exhibit high coherence across electrode pairs, with no apparent decrease with cortical distance, and their structure and coherence remain highly similar under distinct behavioural states (Leopold et al., 2003). Thus, widespread coherent fluctuations over very long timescales exist in the neuronal activity of the awake monkey brain that are comparable to fMRI resting-state fluctuations.

Similar fluctuations have also been shown in intracranial electrocorticography (ECoG; i.e. surface electrode) recordings in humans (He et al., 2008;Nir et al., 2008). Datasets of bihemispheric recordings obtained in the auditory cortex of individuals undergoing presurgical clinical testing were used to study the temporal and spatial profiles of spontaneous LFP activity under awake and asleep conditions (Nir et al., 2008). Slow (<0.1 Hz) fluctuations in the LFP activity were found, which were evident mainly in neuronal firing rate and in gamma (40-100 Hz) power modulations. Importantly, there were significant interhemispheric correlations between functionally similar areas, which were enhanced during rapid eye movement (REM) and stage 2 sleep (Nir et al., 2008) (Fig 1.9).

Spatial specificity in spontaneous neuronal activity was also observed in slow ECoG signals (<0.1 Hz) and gamma power modulations recorded from sites within the sensorimotor system, which showed significantly higher correlations among each other than to sites outside this network (He et al., 2008). These correlations persisted across wakefulness, slow-wave sleep, and rapid eye movement sleep. Taken together, these data argue for the existence of functional networks in the spontaneous LFP power fluctuations in the human brain (He et al., 2008;Nir et al., 2008).

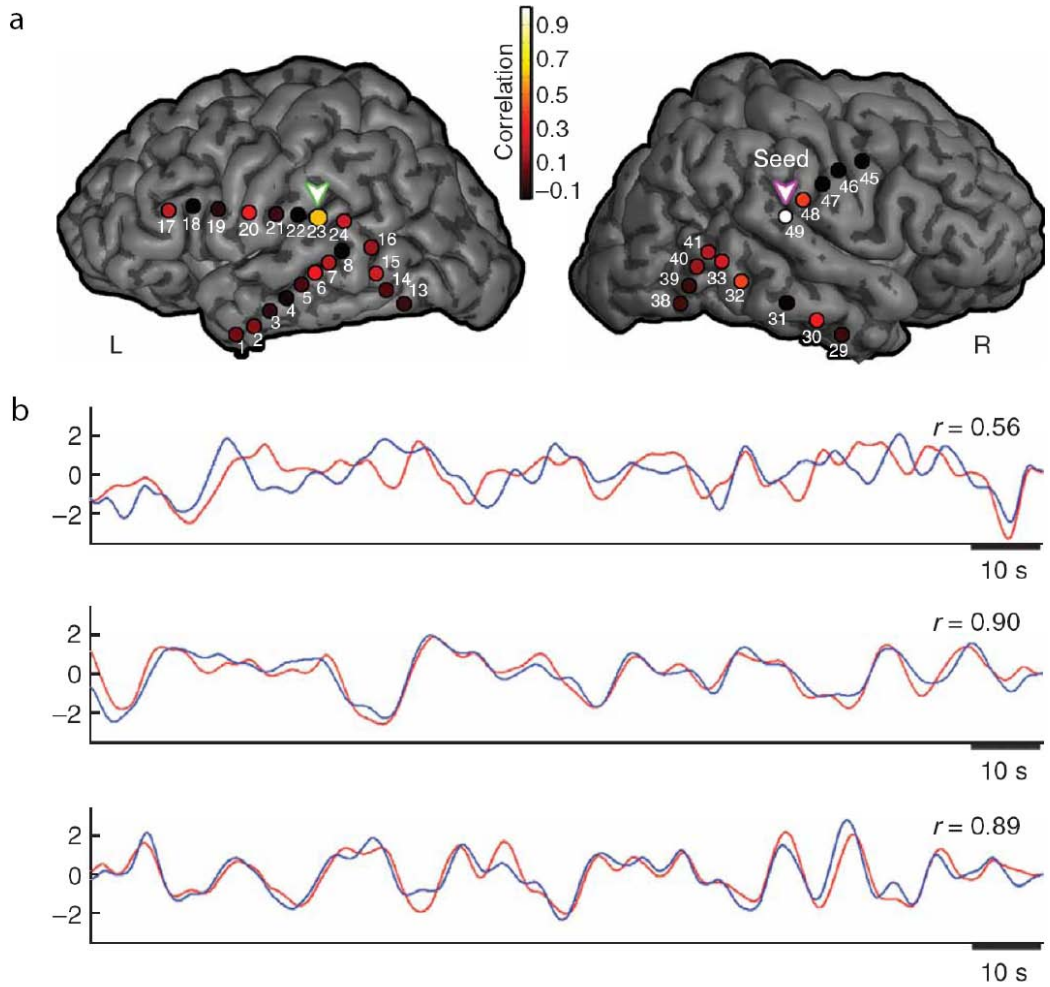

Figure 1.9 Interhemispheric correlations in ECoG gamma power fluctuations. (a) *Correlations of all electrode sites with a site in right auditory cortex (termed 'seed'). The strongest correlation in the left hemisphere (marked with an arrow) is found in a corresponding anatomical location.* ***(b)*** *Correlated fluctuations between the electrode sites marked with arrows in* ***a*** *during wakeful rest (top panel), REM sleep (middle panel), and stage 2 sleep (bottom panel). Adapted from Nir et al., 2008.*

A more direct comparison between fMRI resting-state fluctuations and its underlying neural activity has been made using simultaneous EEG-fMRI recordings (Goldman et al., 2002;Laufs et al., 2003;Mantini et al., 2007). Rather than concentrating on gamma power fluctuations, most of these studies have focused on correlations between the BOLD signal and alpha power, the rationale being that alpha band activity is the hallmark of wakeful rest and sleep (Berger, 1929). Alpha power is negatively correlated with spontaneous BOLD fluctuations in the occipital cortex (Goldman et al., 2002;Moosmann et al., 2003) and in superior parietal and inferior frontal regions (Goldman et al., 2002;Laufs et al., 2003), which are areas commonly thought to be part of the default mode network. Correlations between the BOLD signal and power in even lower frequencies (delta band, 2-5 Hz) were found in anaesthetised rats (Lu et al., 2007). An interesting approach was taken by Mantini et al (2007), who performed independent component analysis (ICA) on spontaneous BOLD data and found six resting-state networks. These networks were separately correlated with five frequency bands (delta, theta, alpha, beta, and gamma) and found to possess their own specific electrophysiological signature, consisting of a particular combination of frequency bands (Mantini et al., 2007). Thus, spontaneous fMRI and neuronal fluctuations correlate across multiple frequencies and in multiple regions.

The relationship between slow fMRI fluctuations and underlying neural fluctuations has been most directly demonstrated in anaesthetised monkey (Shmuel and Leopold, 2008). Using simultaneous fMRI and intracortical neurophysiological recordings in the visual cortex, slow fluctuations in the fMRI and the LFP signal could be compared directly. This comparison revealed strong correlations between the spiking rate of the small network of neurons in the vicinity of the recording electrode, and slow fluctuations in the fMRI signal in the entire visual cortex. Slow power changes in the multi-unit activity (>100 Hz) and LFP gamma band (25-80 Hz) also correlated strongly with the fMRI signal. In order to look at the temporal evolution of this correlation, the gamma power signal was artificially shifted ahead of the fMRI signal in steps of 1 second and the correlation between the two signals was computed each time. In other words, this analysis shows what the correlation looks like

when changes in the gamma power precede changes in the fMRI signal. Since the BOLD signal responds sluggishly to stimulation, peaking typically at a delay of 6-8 seconds (Aguirre et al., 1998b), one might expect that changes in the BOLD signal will correspond best to changes in the LFP signal that happened 6-8 seconds earlier. This is exactly what was found (Shmuel and Leopold, 2008). Moreover, the correlation exhibited a wave-like pattern that slowly traversed the visual cortex (Fig 1.10). This study unequivocally established the existence of a coupling between slow fluctuations in the fMRI signal and underlying fluctuations in neural activity.

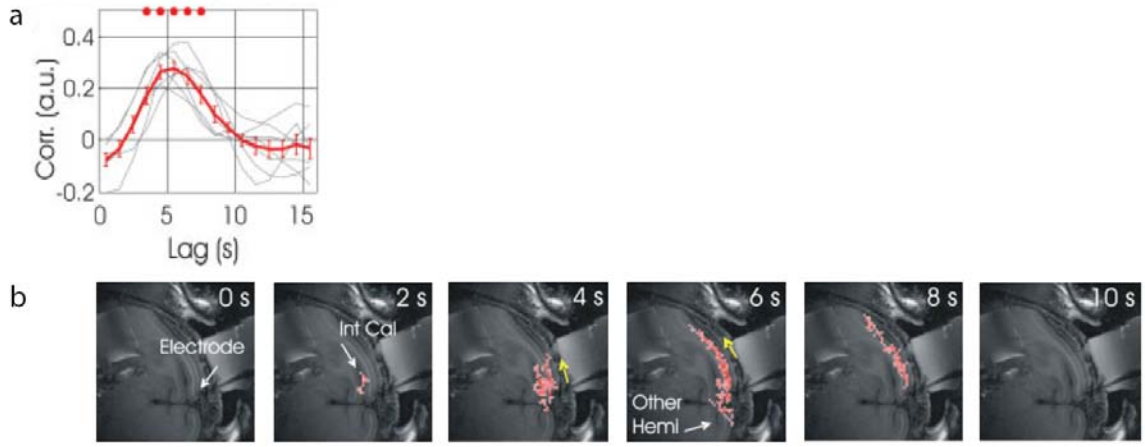

Figure 1.10 Spatial and temporal evolution of LFP-fMRI correlation. (a) *Correlation between gamma power and fMRI signal as a function of the shift between the two signals. When the fMRI signal is lagging the LFP signal by about 6 seconds, the correlation is strongest.* ***(b)*** *The correlation slowly traverses visual cortex. The labels '0 s', '2 s' etc mark the shift between the BOLD and the LFP signal. Intermediate steps of 1, 3, etc seconds have been omitted. Adapted from Shmuel and Leopold, 2008.*

The correlation between the spontaneous fMRI signal and slow LFP or EEG activity suggests that modulations in both signals share a common, perhaps subcortical origin. BOLD resting-state fluctuations in both cortical hemispheres are strongly correlated to fluctuations in their contra- and ipsilateral thalamus (Zhang et al., 2008), thus highlighting the potential importance of thalamocortical pathways in the resting state. More research is needed to establish the origin of the slow fluctuations in spontaneous brain activity.

1.4.7 Summary

In summary, spontaneous brain activity appears as slow (<0.1 Hz) fluctuations in the fMRI BOLD signal. These fluctuations are spatially coherent within several functional networks. These networks persist under a range of behavioural conditions and correlate well with structural connectivity, suggesting they reveal an intrinsic property of brain functional organisation. The spontaneous fluctuations are partly vascular, partly neural in origin. They are positively correlated with slow fluctuations in gamma power, and negatively correlated with modulations in alpha power. The origin of these neuronal fluctuations is not yet understood.

1.5 Spontaneous activity and behaviour

1.5.1 Spontaneous activity and perception

The predictive coding account of spontaneous neural activity (see 1.3.3) relates prestimulus spontaneous activity to the neural processing of subsequent sensory stimuli. It does not encompass the behavioural outcome of that neural processing, in the form of perception of the sensory stimulus or a motor response. Put simply, does spontaneous brain activity influence perception or behaviour? There are several studies that have addressed this question, most notably EEG and fMRI studies.

1.5.2 Prestimulus alpha activity

The first study to reveal an effect of prestimulus electrophysiological activity on subsequent stimulus perception was performed using multiple electrode recordings in monkey primary visual cortex (Super et al., 2003). In search of the neural correlates of states of inattention or absent-mindedness, this study found that for a detected stimulus, the preceding spiking activity and amount of synchrony between neurons was stronger than for

an undetected stimulus. This implies that the strength of neural activity and the functional connectivity between neurons in V1 is a predictor of subsequent awareness of a stimulus (Super et al., 2003).

EEG measurements show that especially neural activity in the alpha frequency band (8-14 Hz) has an effect on stimulus detectability (Mathewson et al., 2009;Romei et al., 2008;Thut et al., 2006). Posterior alpha band activity correlates inversely with covert attention to a particular location of the visual field; that is, alpha band activity is weakest in the cortical region corresponding to the attended location (Thut et al., 2006). Furthermore, these decreases in alpha activity correlate with behavioural performance in target detection at that location; thus, inhibition of alpha activity facilitates stimulus detection (Thut et al., 2006). Also without the explicit manipulation of attention, prestimulus alpha band activity has an adverse effect on stimulus detection; identical TMS pulses are more likely to induce an illusory visual percept (phosphene) when preceding alpha band activity is low (Romei et al., 2008). There is therefore a direct link between alpha band fluctuations and cortical excitability. These fluctuations are spatially specific and happen over short (subsecond) timescales.

Recent evidence has indicated that not only prestimulus alpha activity, but also prestimulus gamma activity might play a role in subsequent stimulus awareness (Wyart and Tallon-Baudry, 2009). Magnetoencephalography (MEG) measurements during a stimulus detection paradigm demonstrated a suppression of alpha band activity in lateral occipital areas when the subject attended to the stimulus location. This produced a shift in prestimulus baseline activity that could predict subsequent stimulus detection. Gamma band fluctuations in the same areas also predicted stimulus awareness, but were not affected by spatial attention. Instead, decision-making models showed that gamma band activity behaved as a decision bias at stimulus onset, irrespective of subsequent stimulus processing (Wyart and Tallon-Baudry, 2009). Thus, the intimately linked phenomena of attention and awareness might be related to distinct neural processes that independently modulate stimulus perception.

Not only the power of alpha fluctuations, but also their phase affects stimulus perception (Busch et al., 2009;Mathewson et al., 2009). When visual stimuli are presented near threshold, their detection probability is strongly dependent on the phase of spontaneous EEG oscillations in the low alpha and theta bands just before (~100 ms) stimulus onset (Busch et al., 2009). The 'ideal' phase was different for each observer, although in a different, metacontrast masking paradigm, observers were consistently less likely to perceive the target when it was presented in the trough of the alpha wave (Mathewson et al., 2009). Based on these findings, it is argued that the cortex goes through microstates (i.e. very fast states) of excitability (Busch et al., 2009;Mathewson et al., 2009). Very slow states of excitability, on the other hand, might also play a role; fluctuations in detection performance of a somatosensory stimulus over the time course of minutes are significantly correlated with the phase of ultraslow (0.01–0.1 Hz) EEG fluctuations (Monto et al., 2009).

1.5.3 Predictive BOLD activity

Correlations between spontaneous fluctuations in the 0.01-0.1 Hz range and behavioural performance should in principle also be detectable using fMRI. Compared to the vast body of literature on resting-state functional networks (Fox et al., 2005;Moeller et al., 2009), comparatively little research has been done in this area, yet a number of neuroimaging studies have found an effect of spontaneous BOLD fluctuations on stimulus-evoked brain activity and behaviour (Boly et al., 2007;Fox et al., 2006b;Fox et al., 2007;Hesselmann et al., 2008a;Hesselmann et al., 2008b).

Much like electrophysiological responses (Snowden et al., 1992;Vogels et al., 1989), the BOLD response to a repeated stimulus displays trial-to-trial variability (Pessoa et al., 2002;Pessoa and Padmala, 2005;Ress et al., 2000;Wagner et al., 1998), but the source of this variability remains unknown. Trial-to-trial variability in single neurons has been shown to be attributable almost entirely to spontaneous activity; a fixed amount of stimulus-evoked activity is added to a variable amount of spontaneous activity (Arieli et al., 1996). The

contribution of spontaneous activity to inter-trial variability has been assessed for the BOLD response as well (Fox et al., 2006b). Subjects were engaged in a simple button pressing task with their right index finger. Exploiting the fact that right and left somatomotor cortex are consistently correlated in their spontaneous activity (Biswal et al., 1995;Cordes et al., 2000;Lowe et al., 1998;Xiong et al., 1998), activity in the right motor cortex (RMC) served as an estimate of the spontaneous activity in the left motor cortex (LMC), which was activated by the button presses. Right-hand button presses do not yield a discernible BOLD response in RMC; thus, activity in the RMC is truly a measure of spontaneous activity. The BOLD response to the button presses in the LMC contained a mixture of task-evoked and spontaneous activity; the spontaneous activity could be subtracted from this mixture using the estimate provided by the RMC. This approach led to a significant (40%) reduction of the variability in the BOLD response in LMC (Fox et al., 2006b) (Fig 1.11). Thus, 40% of the trial-to-trial variability in the BOLD response could be attributed to spontaneous fluctuations. The magnitude of task-evoked activity in a particular trial did not depend on whether the underlying spontaneous activity was high or low on that trial, leading to the conclusion that spontaneous and task-related activity are linearly superimposed in the human brain (Fox et al., 2006b).

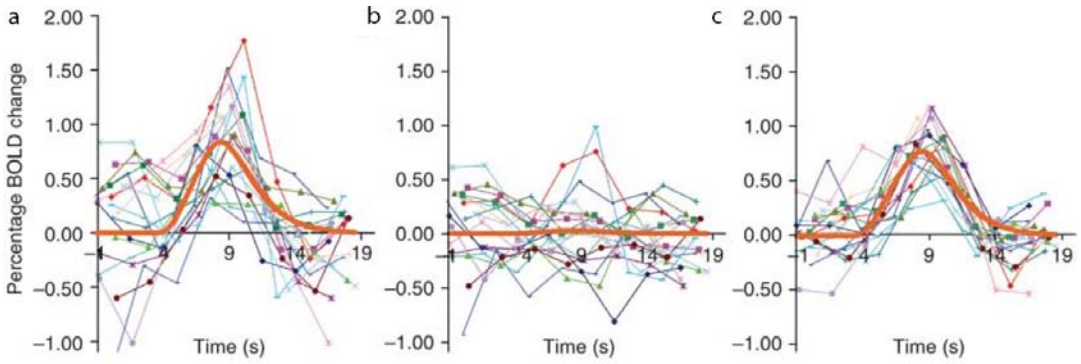

Figure 1.11 The contribution of spontaneous activity to inter-trial variability. (a) *BOLD responses in LMC to individual button presses (thin lines; average is the thick red line).* ***(b)*** *The corresponding activity in RMC for each button press.* ***(c)*** *BOLD responses in LMC after subtraction of the spontaneous fluctuations measured in RMC; there is a significant reduction in trial-to-trial variability. Adapted from Fox et al., 2006b.*

Variability in task-evoked activity thus depends on fluctuations in spontaneous activity. Using the same task, this conclusion was taken one step further by showing that variability in *behaviour* also depends on spontaneous brain activity (Fox et al., 2007). Activity in LMC and trial-to-trial variability in button press force are well correlated; BOLD responses to hard button presses are significantly higher in the first half of the response compared to BOLD responses to soft button presses. Interestingly, this same significant difference exists in RMC, which is not activated by the button presses. Subtracting the RMC estimate of the spontaneous activity in LMC (analogous to Fox et al., 2006b) abolishes this difference between hard and soft button presses. In this way, the majority (74%) of the relationship between spontaneous force variability and BOLD activity in LMC can be attributed to spontaneous fluctuations in activity (Fox et al., 2007). Spontaneous activity therefore has an effect on trial-to-trial variability both in the neuronal and in the behavioural response to a stimulus.

Effects of spontaneous activity on behavioural variability have also been demonstrated in the perceptual domain. Identical stimuli presented over repeated trials can yield strikingly different percepts (Sergent et al., 2005), which might be related to fluctuations in spontaneous activity. In order to test this hypothesis, Boly and colleagues (2007) administered somatosensory (laser) stimuli at detection threshold to the left hand of their subjects. They then examined brain regions that showed an activity difference between perceived and unperceived stimuli just *before* actual onset of the stimuli. They found a positive relationship between conscious perception of the stimuli and prestimulus levels of activity in medial thalamus and the lateral frontoparietal network (Boly et al., 2007), areas which are thought to be related to vigilance. Negative correlations with stimulus perception were found in a set of regions encompassing the posterior cingulate and the temporoparietal cortices, which are part of the default mode network. These results show that prestimulus baseline activity in certain regions of the brain can have a direct effect on somatosensory perception. However, it is not clear whether these prestimulus activity levels truly reflect ‘spontaneous activity’ or whether they are related to fluctuations in attention.

Fluctuations in attention are less of a concern in two studies investigating the effect of prestimulus activity on visual perception (Hesselmann et al., 2008a;Hesselmann et al., 2008b). An ambiguous stimulus, Rubin's face-vase figure, was presented briefly to subjects at variable intervals of >20 s. Brain activity was recorded while subjects reported whether they perceived the stimulus as two faces or as a vase. Activity in the fusiform face area (FFA), a cortical region preferentially responding to faces, was higher when subjects perceived two faces compared to the vase, and importantly, this activity difference was present before presentation of the stimulus (Hesselmann et al., 2008a). Thus, prestimulus activity in the FFA predicted the subsequent percept. This result was confined to the right FFA and not present in a number of control regions. Furthermore, the shape of the BOLD response to faces or vase percepts differed significantly, and this difference depended on the level of prestimulus activity, leading these researchers to conclude that spontaneous and stimulus-evoked activity interact in a nonlinear way (Hesselmann et al., 2008a). Similar effects of prestimulus activity on subsequent perception of an ambiguous stimulus were found in the motion-sensitive occipito-temporal cortex (hMT+), which exhibited both a higher BOLD response, and higher prestimulus baseline activity, to a dynamic random dot display that was perceived as coherent motion compared to random motion (Hesselmann et al., 2008b). Again, the relation between spontaneous and evoked activity was not additive but interacted with perceptual outcome (Hesselmann et al., 2008b).

The nonlinear interaction between ongoing and evoked brain activity has been related to the framework of predictive coding, which has been discussed earlier in the context of electrophysiology data (Engel et al., 2001) (see 1.3.3). Briefly, predictive coding states that the brain constantly matches incoming sensory information to existing templates, or priors (Summerfield et al., 2006). The outcome of this matching can be either a low or high prediction error, which is used to adjust the priors. Spontaneous activity fluctuations might carry these dynamic predictions or priors. The priors and the incoming stimuli might then interact to produce the prediction error, which might also contribute to the stimulus response, and this could explain the observed nonlinear interactions (Hesselmann et al.,

2008a;Hesselmann et al., 2008b). Interesting in this respect is a study that looked specifically at brain regions predictive of an error response (Eichele et al., 2008). They found a set of brain regions, all part of the default mode network, in which activity levels predicted performance errors up to 30 s before the error was made. These areas might be involved in updating the dynamic predictions posited by the predictive coding framework.

In summary, therefore, spontaneous brain activity influences neuronal and behavioural variability in responses to perceptual stimuli. Whether ongoing and stimulus-evoked brain activity are linearly superimposed, or interact in a nonlinear way, remains to be determined.

1.5.4 Fluctuations in visual awareness

In most of the studies described above, stimuli were presented at perceptual threshold and the influence of spontaneous activity on detection probability of the stimuli was measured. A much more striking example of identical perceptual input leading to different percepts is provided by bistable perception. Examples of bistable perception include binocular rivalry and ambiguous figures such as the well-known Necker cube (Blake and Logothetis, 2001). What these phenomena have in common is identical retinal input resulting in virtually binary switches in perception; either one of the two alternative perceptual interpretations of the same physical input is favoured at any given point in time. This phenomenon was cleverly exploited by Hesselmann and colleagues (2008a), who investigated the influence of spontaneous activity on perception of Rubin's ambiguous face/vase figure. However, they presented their stimuli briefly, allowing only for one perceptual interpretation on any given trial. Prolonged viewing of bistable stimuli leads to fluctuations in perception, and since the retinal input remains identical, these fluctuations in perception must be caused by fluctuations in underlying brain states (Blake and Logothetis, 2001).

Much research has been devoted to bistable perception within the context of visual awareness. In particular, where in the brain these fluctuations in brain state occur has been

the topic of intense investigation. Bistable perception has been studied at all levels of the visual hierarchy, from subcortical and early sensory areas, through extrastriate areas, to non-sensory association cortices. Most of this work has focused on binocular rivalry. FMRI studies in humans have repeatedly demonstrated strong effects of binocular rivalry on brain activity in V1 (Polonsky et al., 2000;Tong and Engel, 2001). Moreover, the fluctuations in perception during binocular rivalry can be predicted for extended periods of time from BOLD signals in V1 alone (Haynes and Rees, 2005). Even BOLD signals in the lateral geniculate nucleus (LGN) correlate with the dominant percept during rivalry (Haynes et al., 2005;Wunderlich et al., 2005). We can thus conclude that fluctuations in brain activity at anatomically very early processing stages correlate well with perceptual dominance of bistable stimuli (Sterzer et al., 2009). However, this does not imply that perceptual fluctuations are initiated in these low-level visual areas.

In addition to early visual areas, extrastriate visual areas also demonstrate strong correlations between brain activity and subjective perception (Sterzer et al., 2009). For example, BOLD signals measured in the fusiform face area (FFA) are greater during face perception in Rubin's face/vase illusion (Andrews et al., 2002), and brain activity in motion-sensitive area V5/MT allows accurate prediction of perceptual states during ambiguous structure-from-motion (Brouwer and Van Ee, 2007). Studies specifically looking at perceptual transitions (as opposed to perceptual states) have consistently observed transition-related activity in extrastriate visual areas that are tuned to the visual feature or attribute that is perceived to change (Sterzer et al., 2009). For instance, perceived changes in motion direction are associated with activations in V5/MT (Castelo-Branco et al., 2002;Sterzer et al., 2003). The finding of increased activity in extrastriate areas during perceptual transitions suggests that these areas play an important role in perceptual fluctuations, yet does not provide definitive proof of causality.

Transient fMRI signal increases associated with perceptual transitions are not only observed in extrastriate visual areas but also in parietal and frontal regions (Kleinschmidt et al., 1998;Lumer et al., 1998). Interestingly, although extrastriate areas are equally activated

by unambiguous perceptual changes (i.e. changes in perception due to a stimulus change), parietal and prefrontal regions show greater activation during ambiguous (bistable) perceptual alternations (Lumer et al., 1998). It is difficult to disentangle whether these activity increases are the *result* of activity differences in earlier visual areas, communicated through feedforward processing, or the *cause* of activity differences in these earlier areas, fed back to the visual system through recurrent processing. Chronometric analysis of BOLD activity increases associated with spontaneous changes in apparent motion perception show that activation of the prefrontal cortex precedes that of V5/MT during bistable motion perception, relative to unambiguous perceptual changes (Sterzer and Kleinschmidt, 2007). This temporal precedence of BOLD activations in prefrontal cortex argues for an active role for high level, non-sensory areas in perceptual fluctuations, which are making inferences about the bistable perceptual input. In such a framework, bistable perception can be conceived of as a frequent re-evaluation of the current interpretation of the sensory input (Leopold and Logothetis, 1999).

The current view of bistable perception that has emerged from these studies is that bistable perception arises from interactions between low-level (sensory) and high-level (cognitive) areas, with non-sensory association cortices initiating perceptual fluctuations based on the outcome of their inference (Sterzer et al., 2009). Consistent with this, many instances of bistable perception can be influenced both by low-level sensory factors such as stimulus contrast and brightness (Kaplan and Metlay, 1964;Mueller and Blake, 1989), as well as high-level factors such as grouping (Fang et al., 2008) and decision criteria on the visibility of a stimulus (Caetta et al., 2007).

A particularly interesting case in this respect is another example of bistable perception called motion-induced blindness. Motion-induced blindness (MIB) is a striking phenomenon in which perceptually salient stationary visual targets repeatedly disappear when superimposed on a field of moving distracters (Fig 1.12) (Bonneh et al., 2001). Target disappearance in MIB is influenced by low-level sensory factors. For example, the targets disappear more often at increased eccentricity (Hsu et al., 2004) and when they are smaller

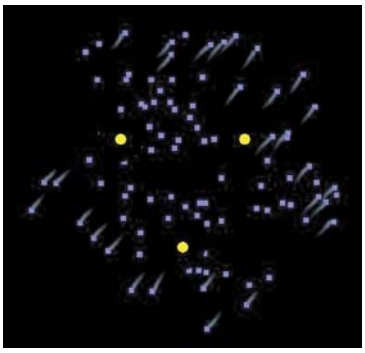

Figure 1.12 Motion-induced blindness. *In the dynamic display, the three yellow dots are stationary; the blue dots move. Upon fixation at the centre, the yellow dots repeatedly appear and disappear from awareness. Adapted from Bonneh et al., 2001.*

(Bonneh et al., 2001). MIB is also prone to the boundary adaptation effect, consisting of the fading of the boundaries of the targets, followed by interpolation of the surrounding distracter elements (Hsu et al., 2006). In addition to these low-level sensory factors, higher-level factors also influence MIB. Disappearance of the targets is subject to gestalt-like grouping effects; the targets tend to disappear together rather than separately when they form good gestalts. More specifically, when two Gabor patches are presented as targets, they tend to disappear together when they are collinear, and in alternation when their orientation is orthogonal (Bonneh et al., 2001). MIB thus seems to be dependent on low-level visual areas such as V1 as well as on higher-level areas. What distinguishes MIB from other types of stimuli fading from awareness, such as Troxler fading (Troxler, 1804) and filling-in of artificial scotomas (Ramachandran and Gregory, 1991), are its interesting dynamics. Disappearance of the targets typically occurs following very brief observation periods and subsequent fluctuations of awareness of the targets are rapid, in the order of several seconds (Bonneh et al., 2001). It seems, therefore, that the fluctuations in internal state of the brain leading to target disappearance and reappearance, are of a more dynamical kind than in other types of perceptual fading. These dynamics, as well as the supposed interplay between low-level and higher-level visual areas, make MIB an interesting model system for the study of the influence of internal brain state on visual awareness.

1.5.5 Manipulating internal dynamics: attention

Thus far, the spontaneous nature of ongoing brain activity has been emphasised. Although fluctuations in spontaneous activity might influence factors such as perception and behaviour (see 1.5.2 and 1.5.3), the influence of any factors on spontaneous activity itself has not been discussed. The persistence of spontaneous fluctuations throughout several stages of awareness, including sleep (Horovitz et al., 2008) and anaesthesia (Vincent et al., 2007), makes it likely that these fluctuations are not under cognitive control and therefore truly spontaneous in nature. However, when we look at it from a broader perspective and acknowledge these spontaneous fluctuations as one factor contributing to the 'internal state' of the brain, we can distinguish several other contributing factors too. The brain is not a passive, stimulus-driven device; rather, it actively interacts with the environment through its internal state and constructs perceptual experiences (Engel et al., 2001). One such factor influencing the internal state of the brain is endogenous attention.

The effect of attention on visual processing has been demonstrated in countless experiments (for a review of the neuroimaging literature, see Pessoa et al., 2003; for a review of the electrophysiology literature, see Reynolds and Chelazzi, 2004), and giving a comprehensive overview goes beyond the scope of this introduction. Therefore the focus will be on the effect of attention on the internal brain states underlying visual awareness. As has just been discussed, many bistable phenomena such as binocular rivalry and motion-induced blindness depend on low-level sensory factors such as stimulus contrast and size (Bonneh et al., 2001;Mueller and Blake, 1989). However, attention equally plays a role in bistable perception. Most studies investigating the effect of attention on bistable perception have focused on voluntary control over the perceptual alternation rate of the bistable stimuli. For example, attentional control over perceptual reversals of ambiguous figures is associated with activity in both frontal (Windmann et al., 2006) and posterior parietal (Pitts et al., 2008;Slotnick and Yantis, 2005) areas. Selective attentional control over perceptual alternations in binocular rivalry is considerably weaker than control over alternations in

other forms of bistable perception, such as Necker cube or face/house reversals (Meng and Tong, 2004;Van Ee et al., 2005). Attention thus affects the temporal dynamics of the internal brain states underlying bistable perception.

Several studies have now also investigated the effects of directing attention directly at the bistable stimulus. This has led to the somewhat counterintuitive finding that attended stimuli disappear more often from awareness than unattended stimuli (De Weerd et al., 2006;HaiYan et al., 2007;Lou, 1999), despite the prevailing idea that attention enhances visual processing (Reynolds and Chelazzi, 2004). Attention thus has a direct effect on stimulus awareness in bistable perception. This is in line with Bonneh et al (2001), who postulated that disappearance of the targets in motion-induced blindness might reflect a disruption of attentional switching between targets and distracters (Bonneh et al., 2001).

1.5.6 Summary

To summarise, fluctuations in spontaneous activity influence perception, as several lines of evidence suggest. First of all, prestimulus alpha power and phase have a direct effect on subsequent stimulus detection. Several neuroimaging studies have demonstrated that also on a much slower timescale, prestimulus activity affects the behavioural response to a subsequent stimulus. This becomes especially evident in bistable perception, where fluctuations in the internal state of the brain lead directly to fluctuations in visual awareness. These internal brain states, to which the spontaneous brain activity contributes, are under the influence of endogenous factors such as attention.

1.6 Conclusions

Cognitive neuroscience has traditionally focused on brain activity evoked by a task or stimulus. However, the brain is very active even in the absence of explicit input or output. This spontaneous brain activity is present at all timescales; as spontaneous neuronal firing measured by electrophysiology, and as slow, so-called resting-state, fluctuations in the BOLD signal measured by functional magnetic resonance imaging (fMRI). Spontaneous brain activity is the dominant component of the total activity of the brain; this is evident on the one hand in the large resting energy consumption of the brain, and on the other hand in the temporo-spatial coherence of spontaneous brain activity, which is only slightly altered by sensory input. This coherence is present on the small spatial scale of ocular dominance columns measured by optical imaging, as well as in functional networks that span the entire cortex and are measured by fMRI. The functional significance of spontaneous brain activity is unclear; it might encode dynamic predictions about forthcoming sensory events. It certainly influences perception and behaviour by increasing the neuronal and behavioural variability in evoked responses to perceptual stimuli. This is especially evident in bistable perception, where fluctuations in the internal state of the brain lead directly to fluctuations in visual awareness. Spontaneous fluctuations in brain activity act in concert with other factors such as endogenous attention in influencing these internal brain states.

1.7 Present thesis

This thesis explores the relationship between spontaneous and evoked brain activity from several angles and using a combination of several experimental techniques. In Chapter 2, the basic steps for measuring spontaneous activity are outlined for electrophysiology in awake monkeys and functional MRI in monkeys and humans. Chapter 3 examines the relationship between spontaneous and evoked activity from the point of view of energy expenditure. Using a computational approach, I calculate the amount of energy spent by the

brain on making a perceptual decision in relation to the amount of energy spent on spontaneous activity. In Chapter 4, I explore the nature of the spontaneous activity fluctuations commonly found in the BOLD signal using simultaneous fMRI and electrophysiological recordings in awake monkeys. Specifically, I investigate the spatial and temporal properties of the relationship between spontaneous BOLD fluctuations and their underlying neural fluctuations. In Chapter 5, I investigate the influence of spontaneous BOLD fluctuations in primary visual cortex on visual perception in an fMRI experiment in humans. Chapter 6 examines the influence of the brain's fluctuating internal state on visual awareness, using motion-induced blindness as a model system in another human fMRI experiment. In Chapter 7, I describe a behavioural experiment to investigate the influence of endogenous attention on these fluctuating brain states underlying motion-induced blindness. Finally, in Chapter 8, these results are placed in the broader context of the study of spontaneous brain activity. Taken together, these findings will hopefully convince the reader that the component of brain activity that lies beneath the surface, is worth investigating.

Chapter 2 Measuring Spontaneous Activity

2.1 Introduction

As mentioned in Chapter 1, a variety of methods are used for the experiments described in this thesis, including computational neuroscience, electrophysiology in awake monkeys, fMRI in monkeys and humans, and behavioural experiments. This chapter outlines the main methodological issues in recording and analysing spontaneous brain activity using electrophysiology, fMRI, and a combination of the two. First a quick overview of each method is given, after which issues specific to measuring spontaneous brain activity are highlighted.

2.2 Electrophysiology

2.2.1 Overview

In vivo electrophysiology involves inserting one or several electrodes into the brain of a living animal in order to detect electrical activity that is generated by neurons in the vicinity of the electrode tip. Electrodes are usually very fine wires made from tungsten or platinum-iridium alloys that are insulated except at their extreme tip. Depending on the size of the electrode tip, the activity of a single or multiple neurons may be recorded; these methods are called single-unit and multi-unit recordings respectively. In single-unit recording, the signal that is being detected consists of the voltages generated extracellularly when the neuron generates an action potential (see 1.2). Typically these voltages are ~0.1 mV in magnitude. The extracellular voltage changes follow the temporal profile of the action potential, i.e. when visually displayed, they have the characteristic shape of a spike. This shape helps in

isolating the neuron that is being recorded from, from nearby neurons that might display a different spike shape; a procedure called spike sorting.

Single-unit recordings are mainly conducted in the context of an experimental paradigm where the effect of the stimulus or task on the firing rate of a single neuron may be of interest. Before starting the experiment, single neurons need to be isolated. This is usually done by playing the neural signal detected by the electrode over a speaker and advancing the electrode through the brain while the animal is performing the task (Fig 2.1a). When the electrode tip enters grey matter, the speaker output sounds like white noise. A series of stimuli that are known to elicit a neuronal response, are shown once the electrode is suspected to be in the correct area. For example, a bar of light might be moved back and

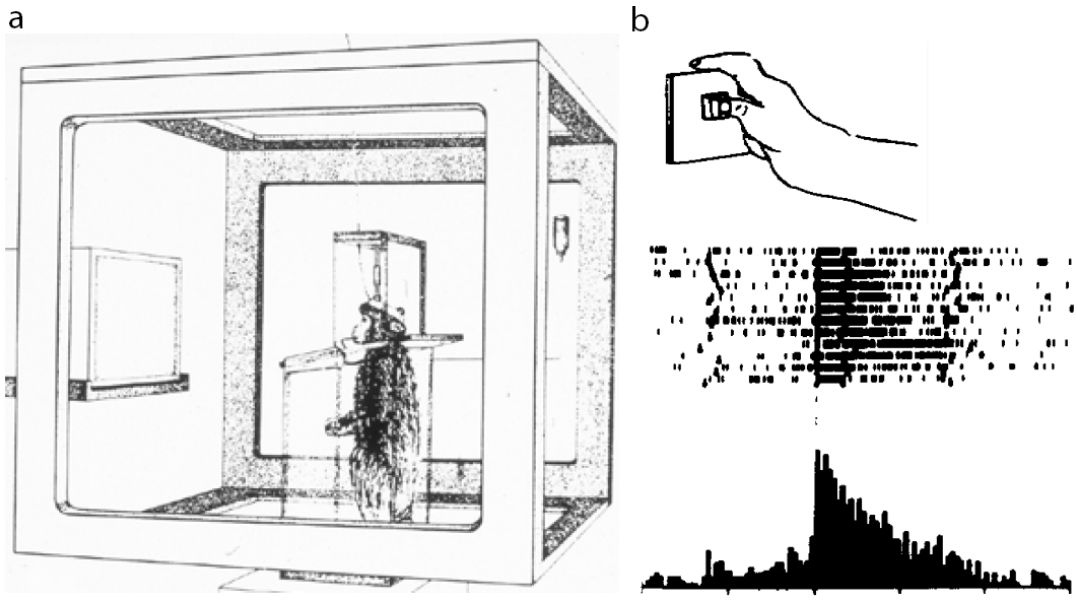

Figure 2.1 Electrophysiological recording in awake monkey. (a) *The monkey sits upright in a Faraday-shielded booth, which allows artefact-free recording of neuronal activity through an opening in the skull called a chamber. Meanwhile, the monkey looks at a screen on which stimuli can be displayed.* ***(b)*** *Example of a spike density histogram. Raster plots (middle) show the response of a typical M1 neuron to a grasping movement (top). Dots are individual spikes; lines are individual trials. Below is the spike density histogram showing the average response of this neuron to the grasping movement. Adapted from Jeannerod et al., 1995.*

forth in various orientations to find the region of visual field, preferred direction, and preferred speed of the local neuronal population. Once the correct area is found, the firing rate of cells within earshot will increase dramatically when the stimulus is presented and stop abruptly with cessation of the stimulus. Once the electrode tip is positioned near a single neuron, the experimental task may begin. During the experiment, the electrode is connected to an analog-to-digital converter which measures the electric potential difference (measured in Volts) between the electrode and a reference electrode. The signal is then amplified and recorded in a continuous manner using specifically designed software. Modern experimental techniques allow several or even a whole grid of electrodes to be inserted into the brain at once. Electrodes can also be permanently implanted into the brain, which reduces set-up time before each experiment dramatically. Analysis of single-unit data typically involves averaging the spikes elicited in response to the stimulus in a spike density histogram (Fig 2.1b). Averaging has the additional advantage of getting rid of any noise in the data, such as noise from the net frequency (50 Hz).

When looking at spontaneous activity of neurons, averaging cannot be done as spontaneous activity is a continuous signal not time-locked to any stimulus. To prevent noise in the signal, care should be taken that the recording booth is well shielded. Furthermore, spontaneous activity of single neurons depends strongly on the activity of neighbouring neurons (Fiser et al., 2004;Kenet et al., 2003;Tsodyks et al., 1999). Therefore multi-unit recording is a more appropriate method than single-unit recording for measuring spontaneous neuronal activity. The activity of multiple neurons that is detected in this way is called the local field potential.

2.2.2 Local field potential

The local field potential (LFP) is a measure of combined electrical activity within a volume of neural tissue (Mitzdorf, 1985). It reflects the aggregate electrical activity from neurons within 50-250 μm of the recording electrode (Katzner et al., 2009), as well as slower

ionic events from within 0.5-3 mm from the electrode tip (Juergens et al., 1999). The LFP signal is typically low-pass filtered at ~300 Hz, to filter out the quick fluctuations in extracellular potential that are caused by action potentials. The LFP is thus composed of the more sustained currents in the tissue. A major component of these slow currents is the postsynaptic potential (PSP), which is the change in membrane potential of the postsynaptic neuron induced by neurotransmitter binding (see 1.2). Excitatory (EPSPs) and inhibitory (IPSPs) postsynaptic potentials are the main constituents of the LFP signal (Mitzdorf, 1987).

Since postsynaptic potentials are generated in the dendrites of postsynaptic neurons and carry the incoming signal in this way, the LFP is believed to represent the synchronised input into an observed area, as opposed to spiking activity, which represents the output from the area. The LFP as a measure of input into an area is biased by the geometric configuration of the contributing neurons. Pyramidal cells have an open field geometrical arrangement where the dendrites face one direction and the somata another. Simultaneous activation of dendrites in these cells produces a stronger dipole than in cells with more radially arranged dendrites. Therefore the LFP is dominated by pyramidal cell activity (Logothetis, 2003).

2.2.3 Band-limited power

The many neuronal sources that contribute to the LFP signal turn it into a complex signal composed of fluctuations at many different frequencies. The contribution of these different frequency components may be assessed using a Fourier transform. Typically, the LFP signal is split into frequency bands according to classically defined electroencephalographic (EEG) conventions; the delta (2-5 Hz), theta (5-8 Hz), alpha (8-14 Hz), beta (14-25 Hz), and gamma (25-100 Hz) band. The frequencies above ~300 Hz are termed multi-unit activity (MUA) and are assumed to reflect spiking activity in the form of fast action potentials (Logothetis et al., 2001). MUA therefore reflects different synaptic processes than the LFP and is usually filtered out. The different frequencies are thought to be an index of various cognitive processes. Alpha band activity is mostly associated with drowsiness (Berger, 1929), whereas

synchronous gamma band activity is assumed to play an important role in anticipation and visual feature integration across different brain areas (Engel et al., 2001;Fries et al., 2001b).

Spontaneous brain activity is not only apparent in these fast fluctuations, it also fluctuates at a much slower timescale (Fox and Raichle, 2007;Monto et al., 2009). In order to effectively capture these slow fluctuations in the LFP signal, one can look at the band-limited power (BLP) signal. This is obtained by first splitting the LFP signal into frequency bands, and then rectifying these signals by taking their absolute value (Leopold et al., 2003) (Fig 2.2). The rectification step provides a measure of the time-varying envelope amplitude of each frequency band. The rectified signal can contain arbitrarily low frequencies, and is no longer a measure of voltage but rather power (or, more accurately, the square root of the power). It can therefore adequately represent arbitrarily slow fluctuations in spontaneous neural activity, as has indeed been shown (Leopold et al., 2003).

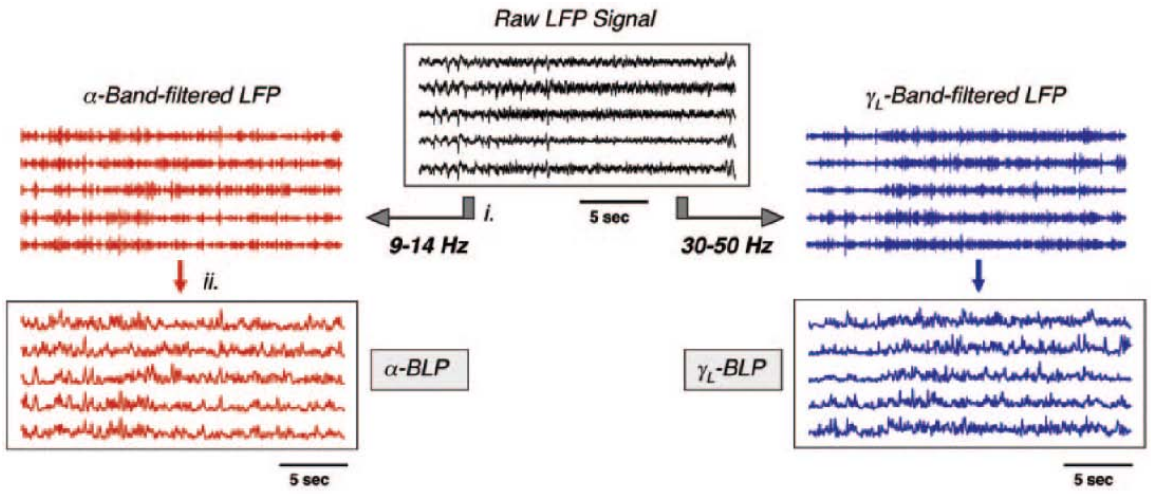

Figure 2.2 Band-limited power. *The raw LFP signal is split into several frequency bands; alpha (9-14 Hz) and low gamma activity (30-50 Hz) is shown here. Both signals are then rectified; this gives the band-limited power or BLP. Adapted from Leopold et al., 2003.*

2.2.4 Coherence

The combination of LFP and BLP can sufficiently represent the temporal properties of spontaneous neuronal activity over a large range of timescales (milliseconds to minutes). Spontaneous activity is manifest on various spatial scales too; the ongoing activity in a single neuron is highly dependent on the spontaneous activity of the surrounding network (Kenet et al., 2003;Tsodyks et al., 1999). The spatial extent of spontaneous activity can be investigated using multi-electrode arrays (Fiser et al., 2004;Leopold et al., 2003) and quantified using the measure of coherence.

Coherence detects common correlated components in two time-varying signals recorded from different locations (these can be LFP or BLP signals), and these values are presented as a function of frequency. If at a certain frequency band the coherence value is relatively high compared to other frequency bands, we can conclude that the two signals are synchronised at that frequency band (Zhan et al., 2009). Prestimulus synchronous activity, especially in the gamma band, is an important predictor of the evoked neuronal response to a visual stimulus (Fries et al., 2001b).

2.2.5 Summary

Electrophysiology in awake monkeys involves the recording of electrical activity generated by neurons around the measuring electrode. This can be either a single neuron (single-unit recording) or multiple neurons (multi-unit recording). Single-unit recording is often used in task-related experiments; multi-unit recording is the main method of choice for recording spontaneous activity. The signal measured by multi-unit recording is the local field potential (LFP), which is believed to represent the synchronised input into an observed area. Band-limited power and coherence are two concepts in the analysis of LFP data which provide useful tools for studying spontaneous neuronal activity.

2.3 Functional MRI

2.3.1 Overview

Magnetic resonance imaging (MRI) makes use of the magnetic properties of tissue to noninvasively map the structure and function of the brain (Kandel et al., 2000). Hydrogen atoms in brain tissue rotate around their axis, acting as small magnets with their own dipole. Normally, these hydrogen atoms are directed at random (Fig 2.3a), but when placed inside the strong magnetic field (B_0) that is present inside an MRI scanner, their axes become aligned (Fig 2.3b). A second magnetic field formed by a radio frequency pulse is then applied to the tissue and causes the hydrogen atoms to start wobbling around their axes. This wobbling is called precession. Precession creates a rotating magnetic field that changes in time, which generates an electric current. Ultimately it is this electric current that is measured in MRI. When the radio frequency pulse is turned off, the hydrogen atoms in the tissue relax. They fall out of synchrony with each other and their axes become aligned with the original magnetic field again (Fig 2.3c).

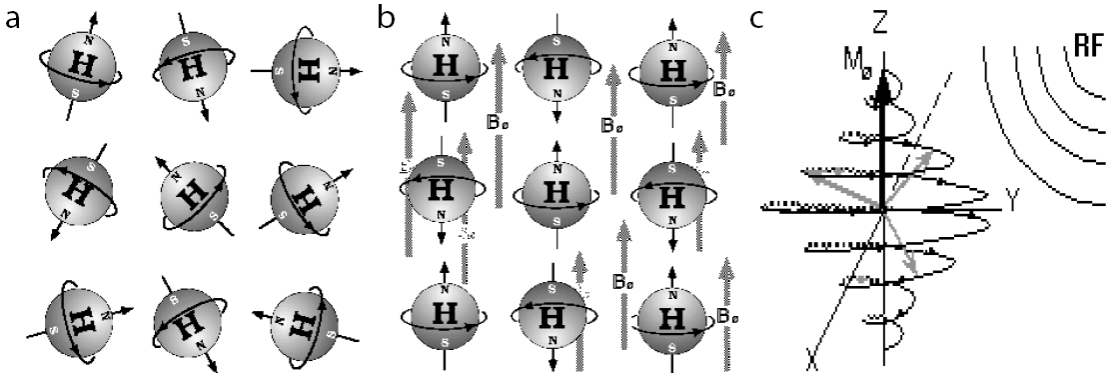

Figure 2.3 Basics of MRI. (a) *Hydrogen atoms spin around their own axes, acting like little magnets.* ***(b)*** *When a uniform magnetic field (B_0) is applied, all hydrogen atoms align their axes.* ***(c)*** *Subsequently applying a radiofrequency (RF) pulse causes the aligned atoms to precess about the Z axis (illustrated by the circles) and dephase with the other atoms about the x and y axes (not shown). Adapted from www.simplyphysics.com.*

MRI measures the rate of two relaxation processes, characterised by time constants T_1 and T_2. The relaxation component emphasised in the T_1 weighted image is the 'righting' of tipped hydrogen atoms as they realign with the original magnetic field. The rate of this relaxation is influenced by nonexcited molecules in the surrounding tissue. In a T_2 weighted image the falling out of synchrony or the 'dephasing' of rotating hydrogen atoms is emphasised. Dephasing results largely from loss of energy to spinning hydrogen atoms nearby. It can also result from local inhomogeneities in the magnetic field; this time constant is called T_2^* and is essentially what is measured in functional MRI. Hydrogen atoms have different T_1 and T_2 time constants depending on whether they are embedded in fat, cerebrospinal fluid, white matter, or grey matter.

In order to localise the location of the hydrogen atoms in the three-dimensional volume of the brain, magnetic gradients are applied alongside the radiofrequency pulses. These gradients are magnetic fields in which the strength of the field changes gradually along an axis. Applying gradients along three axes subdivides the tissue: one gradient is used to excite a single slice of the subject's brain, two more gradients subdivide that slice into rows and columns. This approach results in a single measurement from a cube of brain tissue called a voxel.

Functional MRI (fMRI) measures differences in magnetic properties related to neural activity. When neurons are activated, the supply of blood carrying oxygen and glucose to the active region increases. For reasons that are still unclear, the delivery of oxygenated haemoglobin to the region is greater than local oxygen consumption, resulting in a greater local proportion of oxygenated to deoxygenated haemoglobin. Oxygenated and deoxygenated haemoglobin have different magnetic properties. Deoxyhaemoglobin causes more dephasing than does oxyhaemoglobin, so a decrease in its concentration results in less dephasing and a stronger MRI signal. The ratio between oxyhaemoglobin and deoxyhaemoglobin as an index of brain activity is captured in the blood oxygen level dependent (BOLD) signal (see 2.3.2). Since the blood supply to an active brain region is slow, the BOLD signal typically peaks 6-8 seconds after the neuronal population in that

brain region has become active; that is, it has a low temporal resolution. The spatial resolution of the BOLD signal is confined to the size of the voxels; typically 3x3x3 mm in a functional scan, and the point spread function (the amount of 'blurring') of the haemodynamic response.

A typical fMRI experiment administers a certain task or stimulus (such as moving dots) to the subject and measures the resulting changes in BOLD signal and behaviour. Typically, the task consists of several conditions (e.g. moving dots and static dots), which are designed only to differ in the parameter of interest (movement). By comparing the BOLD signal induced by these conditions to each other, the modulation of the BOLD signal attributable to the experimental parameter of interest can be extracted (e.g. a modulation of the BOLD signal in V5/MT). This approach allows one to relate brain topography to function (e.g. V5/MT is responsive to movement).

2.3.2 The BOLD response

The BOLD response that is evoked by a task or stimulus has a typical shape (Fig 2.4). The main response is positive and peaks at 6-8 seconds after stimulus onset. Ahead of this positive response, the signal commonly displays an initial small, negative dip. This initial dip occurs within 1-2 seconds of stimulus onset and is thought to be more highly localized than the main BOLD response (Shtoyerman et al., 2000). Use of this more localized negative BOLD signal has enabled imaging of human ocular dominance columns in primary visual cortex with resolution of about 0.5 mm (Yacoub et al., 2008). The BOLD response is usually followed by a second negative dip termed the poststimulus undershoot (Chen and Pike, 2009). The neuronal mechanisms underlying the changes in oxygen concentration that result in this typical shape of the BOLD response remain incompletely understood, and the precise mechanisms behind neurovascular coupling (i.e. the dependency of the vascular response on changes in neuronal activity) are a matter of intense debate.

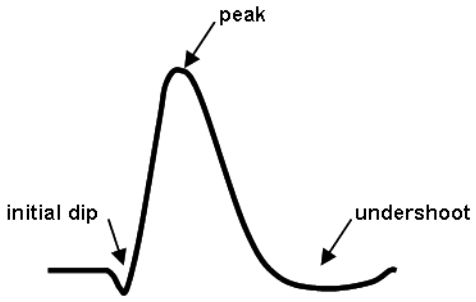

Figure 2.4 The BOLD response. *The initial dip, peak, and undershoot are shown.*

A key player in the coupling between neurons and blood flow is the excitatory neurotransmitter glutamate (see 1.2), which, upon binding to postsynaptic receptors, causes a calcium flux into the neuron which activates nitric oxide synthase and triggers the production of nitric oxide. The nitric oxide diffuses out and dilates smooth muscle surrounding local arterioles, allowing more blood flow to the area (Stefanovich et al., 2007). Glutamate also activates receptors on astrocytes which leads to arachidonic acid production and the release of vasodilatory prostaglandins (Takano et al., 2006). Vasodilation allows for increased blood flow to the active brain region. As the positive peak of the BOLD signal shows, this blood carries more oxygen to the neurons than is consumed. One proposed theory to explain this mismatch between oxygen supply and oxygen consumption is that increases in brain activity are supported by glycolysis (non-oxidative glucose metabolism) (Fox et al., 1988). Thus, the cellular mechanisms and key molecules that link neuronal activity to increased oxygen supply are beginning to be unravelled.

Another approach to studying neurovascular coupling is to correlate the BOLD signal to electrophysiological measures such as multi-unit activity (MUA) and local field potential (LFP). A comparison of single unit data from monkey V5/MT with human fMRI measurements from V5/MT showed that both neuronal firing and BOLD responses increased linearly with increasing motion coherence (Rees et al., 2000). This implies that the BOLD response is well correlated to neuronal spiking. However, subsequent simultaneous electrophysiology – fMRI measurements showed that the BOLD signal is slightly more correlated to the LFP than to the spiking activity in an area, suggesting that the BOLD signal

reflects the input and intracortical processing of a given area slightly better than its spiking output (Logothetis et al., 2001). Both the shape of the BOLD response as well as its relationship to the underlying neuronal activity will be examined in Chapter 4, Neural Basis of Resting-State fMRI Fluctuations.

2.3.3 Data collection

Spontaneous brain activity refers to any component of brain activity that is not attributable to a specific task or stimulus. As such, fMRI studies of spontaneous activity attempt to minimise changes in sensory input. This is achieved by either instructing subjects to fixate on a cross-hair, or to close their eyes and refrain from falling asleep. Ideally, the scanner room is completely dark. Usually, resting-state data are collected for ~5 minutes, using standard scanning parameters for the TR, TE, slice thickness, field of view, and matrix size. In addition, alongside BOLD data acquisition usually data on heart rate and respiration are collected using a breathing belt and pulse oximeter, since these variables can account for a significant fraction of the variance in the resting-state signal (see 1.4.5).

2.3.4 Noise correction

An important difference between task-related fMRI studies and fMRI studies of spontaneous activity is that the former usually involve averaging across many trials. This averaging eliminates noise caused by artefacts such as scanner instability and changes in heart rate and respiration. Since resting-state activity cannot be averaged, a natural concern is that the observed fluctuations are contaminated by or even due to artefacts. Consistent with this concern, spontaneous BOLD fluctuations have been measured in a water phantom (Zarahn et al., 1997).

Artefacts that can contribute to observed fluctuations in the BOLD signal can be instrumental or physiologic in origin. The relative contribution of these artefacts to resting-state BOLD data has been determined (Bianciardi et al., 2009b). In an individual voxel,

thermal noise caused by the scanning environment is a large contributor to the fluctuations in its time course. Fortunately thermal noise is essentially uncorrelated between voxels and cancels out completely when the signal is averaged over multiple voxels. Low-frequency drifts due to scanner instability are another significant source of fMRI signal fluctuations (34.7%), followed by variations in respiration rate (8.6%) and cardiac pulsation (6.6%) (Bianciardi et al., 2009b). This leaves 50.1% of the fluctuations in the resting-state fMRI signal to be attributed to underlying neuronal activity, i.e. the spontaneous fluctuations which are of interest. These measurements were performed at 7T and may slightly differ for measurements done at 3T.

Low-frequency drifts in the signal might be caused by slow changes in head position, baseline physiology, and instrumental conditions such as slow drifts in gain and resonance frequency (Bianciardi et al., 2009b). Spontaneous BOLD fluctuations follow a 1/f distribution, meaning that there is increasing power at lower frequencies (Fox and Raichle, 2007). Much of the lowest frequencies, and therefore also the most power, present in the spontaneous fluctuations can be accounted for by these low-frequency drifts. Usually they are removed simply by high-pass filtering at 0.01 Hz (Biswal et al., 1995). Since frequencies above 0.1 Hz mainly relate to cardiac and respiratory factors (Cordes et al., 2001), the majority of spontaneous BOLD studies also low-pass filter the data at 0.1 Hz. This leaves a signal consisting of frequencies between 0.01–0.1 Hz and spontaneous fluctuations within this frequency range are indeed the ones in which functional networks have been observed (Cordes et al., 2001).

Noise components related to changes in physiological variables, i.e. heart rate and respiration rate, are the most difficult to characterise in terms of both their number and their dynamics. They are commonly modelled using a correction method called RETROICOR (Glover et al., 2000). This method incorporates eight regressors into the design; four for fluctuations occurring at the frequency of the respiration and cardiac cycles (2 sines and 2 cosines), and four for fluctuations at twice that frequency (again 2 sines and 2 cosines). Alternatively, the respiration volume per unit time (RVT) may be estimated for each subject

individually during a cued-breathing condition, which may then be modelled as a separate regressor (Birn et al., 2006). Additional regressors may be the cardiac rate shifted at various time lags with respect to the BOLD signal (Shmueli et al., 2007). Finally, the time course from a region that is likely to have a high degree of physiological artefact relative to the amount of neuronal activity, such as the ventricles, might be included as another regressor of no interest (Fox et al., 2005;Rombouts et al., 2003).

In addition to low- and high-pass filtering and physiological noise correction, data are preprocessed just like in any other fMRI study. Thus, preprocessing of spontaneous BOLD data typically includes realignment of all scans, coregistration to a structural scan or normalisation to a template brain, smoothing, temporal filtering, and correcting for head movement and physiological noise by modelling them as regressors.

2.3.5 Global signal removal

The final preprocessing step that is routinely employed by fMRI resting-state studies, is removal of the spontaneous BOLD fluctuations common to the whole brain, the so-called global signal (Fox et al., 2005;Macey et al., 2004). This can be done either by including the global signal as a linear regressor or by multiplicative scaling, which forces the mean BOLD signal across the whole brain to the same in every scan (Fox et al., 2009). The latter approach is essentially the same as proportional scaling, which is commonly used in task-related studies to remove both intersession (session-to-session) and intrasession (scan-to-scan) variance in the global signal (Gavrilescu et al., 2002). The assumption underlying global signal removal is that these common BOLD fluctuations are caused by physiological (i.e. non-neuronal) factors, and global signal removal has indeed been shown to facilitate the extraction of functional networks from the data (Fox et al., 2009). These functional networks commonly comprise regions with similar functional properties that are positively correlated at rest (Biswal et al., 1995;Cordes et al., 2000). In addition to positive correlations, also negative correlations have been reported. Specifically, negative correlations have been

observed between two sets of regions, one exhibiting activity *increases* during attention demanding tasks, and the other exhibiting activity *decreases* during the same tasks (the so-called default mode network) (Fox et al., 2005). These anticorrelations have been taken as evidence that certain differences between brain regions are an intrinsic feature of the brain's organisation (Fox et al., 2005).

However, the interpretation of observed anticorrelations in resting-state BOLD data is less straightforward than originally thought (Fox et al., 2009). Specifically, the effect of global signal removal on these anticorrelated networks has been called into question (Murphy et al., 2009). In task-related studies, global normalisation of the brain activity level can introduce artefactual deactivations in the data (Aguirre et al., 1998a;Gavrilescu et al., 2002). Similarly, global signal removal forces the distribution of correlation values across the whole brain to be centred on zero. Therefore, global signal removal mandates the observation of negative correlations (Fox et al., 2009). Along these lines, simulations have shown that small phase differences between regions can lead to spurious negative correlation values (Murphy et al., 2009). A concern is, therefore, that the observed anticorrelations (Fox et al., 2005) are not actually present in the data, but merely an artefact caused by global signal removal.

However, further investigations into the nature of the global signal have shown that it is indeed global, and not residing preferentially in systems exhibiting anticorrelations. Furthermore, global signal removal leads to an improvement of the correspondence between resting-state correlations and structural connectivity (Fox et al., 2009). Taken together, these findings suggest that global signal removal is a valid preprocessing step, but must be taken with caution, especially when anticorrelations are subsequently observed.

2.3.6 Extracting functional networks

Once the data have been preprocessed, further analysis depends on the type of question that is being addressed. Studies investigating the effect of spontaneous BOLD fluctuations

on behaviour typically focus on one particular brain area (Fox et al., 2006b;Hesselmann et al., 2008a). For extracting functional networks from resting-state data, several methods are commonly used. The simplest technique is to extract the BOLD time course from a voxel or a region of interest and to determine the temporal correlation between this extracted signal and the time course of all other voxels in the brain (Fox and Raichle, 2007). This approach is called the 'seed voxel' or the 'seed region' approach (Fig 2.5) and is widely used owing to its inherent simplicity and ease of interpretation (Biswal et al., 1995;Cordes et al., 2000;Fox et al., 2006b;Fransson, 2005;Hampson et al., 2002;Vincent et al., 2007). However, it has some disadvantages. The results are dependent on the *a priori* choice of the seed region, and multiple systems cannot be studied simultaneously. In response to these limitations, other techniques for extracting functional networks have been proposed.

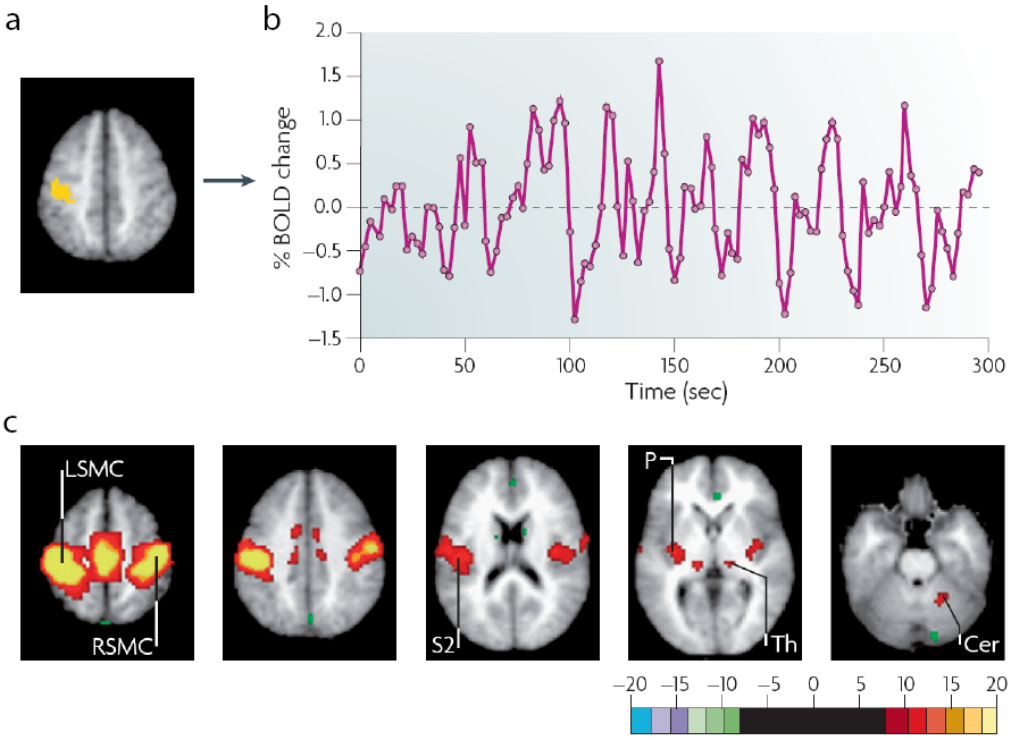

Figure 2.5 Seed-region approach. ***(a)*** *Seed region in the left somatomotor cortex (LSMC).* ***(b)*** *Time course of spontaneous BOLD fluctuations in the seed region acquired during rest.* ***(c)*** *Statistical z-score maps showing voxels that are significantly correlated with the extracted time course. RSMC, right somatomotor cortex, S2, secondary somatosensory cortex, P, putamen, Th, thalamus, Cer, cerebellum. Adapted from Fox and Raichle, 2007.*

Independent component analysis (ICA) has proven to be another popular method for analysing spontaneous BOLD data (Beckmann et al., 2005;Kiviniemi et al., 2003;Van de Ven et al., 2004). A fully automated algorithm decomposes the entire BOLD data set into components that are maximally independent in a statistical sense. Each component is associated with a spatial map that reveals how much of the data in each voxel can be explained by that particular component. Some maps reflect noise components, while others reflect functional networks. The advantages of this approach are that it is entirely data driven and that it automatically isolates noise components. However, the interpretation of these maps is not automated, introducing a potential source of bias into the method. Furthermore, the maps are highly dependent on the number of components the algorithm is instructed to produce. Combining the seed region and the ICA approach (Seeley et al., 2007) can provide converging evidence for the existence of certain functional networks and increase confidence in the results.

2.3.7 Improving task-related analysis

Task-related fMRI studies typically discard spontaneous fluctuations in the BOLD signal by averaging over many trials; those studies that do take spontaneous BOLD fluctuations into account typically have those fluctuations as their focus of study. An interesting alternative approach has been taken in a number of studies seeking to improve the signal to noise ratio (SNR) of task-related designs by using spontaneous activity (Bianciardi et al., 2009c;De Zwart et al., 2008). Spontaneous BOLD fluctuations compromise the detection of stimulus-evoked responses and as such can be viewed as noise. In this approach, an initial estimate of the brain region activated by the stimulus or task is obtained using conventional statistical analysis. By collecting a short (1-2 min) resting-state reference scan, the spontaneous BOLD fluctuations can be measured in this estimate of the active region and correlated with all other regions of the brain. A significantly correlated region is then taken as a reference region and the spontaneous fluctuations present in this reference region are

incorporated as a regressor of no interest in the actual analysis of the data (De Zwart et al., 2008). This approach is similar to that of Fox and colleagues (2006b). Correcting for spontaneous fluctuations in this way improved the average t-score of the activated voxels by 11.3% and led to a 24.2% increase in size of the activated brain area (De Zwart et al., 2008). When principal component analysis (PCA) is used on the spontaneous fluctuations in the reference region to derive multiple regressors of no interest, the improvement is even substantially higher (Bianciardi et al., 2009c).

2.3.8 Summary

In summary, the basics of measuring spontaneous fluctuations using fMRI, including the physics underlying the BOLD signal and data collection, are the same as in any task-related fMRI study. Special attention should be paid to noise correction, as no averaging across trials is done. Low frequency scanner drifts are typically removed by high-pass filtering; variance due to changes in heart rate and respiration is removed by including them and their harmonics as regressors of no interest into the design. The global signal common to all brain voxels can also be removed, though this should be done with caution. Once the data are preprocessed, functional networks can be extracted using either the seed region approach or ICA. In task-related experiments, the spontaneous fluctuations themselves might be modelled as a regressor of no interest to improve SNR.

2.4 Simultaneous fMRI and electrophysiology

2.4.1 Overview

Both electrophysiology and functional MRI have their limitations. FMRI provides whole brain coverage, but at the expense of temporal resolution, while *in vivo* electrophysiology has excellent temporal resolution, but allows data collection only at a very local scale.

Combining these two techniques can thus yield insights beyond those obtained by each technique individually. Electrophysiology in awake monkeys within the MRI scanner was first used to investigate the neural basis of the evoked BOLD response (Logothetis et al., 2001). Now this combined technique is starting to be applied successfully to the study of spontaneous activity (Shmuel and Leopold, 2008), although it remains technically very challenging.

2.4.2 Data collection

Several issues should be addressed when applying neurophysiological techniques in the context of magnetic resonance imaging. All equipment should be MR compatible; this includes LFP electrodes made of platinum-iridium and coated with glass (Logothetis et al., 2001) as well as MR compatible holders to hold the electrodes in place. Acquiring MRI data involves applying RF gradients to the brain (see 2.3.1); these fast switches in the magnetic field induce a large artefact in the electrophysiological signal. Removal of this artefact is the prime hurdle in simultaneous fMRI-electrophysiology. Ideally, the signal is amplified and digitised within the scanner bore before leaving the scanning room through optical fibres (Allen et al., 2000). The (MR compatible) amplifier should allow sampling of the electrophysiological signal at high temporal rate and within a large amplitude range, since the RF gradient artefact contains high frequency and large amplitude components, and the signal should not be clipped for artefact correction (see 2.4.3) to work (Laufs et al., 2008). In order to aid artefact removal even more, electrophysiological sampling should be synchronised with the MR sequence.

The primary safety risk to the monkey is heating arising from interaction of the radiofrequency (RF) fields with the electrophysiology equipment. Maximum heating will occur when a conductor is resonant at the frequency of the RF gradient. This can occur in a single wire and cause dangerous heating in tissue, especially at the end of the wire (Konings et al., 2000). For simultaneous LFP-fMRI recordings, this means heating of the neuronal

tissue directly. Heating can be prevented by minimising the length of wires, avoiding loops in the wires, and, where possible, the use of optical cables.

2.4.3 Artefact correction

The artefact induced by the switching of the RF gradients is dependent on a combination of factors including the field strength of the scanner, the orientation of the gradients, wire vibration, and the positioning of recording equipment relative to the RF coil (Laufs et al., 2008). Despite completely obscuring the electrophysiological signal, in principle it is easy to remove, owing to its periodicity and stable shape. The most common method for artefact correction is to create a template of the artefact, that can then be subtracted from the data, allowing the biological signal to be recovered (Allen et al., 2000;Laufs et al., 2008) (Fig 2.6). The artefact can also be removed using principal component analysis to determine the artefact shape (Niazy et al., 2005). A rather different approach is the 'stepping stone' technique, which entails avoiding sampling the electrophysiological signal during periods of gradient switching in the MRI pulse sequence altogether, and limiting sampling to periods without gradient switching (Anami et al., 2003). This places constraints on both the electrophysiology and fMRI data acquisition – the electrophysiology data are not continuous, and a sparse scanning sequence (i.e. one with a 'gap' between successive volume acquisitions) has to be used. However, this can be the only option available if the gradient artefact saturates the amplifier and the shape of the artefact cannot be determined.

2.4.4 LFP predicting fMRI

Simultaneous electrophysiological (EEG or LFP) and fMRI data are commonly collected with one of two purposes in mind. First, fMRI can be used to determine the source of the electrophysiological signal. This concerns EEG data for obvious reasons, and is important for the localisation of epileptiform activity (Laufs and Duncan, 2007).

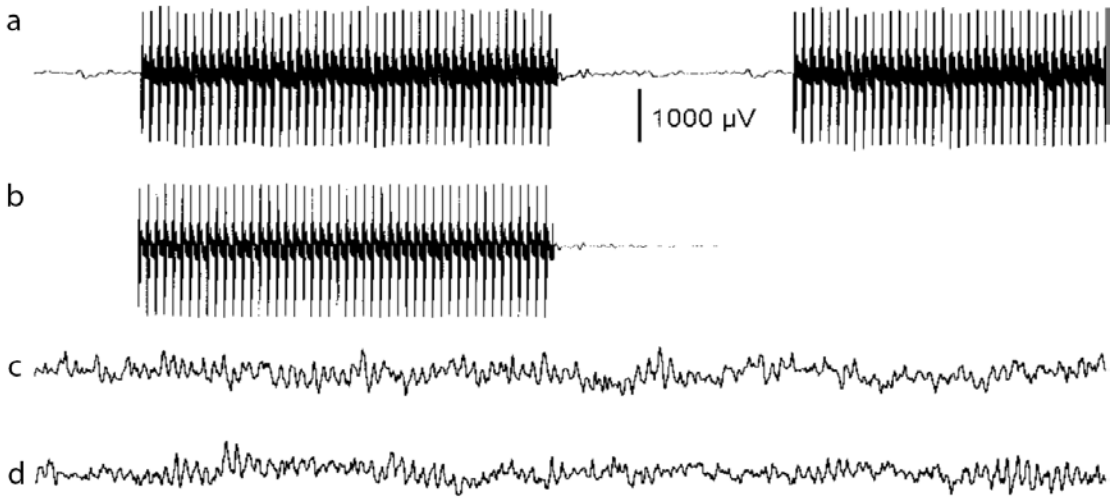

Figure 2.6 Artefact correction of electrophysiology data. ***(a)*** *Raw electrophysiology signal contaminated by the scanner artefact.* ***(b)*** *The isolated artefact template.* ***(c)*** *Electrophysiology signal after the artefact has been subtracted.* ***(d)*** *Raw electrophysiology signal of the same subject recorded outside the scanner. Adapted from Allen et al., 2000.*

Second, the electrophysiology and fMRI data can be used to investigate the various functional states of the brain. This is especially interesting in the context of spontaneous fMRI fluctuations, which have been shown to persist across several behavioural states (Horovitz et al., 2008;Vincent et al., 2007). More specifically, electrophysiological data can be used to predict variance in the fMRI data, by including them as regressors into a design matrix. For example, sleep spindles identified in EEG data are used to define events in fMRI analysis (Laufs et al., 2007). Generally, this approach is based on transforming the electrophysiological data into a set of regressors for the fMRI data, using sophisticated forward biophysical models which involve convolving the EEG data with a standard haemodynamic response function (HRF) (Salek-Haddadi et al., 2003).

An easier and more assumption-free method to predict the fMRI signal from the electrophysiological (LFP) data is to artificially shift the two signals with respect to each other. This is the approach that has been taken in this thesis (see 4.2.9). The BOLD response is typically sluggish, peaking at a lag of 6-8 seconds (Aguirre et al., 1998b). In order to

assess temporal precedence of the LFP signal, this signal may be shifted forward in time. If fluctuations in the LFP and the fMRI signal have the same underlying origin and therefore follow a similar time course, but the fMRI time course is delayed in time, one would expect to observe the highest correlation between these two signals when the LFP signal is shifted forward in time by 6-8 seconds. This is indeed what was found in visual cortex (Shmuel and Leopold, 2008).

The temporal relationship between the LFP and the fMRI signal might be assessed using this 'artificial time shifting' approach. The spatial relationship between the two signals can be assessed by correlating the LFP signal with the time course of all the voxels in the brain, another analysis method employed in this thesis (see 4.2.9). This approach is reminiscent of the seed region approach to extract functional networks from resting-state fMRI data (see 2.3.5).

2.4.5 Summary

The marriage of two very different techniques for recording brain activity, electrophysiology and fMRI, is promising because of the new insights it can give us into spontaneous brain activity and brain function more generally. However, this approach is not without problems. The main concern during data collection is subject safety; the main concern during data analysis is correction of the artefact induced by switching of the RF gradients. Artefact correction can be done by using a template of the artefact or by avoiding the artefact altogether. Simultaneous electrophysiology – fMRI data have mainly been used in the study of epilepsy and in the study of the influence of behavioural states on brain activity. The main focus of the latter is the causal influence of the electrophysiological signal on the fMRI signal, which can be most easily assessed by temporally shifting the two signals with respect to each other.

2.5 Conclusions

Electrophysiology, functional MRI, as well as the two in concert, have all proven to be useful methods for the study of spontaneous brain activity. In electrophysiology, spontaneous brain activity is most effectively captured in the LFP signal as measured by multi-unit recording. In order to study the LFP signal at a timescale accessible to fMRI, it can be converted to the measures of band-limited power (BLP) and coherence. The BLP signal can then be correlated to fMRI measurements collected simultaneously and artificially shifted in time to assess its predictive value. It can also be used as a seed region, which together with ICA is the most common method to extract functional networks out of fMRI data.

A large concern in all methods is noise correction, as spontaneous brain activity is a continuous signal and inherently cannot be averaged. In electrophysiology, noise correction is done at the data collection stage by ensuring that the recordings are done in a properly shielded electrophysiology booth. In fMRI, scanner drifts, physiological noise (changes in heart rate and respiration), and sometimes the global signal common to the entire brain, are removed. In simultaneous fMRI and electrophysiology, the artefact caused by scanner gradient switching should be removed.

The following five experimental chapters will show how these techniques, in combination with computational neuroscience and behavioural experiments, have been employed in the study of several aspects of spontaneous brain activity.

Chapter 3 Cortical Energy Needed for Conscious Perception

3.1 Introduction

As mentioned in Chapter 1, General Introduction, the brain requires a large amount of energy to power its spontaneous activity. This large energy consumption at rest is remarkable, given that there is a finite amount of oxygen and glucose available in the body; the brain is therefore a metabolically expensive organ. Because neuronal activity is so highly energy demanding, glucose and oxygen are distributed to the brain areas that need them most by increasing blood flow in regions where neurons are active. This regional neuronal activity, over and above the spontaneous activity, is typically evoked by an external task or stimulus.

To date, it has remained unclear how much evoked neuronal activity, and hence, cortical energy use, underlies these increases in blood flow. Traditional analyses of sensory systems assume that external stimuli evoke action potentials in neurons that have receptive fields tuned to particular features of the stimuli (Hubel and Wiesel, 1998): in this view, spontaneous neuronal activity merely provides a 'noise' background against which a signal representing sensory input must be detected (Barlow, 1957), and sensory input should greatly increase cortical energy use. Recently, however, it has been suggested that incoming sensory information produces only small changes to the ongoing dynamic pattern of activity in cortical neurons (Arieli et al., 1996;Fiser et al., 2004), implying that sensory input alters cortical energy use only slightly.

The blood flow increase associated with increased neuronal energy use is the basis of functional imaging techniques such as positron emission tomography (PET) and blood oxygen level dependent functional magnetic resonance imaging (BOLD fMRI). Increases in energy expenditure due to an external stimulus or task are thus directly relevant for these

techniques; large increases in energy consumption will result in robust increases in blood flow that are easily detectable by functional imaging, while small increases in energy usage may go unnoticed. However, blood flow measurements cannot be used to calculate the energy usage supporting a cognitive task, because blood flow increases are generated by a variety of neurotransmitter-mediated mechanisms (Drake and Iadecola, 2006) rather than being driven directly by energy use. In brief, glutamate released by neural activity activates a calcium flux into neurons which activates nitric oxide synthase leading to release of the vasodilator nitric oxide (Faraci and Breese, 1993), and also activates metabotropic glutamate receptors on astrocytes which leads to arachidonic acid production by phospholipase A2 and ultimately to the release of vasodilatory prostaglandins (Zonta et al., 2003). Furthermore, there may be complex changes in the fraction of energy provided by glycolysis and oxidative phosphorylation during and after neural activity (Fox et al., 1988;Gjedde et al., 2009;Kasischke et al., 2004). In addition to this, the blood flow response following neural activation occurs over a volume significantly larger than that of the activated neural tissue (Malonek and Grinvald, 1996).

In order to calculate the energy usage associated with evoked brain activity, we therefore turned to electrophysiological measurements. We estimated, from electrophysiological data in primates, the local cortical energy use associated with conscious perception of a stimulus property in three different sensory modalities: vision, touch, and hearing (Fig 3.1). We adopted a philosophy similar to that in many functional imaging experiments, by comparing the energy use powering neural responses to two types of stimuli which differ only in the conscious perception of a particular stimulus attribute, such as motion coherence or colour (McKeefry et al., 1997;McKeefry and Zeki, 1997;Phillips et al., 1997). Because of the importance of conscious perception for determining behaviour, one might expect that the perception of a stimulus attribute would be associated with a set of neurons increasing their firing robustly. However our results show that, although the unconscious representation of information from which a percept is derived can involve a large increase in neural firing rate, conscious perception, i.e. the change from not being able to distinguish two stimuli to

perceiving them as different, is associated with a surprisingly small change in mean neuronal firing rate and energy consumption.

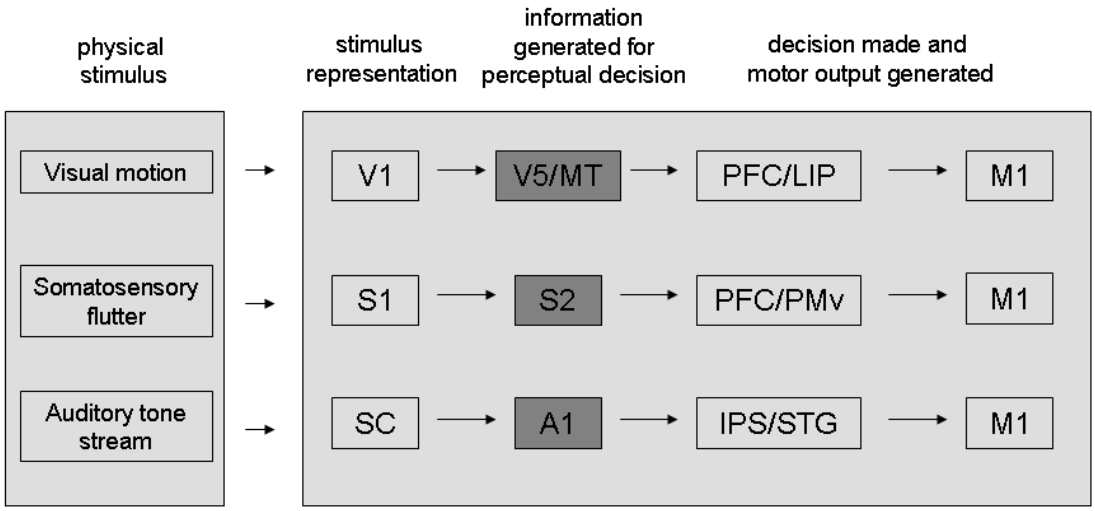

Figure 3.1 Brain regions involved in the perceptual tasks*. Incoming stimuli (left) are represented as neural firing in areas such as V1, S1 and SC. Areas V5/MT, S2 and A1 are the first areas where firing rate provides enough information allowing a decision on the presence of a percept of visual movement, altered skin vibration ('flutter') frequency or the grouping of sounds ('tone stream segregation'). Subsequent areas may make the perceptual decision and generate motor output (note that although we show a pure feedforward flow of information, in reality there are also reverse interactions between different areas which probably contribute to the perceptual decision). V1, primary visual cortex; S1, primary somatosensory cortex; SC, superior colliculus; V5/MT, middle temporal area; S2, secondary somatosensory cortex; A1, primary auditory cortex; PFC, prefrontal cortex; LIP, lateral intraparietal area; PMv, ventral premotor area; IPS, intraparietal sulcus; STG, superior temporal gyrus; M1, primary motor cortex.*

3.2 Materials and Methods

3.2.1 Overview of approach

We identified tasks that have been studied psychophysically and electrophysiologically in monkeys, as well as psychophysically and by functional imaging in humans. These tasks were detection of movement of random dot stimuli (Fig 3.2a), detection of flutter vibration applied to the skin (Fig 3.2b), and detection of auditory tone stream segregation (Fig 3.2c), and are described in detail in subsequent sections. Electrophysiological single unit data from monkeys were used to evaluate the change in mean neuronal firing rate occurring in cortical areas which are associated with the detection of visual motion, skin vibration frequency or sound frequency (Fig 3.1). This change in firing rate was then converted into an estimated fractional change of energy use in that area, using an energy budget for the cerebral cortex (Attwell and Laughlin, 2001) which predicts the energy consumed on different subcellular processes underlying neural information processing. For each task (and associated brain area) considered, the aim was to evaluate the change in action potential firing, and hence the extra energy needed, for perception, above that needed merely to represent stimuli which do not produce a conscious percept, since this is the change in energy consumption between brain activation states that are commonly compared in functional imaging experiments (McKeefry et al., 1997;McKeefry and Zeki, 1997;Phillips et al., 1997).

In the first three sections below, we assess the change in firing rate of cortical pyramidal cells in the three cortical areas when a stimulus is at the threshold of conscious perception for the perceptual tasks considered. This is followed by an explanation of how we converted changes in pyramidal cell firing rate into changes of cortical energy use, and an assessment of the change in firing rate and energy use for perception of reliably detected stimuli (i.e. stimuli that are well above threshold).

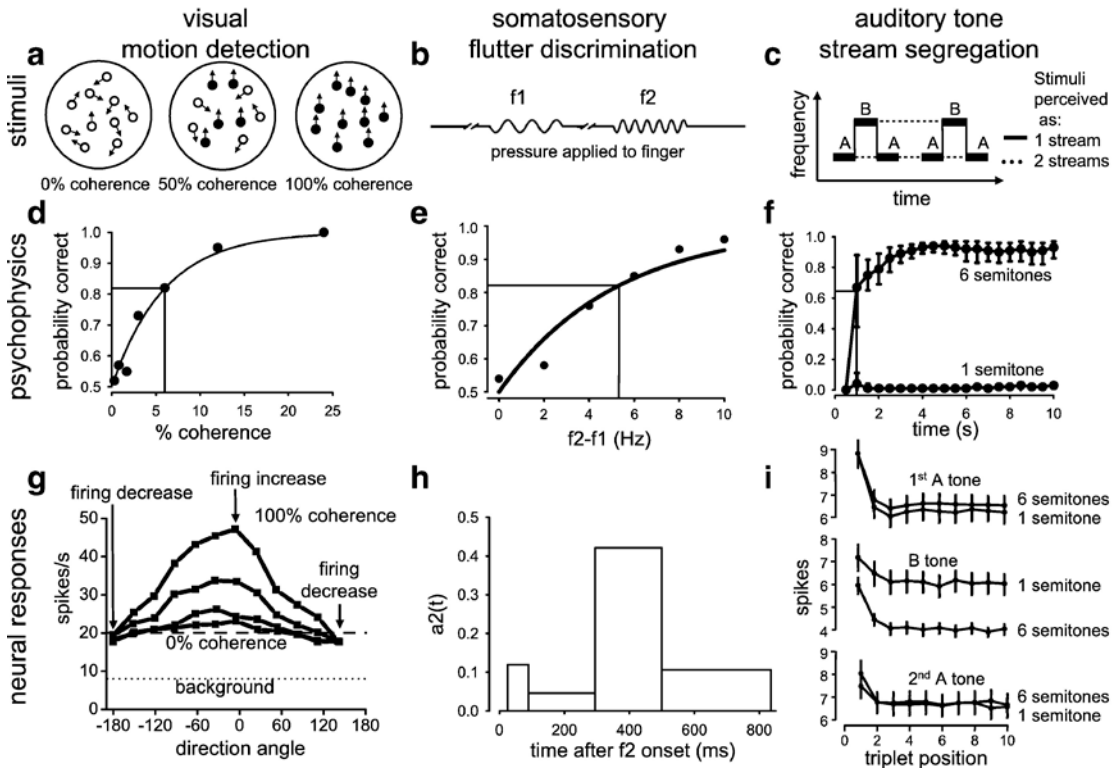

Figure 3.2 Perceptual tasks, psychophysical responses, and cellular responses*. **(a-c)** Stimulus schemata for the three tasks considered. **(a)** Three different levels of coherence in the visual motion task. At 0% coherence, all dots move randomly. As coherence increases, more dots move in a coherent fashion in one direction (black symbols) while the others move randomly. **(b)** Somatosensory task, showing a frequency discrimination trial where the second stimulus (f2) has a higher frequency than the first stimulus (f1). **(c)** Auditory percepts during stream segregation. The stimuli (repeating triplets of different frequency tones, ABA) are perceived as a single stream of connected tones (solid lines) or as two monotonic streams playing in parallel (dashed lines). **(d-f)** Psychometric curves for visual motion (**d**), somatosensory (**e**), and auditory (**f**) tasks. Black lines indicate threshold values for perception of random dot coherence, difference in flutter frequency (f1-f2), and time for build-up of auditory stream segregation. **(g-i)** Neuronal responses evoked by the tasks. **(g)** Direction tuning functions for a V5/MT neuron at increasing motion coherences (bottom to top). For stimuli close to the preferred direction, increased coherence increases firing, but as the orientation approaches the opposite direction, the rate decreases below the rate with a 0% coherence signal (arrows). **(h)** Average firing rate parameter a2 (see 3.2.3) for S2 neurons during f2 presentation. The dependence of the firing rate on f2 changes over time. **(i)** Spike counts evoked in A1 neurons with best frequency A, by the A and B tones in repeating ABA triplets.*

3.2.2 Detection of visual motion

For the visual modality, we analysed detection of movement in random dot visual stimuli, which has been studied psychophysically and electrophysiologically at the single unit level in monkeys (Britten et al., 1992;Britten et al., 1993), as well as psychophysically (Britten et al., 1992) and by fMRI (Rees et al., 2000) in humans. An array of moving dot stimuli is presented (Fig 3.2a), with the dot intensity well above the threshold for visibility, in which a certain percentage (X) of dots move in the same direction (termed X% coherence), and the observer has to decide what the general direction of motion is. A neural substrate contributing to this decision is likely to be the middle temporal visual area (V5/MT). This is the first area on the visual pathway in which the responses of most monkey neurons (up to 97%) are directionally selective (Van Essen et al., 1981), and is activated when humans view moving stimuli (Zeki et al., 1991). The sensitivity of monkey V5/MT neurons to such stimuli correlates well with the monkeys' psychometric function relating performance to coherence of the motion signal (Britten et al., 1992) (Fig 3.2d). Furthermore, the psychophysical performance of human observers on this task is similar to that of monkeys (Britten et al., 1992), supporting extrapolation from the monkey neuronal firing data to the human cortex. From area V5/MT, information is passed to the prefrontal cortex or lateral intraparietal area, and a behavioural decision based on the perceived motion is made (Huk and Shadlen, 2005;Kim and Shadlen, 1999) (Fig 3.1).

To calculate the energy needed to support the perception of motion in area V5/MT, we need to know the action potential rate of the cells analysing the motion. Monkey V5/MT neurons have a firing rate of ~8 Hz in darkness, and this increases to 20 Hz when the animal views a 0% coherence stimulus of moving dots (Huk and Shadlen, 2005). Increasing the coherence of the stimulus increases the firing of cells tuned to respond to the direction of motion of the coherently moving dots, and decreases the firing of cells tuned to the opposite direction (Fig 3.2g). Psychometric functions (Fig 3.2d) measured psychophysically, or 'neurometric' functions derived by deducing the psychophysical performance of an ideal

observer comparing the responses of neurons tuned to the direction of motion and to the opposite direction, can be fitted by the function

$$p = 1 - 0.5 \exp(-(c/\alpha)^{\beta}) \quad (3.1)$$

where p is the probability of correctly detecting the motion direction (out of two oppositely directed possibilities) at coherence c, α is termed the threshold for detection, and β is a measure of the steepness of the function (Britten et al., 1992;Britten et al., 1993). Detection at threshold (c=α) corresponds to correctly detecting the direction of motion on $1\text{-}0.5*e^{(-1)}$ = 82% of trials. This 82% success rate for detecting motion can be achieved when stimuli have a coherence of 14% (this number is derived from the neuron data in Fig 9a of Britten et al., 1992). Having derived this threshold coherence allows us to calculate the mean firing rate of V5/MT cells when detecting motion. The action potential rate of V5/MT neurons responding to motion in their preferred direction increases with coherence of the stimulus at a rate of 0.39 Hz / (% coherence), while the rate in cells whose preferred direction is opposite to the stimulus decreases at 0.11 Hz / (% coherence) (Britten et al., 1993). Thus, for 14% coherence, these cells will increase and decrease their rate by 5.47 Hz and 1.55 Hz respectively. Adding the 20 Hz firing occurring in the presence of a 0% coherence stimulus (see above), these cells will therefore fire at 25.47 and 18.45 Hz respectively.

A column of V5/MT cells analysing motion in a retinal area (Albright et al., 1984) contains cells responding to all possible directions of motion which, in general, will respond at a rate between the extremes of 25.47 Hz and 18.45 Hz. The firing rate of V5/MT neurons can be expressed as

$$\text{rate} = D \exp(-(x/\sigma)^2) + E \quad (3.2)$$

where x is the angle relative to the preferred direction, σ is the bandwidth of the response and D and E are constants (Britten and Newsome, 1998). Using $\sigma = 88^0$ for 14% coherence (from Fig 3 of Britten and Newsome, 1998), and fitting this equation to firing rates of 25.47

and 18.45 Hz at 0^0 and 180^0, gives D = 7.13 Hz and E = 18.34 Hz. The mean firing rate averaged over all of the cells in the column is thus

$$\int_0^{180} \{ D \exp(-(x/\sigma)^2) + E \} dx/180 = (D/2)*(\sigma/180)*(\sqrt{\pi})*\mathrm{erf}(180/\sigma) + E = 21.4 \text{ Hz}$$

when the motion is perceived at threshold. In contrast, when viewing a 0% coherence stimulus, the firing rate is 20 Hz (see above). Thus, the motion percept is associated with a 7% increase in mean firing rate {100% * (21.4–20)/20}. Perception of motion by V5/MT neurons evokes an increase in firing rate and energy use only because of an asymmetry in the neural responses to motion in the preferred and nonpreferred directions of the cells: stimuli in the preferred direction evoke a larger increase in firing than the decrease of firing evoked by stimuli in the opposite direction (Britten et al., 1993). In principle the system need not be constructed with this asymmetry, and it might be possible for perception to occur with no change of mean firing rate and energy usage at all relative to viewing a 0% coherence stimulus (or even a decrease in mean firing rate and energy usage if the relative strengths of the responses in the preferred and opposite directions were reversed).

3.2.3 Detection of skin vibration

For the somatosensory modality, we analysed the detection of 'flutter', a sensation which is produced when 5-50 Hz vibrations are applied to the skin to activate Meissner's mechano-receptors (Mountcastle et al., 1967). In monkeys, information from these receptors is passed to somatosensory cortical area S1, where neurons are active during the period of vibration, and also to higher-level areas S2 and prefrontal cortex (Romo et al., 2004) (Fig 3.1). In these higher-level areas the neural activity evoked outlasts the period of stimulation, providing a working memory trace that can be used to compare the frequency of a second stimulus (Fig 3.2b) with that of an earlier stimulus (Romo et al., 2004). Both of the individual stimuli should be well above the threshold for detection. In humans, flutter vibration also activates areas S1 and S2 (Maldjian et al., 1999), and in psychophysical experiments (Fig 3.2e) monkeys and humans distinguish the frequency of sequentially applied vibrations with a

similar performance (Lamotte and Mountcastle, 1975). We estimated the energy expended in area S2 to generate neural activity which can support the discrimination of the frequency of two vibration stimuli, i.e. the increase in energy expenditure associated with perception of a frequency difference, above that needed merely to represent two stimuli which are not perceived as different.

Neurons in monkey S2 change their firing when a flutter stimulus is applied, but only 40% of these show a response that depends on the vibration frequency (Romo et al., 2002). Of these frequency-sensitive neurons, 57% show an increase in firing rate with increasing vibration frequency, and 43% show a decrease in firing rate with increasing frequency (Romo et al., 2003). When two stimuli of different frequency, f1 and f2, are applied for 0.5 sec, separated by a few seconds in time (Fig 3.2b), the action potential firing rate response to the second stimulus can be represented as a function of f1 and f2 as follows (Romo et al., 2002):

$$\text{rate}(f1, f2) = a1.f1 + a2.f2 + \text{constant} \qquad (3.3)$$

where a1 and a2 are experimentally determined functions of time that evolve so that for much of the response, a1(t) = -a2(t) and the rate depends solely on the difference in frequency, f2-f1. For an initial frequency of f1= 20 Hz, we evaluated the mean difference in spike count ($\int$rate(f1,f2) dt) averaged over all cells in the case where f2 was sufficiently above f1 to be distinguished perceptually from the case where f2 = f1 = 20 Hz. Using the definition of threshold in eqn. (1), i.e. 82% of behavioural choices correct (Fig 3.2e), and taking correlations between neuronal responses into account (Romo et al., 2003), the threshold for perceiving that f2>f1 is reached when f2 is raised from 20 to 24.6 Hz (from Fig 4 of Romo et al, 2003), and the resulting increase of spike count from eqn. (3.3) is

$$\int \text{rate}(f1=20, f2=24.6)\, dt - \int \text{rate}(f1=20, f2=20)\, dt = 4.6\text{Hz} \cdot \int a2(t)\, dt$$

Remember that a2(t) represents a function that resembles the firing rate of the neurons in response to the f2 stimulus over time. The motor response defining the monkey's choice of

whether f2>f1, starts on average 836 msec after the start of the f2 stimulus (Romo et al., 2002). Mean values of a2(t) were obtained for times 25-90 msec, 90-295 msec, 295-500 msec and 500-836 msec after the start of the f2 stimulus by averaging over the experimental data for cells in Figs 6a, 6b, 6c and 6d respectively of Romo et al., 2002. This procedure gave mean values for a2 of 0.119, 0.046, 0.421 and 0.106 action potentials (respectively) for the four time periods (Fig 3.2h), and thus a mean increase in spike count of 0.64 action potentials per neuron. This mean increase is very low because similar numbers of cells show increases (for which a2 is positive) and decreases (for which a2 is negative) in firing rate in response to the flutter stimuli (Romo et al., 2002). Since only 40% of neurons show responses dependent on the stimulus frequency (Romo et al., 2002), averaged over all the cells in S2 the mean increase of action potentials/neuron is 0.26, for the 3 sec period during which the two stimuli are applied. The baseline firing rate of these cells is ~ 15 Hz (Romo et al., 2002), so this corresponds to an 0.57% increase of firing over the 3 sec trial.

3.2.4 Detection of auditory tone stream segregation

For the auditory modality we studied tone stream segregation. A repeated sequence of (suprathreshold) sound tones alternating between two frequencies, A and B, such as ABA-ABA-ABA (Fig 3.2c), is heard by humans as two separate streams of constant pitch tones if A and B are sufficiently different (i.e. heard as A-A-A- and B-B-B-, with the stream separation building up over time, Fig 3.2f), but as a single tone stream with a galloping rhythm if A and B are close (Bregman and Campbell, 1971). Tone stream segregation has also been demonstrated in psychophysical experiments on monkeys (Izumi, 2002).

A possible neural basis for the phenomenon of tone stream segregation is suggested by experiments on primary auditory cortical (A1) neurons in monkeys (Fishman et al., 2001;Micheyl et al., 2005). For the ABA-ABA-ABA- stimulus, if A and B are sufficiently different, neurons with a best frequency equal to that of the A tone show a different time course of adaptation to the repeated presentation of the A and B tones: although the

responses to both tones decrease over the first few presentations of the tone triplet, the response to the off-best frequency B tone is not only smaller but shows proportionally more adaptation with repeated presentation of the triplet tones (Micheyl et al., 2005) (Fig 3.2i). Similarly, for a neuron with a best frequency equal to that of the B tone, the response to the A tones would decrease more over time than the response to the B tone (Micheyl et al., 2005).

Thus, if the A and B tones are sufficiently separated, after some duration of exposure to the tone sequence, high signal to noise ratio responses will only be produced for the A tones in neurons tuned to the A frequency, and for the B tones in neurons tuned to the B frequency. In contrast, when A and B are close, the extra adaptation to the B tone is hardly seen in neurons tuned to the A frequency (Fig 3.2i), and vice versa, so that information on both tones will be encoded with a high signal to noise ratio by both sets of neurons. This representation of the tone sequence in two discrete sets of cells when A and B are sufficiently different, but in the same cells when A and B are close, is postulated to underlie the different perceptions produced (Micheyl et al., 2005;Fishman et al., 2001). Human magnetoencephalographic (Gutschalk et al., 2005) and fMRI (Cusack, 2005) studies suggest that auditory areas outside A1 may also contribute to the different perceptions produced, perhaps by controlling attention to the information streams produced in cells at different locations in A1.

The change in energy expenditure associated with tone stream segregation in the primary auditory cortex (A1) can be estimated as follows. Psychophysical experiments (Micheyl et al., 2005) on the response of humans to ABA triplet tone sequences applied at 0.5 sec intervals show that if B is 6 semitones ($\sqrt{2}$ -fold) above A in frequency, then stream segregation occurs over a period of seconds, and after 2 presentations of the triplet tone sequence the probability of correctly perceiving the segregated streams reaches 64% (which, since the probability rises from 0 to ~100%, is equivalent to the 82% criterion used in eqn. 1 for an experiment where the probability rises from 50 to 100%, as 82% = 50% + (100-50)%x64%). In contrast, if B is only 1 semitone above A in frequency, or the same as A, then stream segregation does not occur even after 10 sec of the stimulus (Fig 3.2f).

In primary auditory cortical neurons of monkeys with a best frequency of A, Fig 3 of Micheyl et al., 2005 shows that, when B is 6 semitones above A, the first 2 presentations of the triplet tone sequence evoke 8.82 and 6.79 action potentials respectively in response to the two first A tones (a total of 15.61 spikes), 5.97 and 4.46 action potentials in response to the two B tones (a total of 10.43 spikes, much less than for the A tone because of the adaptation described above), and 7.48 and 6.77 action potentials in response to the two last A tones (a total of 14.25 spikes), giving a grand total of 40.29 spikes in response to the 2 triplet sequences (this includes the baseline firing rate of ~25Hz). In contrast, when B is only 1 semitone above A, although the total spikes in response to the two first and two last A tones of the 2 triplets were little changed (15.28 and 14.81 respectively), the total spike number in response to the intervening B tones was increased from 10.43 to 13.69 (because of the absence of the adaptation described above: Fig 3.2i), giving a grand total of 43.78 spikes in response to the 2 triplet sequences.

The difference in total spike count between the responses to the triplets with the B tone 6 and 1 semitones above A is therefore 3.49 spikes, out of a total response of 43.78 spikes when tone stream segregation does not build up. Thus, there is an 8.0% decrease (3.49/43.78) in total spikes occurring associated with the switch from a perception of one tone stream to two separate streams of different tones. This is an overestimate of the change occurring in all of A1, because although a change of this magnitude will occur at the locations in (the tonotopically arranged) A1 where cells have best frequencies of A and B (Fishman et al., 2001), at other locations the difference in firing rate will be smaller.

3.2.5 Relationship between firing rate and energy use

In the Results section (3.3) we use the mean changes of firing of cortical pyramidal cells calculated above to estimate the change of energy use occurring in a cortical area as a result of altered activity in the recorded cells themselves, and in their input synapses and surrounding glia. Cortical energy use initiated by action potentials has components related to

presynaptic and postsynaptic action potentials (Attwell and Laughlin, 2001). On the presynaptic side, energy is used on presynaptic action potentials and transmitter release, and transmitter and vesicle recycling. On the postsynaptic side, energy is used to reverse the ion movements generating postsynaptic action potentials, and for reversal of postsynaptic ion movements generated by transmitter release (Attwell and Laughlin, 2001). Action potential driven signalling energy accounts for ~50-75% of total energy consumption; the remaining 25-50% of brain energy is expended on the resting potentials of neurons and glia, and on non-signalling housekeeping tasks (Attwell and Laughlin, 2001).

3.2.6 Stimuli well above perceptual threshold

For the detection of visual motion calculation described above, if the coherence is twice the threshold value in eqn. (3.1), i.e. 28% then, for a steepness parameter of α=1.4 (Britten et al., 1992), eqn. (3.1) predicts that stimulus motion will be correctly detected 96.4% of the time (Fig 3.2d). Repeating the calculation above (see 3.2.2) for 28% coherence predicts that this highly reliable detection of the motion percept is associated with a 14% increase in mean firing rate. Similarly we repeated the calculation for flutter perception given above, now for comparison of a 30 Hz vibration with a 20 Hz vibration, for which the correct behavioural choice is made 97% of the time (Romo et al., 2003). Averaged over all the cells in S2, the mean increase of action potentials/neuron is then 0.56, for the 3 sec period during which the two stimuli are applied, i.e. a 1.2% increase over the basal firing rate.

For the tone sequence experiment with tone B 6 semitones above A, psychophysical experiments on humans show that perception of the two tone streams reaches its maximum (94% correct) after 5 sec of repeating the tone triplets (Fig 3.2f). Extending to 5 sec the counting of the spikes of monkey A1 neurons (Micheyl et al., 2005) showed that (including the 25 Hz baseline firing rate) the total spike count with B 6 semitones above A was 16.7 spikes less than the 195.8 spikes occurring when B was just one semitone above A, i.e. an 8.5% difference. Thus, in all three cortical areas, the mean change in firing rate used for

conscious perception of stimuli is low, not just at the threshold of perception, but also when perception is highly reliable.

3.3 Results

3.3.1 Visual task

In order to determine the energy needed to support the perception of motion in area V5/MT, we have calculated the action potential rate of the cells analysing the motion. Averaging over cells responding to all directions of motion, for a coherence value which is at the threshold of detection of the motion we have estimated that the motion percept is associated with a 7% increase in mean firing rate (and hence in firing-related energy use) in area V5/MT over that occurring during presentation of a 0% coherence stimulus (see 3.2.2). If action potential driven signalling energy accounts for ~50-75% of the total energy consumption (Attwell and Laughlin, 2001), then this 7% increase of firing rate implies an increase of total local energy consumption of 50-75% of 7% = 3.5-5.3% (Fig 3.3).

3.3.2 Somatosensory task

Neurons in monkey S2 change their firing when a flutter stimulus is applied. When two stimuli of different frequency, f1 and f2, are applied for 0.5 sec, separated by a few seconds in time (Fig 3.2b), the action potential firing rate in response to the second stimulus evolves over time to depend largely on the difference in frequency. For an initial frequency of f1= 20 Hz, we evaluated the mean difference in spike count averaged over all cells for the case where f2 was sufficiently above f1 to be distinguished perceptually from the case where f2 = f1 = 20 Hz. The calculation shows that there is a 0.57% increase in mean firing rate at the threshold of perception in area S2 (see 3.2.3). As above for visual perception, if action potential driven energy use is ~50-75% of the total energy consumption (Attwell and

Laughlin, 2001), the 0.57% increase of firing occurring during flutter detection implies an increase of local energy consumption of 50-75% of 0.57% = 0.29- 0.43% (Fig 3.3).

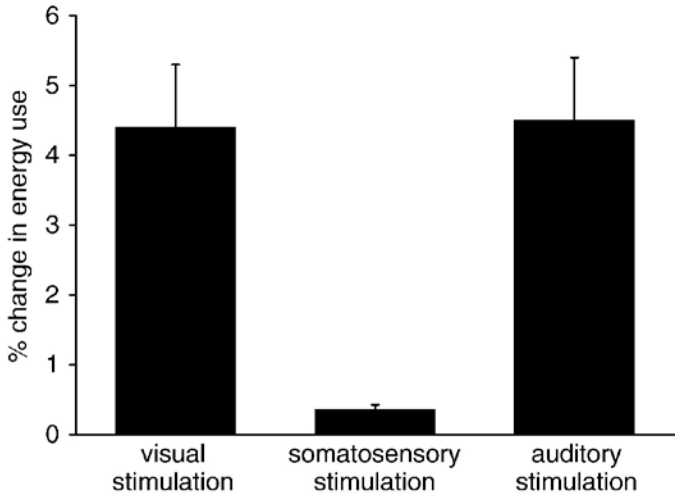

Figure 3.3 Estimated changes in energy use associated with conscious perception*. Bars show mean increase in energy use associated with perception of a moving stimulus, increase in energy use associated with detection of a difference in flutter frequency, or decrease in energy use associated with detection of tone streaming (SEM was calculated from the 2 results obtained assuming that either 50 or 75% of total energy is action potential driven).*

3.3.3 Auditory task

We estimated the change in energy expenditure associated with tone stream segregation in the primary auditory cortex (A1) using electrophysiological data from monkeys recorded during exposure to tone triplets with B tones either 6 semitones or 1 semitone above the frequency of the A tone, for which tone stream segregation does, or does not occur, respectively (Micheyl et al., 2005). These data revealed that there is an 8.0% decrease in total spikes occurring in A1 associated with the switch from a perception of one tone stream to perceiving two separate streams of different tones (see 3.2.4). As above for visual perception, if action potential driven energy use is ~50-75% of the total energy consumption (Attwell and Laughlin, 2001), auditory stream detection will lead to a decrease of local energy consumption of 50-75% of 8% = 4-6% (Fig 3.3).

3.3.4 Supra-threshold stimuli

The calculations above detail the change in cortical energy use associated with the threshold perception of a stimulus attribute. Larger energy changes are expected for stimuli above threshold, but repeating the calculations for this case shows that even well above threshold, where stimulus detection is highly reliable, the fractional change of energy use is still surprisingly small: 7-10.6% for the visual motion task, 0.6-0.9% for the flutter perception task, and 4.3-6.4% for the tone stream segregation task (calculated as above from the mean firing rate changes given in 3.2.6).

3.4 Discussion

3.4.1 Energy used on conscious perception

We have estimated how much brain energy is needed to produce information which can be used to generate a percept, over and above the energy needed to represent the incoming stimuli when the percept is absent. For example, this is the energy needed for visual processing of dot stimuli which move sufficiently coherently to generate a percept of general movement, relative to that needed for processing of the same number of dots which move randomly and so generate no general movement percept. All three cortical areas studied show only a small change of energy usage associated with perception (<6% at threshold, and <11% when perception is reliable), despite the difference in modalities that they serve (vision, touch, audition) and large differences in baseline firing rate, suggesting that this result is of general relevance.

A major reason for the small size of this energy change, at least for the visual motion and somatosensory flutter stimuli considered, is that sensory attributes are encoded across a population of neurons as a mixture of increased and decreased firing. Across the population of neurons considered, therefore, the changes in mean firing rate and energy usage are much

less than would occur if firing simply increased in all neurons with the strength of the sensory attribute. Thus, encoding stimuli across a population of neurons as a mixture of increased and decreased firing confers the advantage that the energy demand of the brain is kept more constant and requires smaller blood flow changes (rather than requiring that blood flow increases dramatically for all sensory input).

For these conclusions to hold for humans, we must assume that experimental measurements of the change of action potential frequency evoked by sensory stimuli in awake monkeys can be extrapolated to humans. While there is no easy way to verify this, the similar psychophysical results (Britten et al., 1992;Lamotte and Mountcastle, 1975;Bregman and Campbell, 1971;Izumi, 2002) obtained in monkey and human for all three sensory stimuli studied suggest that the cellular mechanisms underlying perception are similar in the two species.

If the change in energy use is so small, why has evolution produced systems that increase blood flow when neurons are active? In other words, do active neurons need the blood flow to increase? It is important to note that our predictions of a small increase in firing rate and energy expenditure are only for the perception of a feature of the incoming sensory information. Thus, in the vision example given above, the presence of a zero coherence array of randomly moving dots increases the mean firing rate in area V5/MT from ~8 to ~20 Hz (Huk and Shadlen, 2005). Similarly, neurons representing tactile flutter stimuli can double their firing frequency when the stimulus is present (Romo et al., 2002), and A1 neurons increase their firing 6-fold when a tone is applied (Micheyl et al., 2005). The much larger firing rate changes associated with unconscious information processing than with perception suggest that the changes in energy expenditure associated with conscious perception are much smaller than those associated with the unconscious representation of incoming sensory information, for which the increase in blood flow associated with neuronal activity will be more important.

3.4.2 Relevance to BOLD fMRI

Functional imaging experiments often assess the difference in brain activation for two situations designed to differ only in the perception of some stimulus attribute (McKeefry et al., 1997;McKeefry and Zeki, 1997;Phillips et al., 1997). Our calculations show that, in the tasks we consider, perception is associated with only a small change in energy usage (the exact size of which varies between cortical areas, being an order of magnitude smaller for the somatosensory flutter task than for the visual motion task, and even a decrease in the case of tone stream segregation). For a small increase of neural firing and energy usage it is unclear whether an increase in blood supply is actually needed to power the neural activity, or whether an increased extraction of oxygen and glucose from the blood (driven by the lowered local concentration of these substrates) would suffice. In any case, it does seem likely that any neurotransmitter-mediated (Drake and Iadecola, 2006) increase of blood flow associated with perception need only be small. Interestingly, the blood flow increases generating functional imaging signals are rather small (Raichle and Mintun, 2006), typically less than 5-10%, and the BOLD signal increase associated with the perception at threshold of the stimulus properties considered here is less than 1% in the visual motion (Rees et al., 2000), flutter discrimination (Hegner et al., 2007) and tone stream segregation (Wilson et al., 2007) tasks. It seems possible, therefore, that perception of a stimulus attribute in some brain areas, particularly those where a decrease in the firing of some neurons outweighs an increase in the firing of other neurons and so is likely to lead to a decrease in the total release of glutamate (the main agent thought to trigger vasodilator release and BOLD signals), may fail to be detected as a positive BOLD fMRI signal (cf. Shmuel et al., 2006).

3.5 Conclusion

Our calculations show that the amount of evoked activity that is added to the ongoing spontaneous activity in the cortex when a stimulus is presented, is quite substantial. Conscious perception of a particular attribute of this stimulus, however, is associated with a minute further increase in evoked activity and energy use. The amount of evoked activity in relation to the amount of spontaneous activity has implications for the size of the evoked BOLD response. The relationship between the BOLD signal and spontaneous activity per se, in the absence of any external stimulation, is the topic of the next chapter.

Chapter 4 Neural Basis of Resting-State fMRI Fluctuations

4.1 Introduction

In humans, spontaneous brain activity is typically investigated in the so-called resting state. The resting state is poorly defined, and typically amounts to a subject lying in the scanner with their eyes open or closed, but without an explicit stimulus or task. As mentioned in Chapter 1, General Introduction, under these conditions analysis of the spatiotemporal coherence of brain activity reveals several distinct functional networks (Beckmann et al., 2005;Damoiseaux et al., 2006;Fox and Raichle, 2007). Specifically, resting-state activity encompasses a so-called default-mode network (Greicius et al., 2003), attentional networks (Fox et al., 2006a), networks in visual (Bianciardi et al., 2009a;Eckert et al., 2008), auditory (Cordes et al., 2000), and somatomotor (Biswal et al., 1995;Xiong et al., 1998) cortex, and networks including the thalamus (Zhang et al., 2008), cerebellum (O'Reilly et al., 2009), and basal ganglia (Di Martino et al., 2008). While activity covariation can be attributed to many factors, it is often associated with known anatomical connections (Hagmann et al., 2008;Honey et al., 2009) and as such, appears to be fundamental to the brain's functional organisation.

An important data analysis step used to reveal these functional networks in resting-state fMRI activity has been removal of spontaneous BOLD fluctuations common to the whole brain (the so-called global signal) (see 2.3.5). Global signal correction is common during processing of resting-state fluctuations (Fox et al., 2005;Macey et al., 2004) and is thought to uncover correlations between brain regions that are potentially obscured by fMRI fluctuations of physiological (non-neuronal) origin. For example, it is well known that physiological factors such as changes in heart rate and respiration contribute to fMRI resting-state fluctuations (Bianciardi et al., 2009b;Birn et al., 2006;Wise et al., 2004). On the other

hand, several studies have now suggested that resting-state fluctuations are also partly neural in origin (Bianciardi et al., 2009b;Leopold et al., 2003;Nir et al., 2008;Shmuel and Leopold, 2008). Intracranial electrocorticography (ECoG) recordings in humans display slow fluctuations similar to spontaneous fMRI fluctuations, with significant correlations between functionally related areas. Strong interhemispheric correlations are found in the slow modulation (<0.1 Hz) of spontaneous neuronal firing rate and gamma power (Nir et al., 2008). These correlations are enhanced during rapid eye movement (REM) and stage 2 sleep. Spatial specificity in spontaneous neuronal activity is also observed in slow ECoG signals recorded from sites within the sensorimotor system, which show significantly higher correlations among each other than to sites outside this network (He et al., 2008). The relationship between slow fMRI fluctuations and underlying neural fluctuations has been most directly demonstrated in anaesthetised monkey (Shmuel and Leopold, 2008). In that study, simultaneous fMRI and intracortical neurophysiological recordings in the primary visual cortex revealed a widespread correlation between slow fluctuations in the fMRI signal and fluctuations in the spiking rate and gamma-band local field potential power.

While it is now certain that neural activity underlies at least some portion of fMRI resting-state activity, many questions remain regarding the nature of this coupling. For example, what is the spatial nature of the coupling? In Shmuel and Leopold (2008), neural signals were only measured in the primary visual cortex, and the correlated fMRI activity was not restricted to a region adjacent to the recording electrode, but was found several millimetres from the recording site. It is unknown, however, to what extent the activity in the rest of the brain is correlated with these neural signals. Furthermore, previous analyses have focused mainly on gamma power modulations (Nir et al., 2008;Shmuel and Leopold, 2008); the contribution of other LFP frequencies present in the neural activity to resting-state fMRI fluctuations is unknown. Finally, it is unknown whether the relationship between neural and fMRI signals in the resting state is fixed, or whether the effective neurovascular coupling changes over time. In this chapter, I attempt to address these questions by performing simultaneous local field potential (LFP) and fMRI recordings during the resting state in the

awake monkey, focusing on the spatial, spectral, and temporal properties of the correlation between the signals.

4.2 Materials and Methods

4.2.1 Subjects and procedure

Two healthy adult female monkeys (*Macaca mulatta*), monkey A and monkey V, were used in this study. All procedures followed NIH guidelines, were approved by the Animal Care and Use Committee, and were conducted with great care for the comfort and well being of the animals. Each monkey had an MR-compatible implanted electrode in V1, which allowed for fMRI and neurophysiological testing simultaneously. The electrodes were multicontact electrodes, which permitted electrophysiological recording from all cortical layers simultaneously. Monkey A had two additional electrodes implanted in the frontal lobe (area 6d) and parietal lobe (area 7a). The monkeys were trained to sit quietly in the scanner, having been previously acclimated to the scanner noise, and had no particular behavioural requirements. No monitor screen was present and the monkeys sat in complete darkness. An infrared video camera sitting inside the bore and directed to the monkey's face was used to monitor the animal's behavioural state. The monkeys differed in their behavioural tendencies, with monkey A showing a strong tendency to sleep and monkey V typically remaining alert throughout the session. Together, the animals participated in a total of 52 runs (25 and 27 runs in monkeys A and V, respectively) over a period of several months. Seven runs in monkey A and 19 runs in monkey V were excluded from further analysis, since the data did not show correspondence between the neural and fMRI signals. While such zero-correlation could reflect a genuine absence of physiological correlation in those sessions, such a situation can also arise for any of a number of reasons related to the

electrophysiology or imaging methods. Post-hoc analysis revealed that the absence of any correlation was most likely due to insufficient MION concentration in the blood (see 4.2.5).

4.2.2 Headpost surgery

Monkeys were implanted with posts to immobilize the head and with implantable electrodes under deep isoflurane anaesthesia (1.5-2%). Head restraints were custom-machined using fibreglass (G10) material (McMaster-Carr, Chicago, IL). Following exposure of the skull, the bone was thoroughly cleaned and dried. Eight ceramic screws (Thomas Recording, Giessen, Germany) were attached to the cranium adjacent to the designated position of the head post. Dental lacquer (Copalite) was then applied over the exposed surface, serving to prevent tissue growth under the implant. A thin coat of self-curing denture acrylic (Lang Inc., Wheeling, IL) was first applied to the skull and around the screw heads, ensuring good adherence to the bone and defining the outer margin of the implant. The post was then affixed to this pedestal, once it was dry, with additional layers of acrylic. The fascia and skin were subsequently sewn tight against the margin. Animals received antibiotics and analgesics post-operatively.

4.2.3 Electrode surgery

Each chronic electrode (NeuroNexus Technologies, Ann Arbor, US) was implanted as follows. Implantation positions were decided during an earlier surgical planning session, based on a high-resolution 3D anatomical MRI scan. These positions were located on the monkey's skull during surgery using the Brainsight frameless stereotaxy system (Rogue Research, Montreal, Canada), after which a 4 mm window of bone was opened and the dura mater was reflected. Each multicontact electrode was then inserted, using a Teflon-coated forceps under optical assistance, perpendicular to the pial surface. The electrode was advanced approximately three millimetres, so that the 32 electrode contacts, spaced 100 µm apart, would span the depth of the cortex (Fig 4.1). The window was then filled with

antibiotic-laden agar gel, and was secured by silicone and dental acrylic. An MR-compatible connector attached to the electrode was glued onto the skull adjacent to the window, approximately 8-20 mm from the proximal end of the electrode. Animals received antibiotics and analgesics post-operatively.

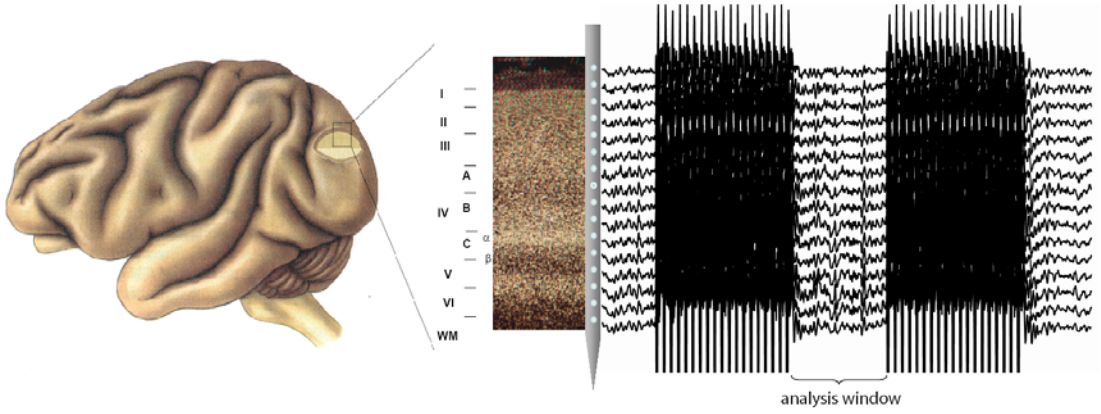

Figure 4.1 Schematic of multicontact electrode and recording. *MR compatible electrodes were implanted in V1 (left), with the contacts spanning the entire width of the cortex. Recordings were heavily polluted by the switching of the MR gradients (right); therefore only LFP signal within time windows during which the gradients were silent was analysed (see 4.2.7).*

4.2.4 MRI scanning

Structural and functional images were acquired in a 4.7 T / 60 cm vertical scanner (Bruker Biospec 47/60, Ettlingen, Germany) equipped with a Bruker gradient coil (60 mT/m, <150 µs). Monkeys were scanned using a custom-built transmit-receive RF coil (width 100 mm) situated over cortical area V1. This coil, while providing the highest signal to noise ratio (SNR) in the occipital lobe, nonetheless provided adequate coverage for most of the brain. At the beginning of each session, active shimming was achieved either by manual manipulation of the gain of the shim coils, or by using the FASTMAP procedure, or a combination of the two. To assess functional cortical activation, a single-shot gradient echo-planar imaging (GE-EPI) sequence was used with a repetition time (TR) of 1.6 s followed by a 1.0 s gap ('sparse scanning paradigm') and an echo-time (TE) of 15.6 ms. Sparse scanning

was employed since switching of the MR gradients caused a large artefact in the LFP signal, which saturated the LFP amplifier and could therefore not be removed from the data by artefact correction (see 2.4.3). Typically, 19 coronal slices were collected with a field of view (FOV) of 90 x 50 mm, matrix size 72 x 40, a slice thickness of 1.5 mm, and a 0.5 mm gap. The in-plane resolution of the functional images was 1.5 x 1.5 mm. Runs consisted of 700 volume acquisitions, lasting roughly 30 min. For 5 runs in monkey A and 3 runs in monkey V, 15 axial slices (matrix size 64 x 128) were collected, in monkey A using the single-shot EPI sequence described above, and in monkey V using a two-shot EPI sequence with a TR of 0.6 s followed by a 1.0 s gap per shot. An infrared video camera inside the bore monitored and recorded the animals' eye movements during most of the scans (22/26).

4.2.5 MION

Prior to scanning, the monkeys were administered a dose of Monocrystalline Iron Oxide Nanoparticles (MION) intravenously. MION is a T2* contrast agent that isolates the regional cerebral blood volume (rCBV) component of the functional activity (Leite et al., 2002). MION boosts the functional signal to noise ratio (SNR) compared to the blood oxygenation level-dependent (BOLD) signal, which was confirmed in pilot runs. We obtained MION from three different sources: (1) Dr. Anna Moore, Martinos Center for Biomedical Imaging, Massachusetts General Hospital, Charlestown, MA, (2) Dr. Gary Griffiths, Imaging Probe Development Center, National Institutes of Health, Bethesda, MD, and (3) BioPal, Inc., Worcester, MA. We determined the dose of MION by monitoring the drop in intensity in the brain following injection. Previous work has shown that a drop of roughly 50% is optimal for good functional imaging (Leite et al., 2002), and this corresponded to roughly 8-10 mg/kg MION, depending on the monkey and batch of MION. Since increased MION (i.e. increased rCBV) leads to decreases in the raw signal associated with function, the polarity of each of our fMRI plots is inverted for clarity.

4.2.6 MRI data analysis

Functional (EPI) raw images were converted from the generic BRUKER into the common AFNI data format. All images of a scan were realigned to correct for motion artefacts using a custom written algorithm (Bob Cox, AFNI). Functional data were registered to the corresponding high-resolution anatomical scan (MDEFT) acquired prior to surgery, using the analysis package mrVista (http://white.stanford.edu). Each voxel's time course was converted into units of percent change by first subtracting, and then dividing by the mean of its time course (Fig 4.2b).

4.2.7 Neurophysiological recordings

The electrodes consisted of a linear array with 100 μm spacing between contacts, spanning from the pia to white matter of the cerebral cortex (Fig 4.2a). The reference was located on the array itself, just above the dura. In total, 4 electrodes were used for electrophysiological recordings; the two electrodes in the primary visual cortex (area V1) in both animals, plus the electrode in the parietal cortex (area 7a) and frontal cortex (area 6d) in monkey A. Recordings of the local field potential (LFP) from the implanted electrodes were conducted inside the scanner bore. Additional recordings were performed outside the scanner, in an RF-shielded booth. Activity was recorded inside the scanner bore using an MR-compatible 32-channel amplifier (BrainAmp, Brain Products, Munich, Germany) with an input range of 16 mV, then passed optically out of the scanner. The amplifier was equipped with a 16-bit A/D converter, and sampled the signal at 5 kHz and at a resolution of 500 nV. The signal was high-pass and low-pass filtered at 0.5 and 1000 Hz, respectively. During simultaneous acquisition, the scanner was synchronised to the electrophysiological data via a brief digital pulse from the scanner delivered at the beginning of each volume acquisition.

4.2.8 Neuronal data analysis

Data were preprocessed using Vision Analyzer Software v1.05 (Brain Products, Munich, Germany). Data were band-pass filtered at 2-80 Hz, down-sampled to 200 Hz, and further analyzed in MATLAB (www.mathworks.com). Only segments of the LFP recorded during the 1 s gap between volume acquisitions were considered for analysis (i.e. no LFP signal obtained during MR image acquisition was analysed) (Fig 4.1). This approach is similar to the stepping stone technique (Anami et al., 2003, see 2.4.3) in eliminating the contribution of gradient switching artefacts in the electrophysiological signal, and provided adequate temporal sampling of the signals of interest. Segments containing clear movement artefacts were removed by an automated algorithm. Within each 1s time window, the frequency-specific power was computed in two ways. First, the magnitude spectrum of the signal was computed for each segment using the fast Fourier transform. This provided a spectral estimate for each time window which, together, resembled a spectrogram with a sampling rate of TR (albeit computed for the gap period only). In a second approach, which was in some ways equivalent, the LFP was first band-pass filtered using a 2^{nd} order Chebyshev filter in the following standard frequency bands: delta (2-5 Hz), theta (4-9 Hz), alpha (8-14 Hz), beta (15-25 Hz), low-gamma (25-40 Hz), and high-gamma (40-80 Hz) and then rectified. The mean over each segment was then computed. This analysis provided six estimates of time varying band-limited power (BLP, or more accurately, band-limited root mean square voltage; see 2.2.3) for each time window, providing six band-limited signals of higher signal to noise ratio than in the first approach (Fig 4.2c). Both approaches gave us estimates of the LFP at each of the 32 contacts on the electrode. While pilot analyses showed that there was some variation in the BLP as a function of cortical depth (data not shown), these differences were minor compared to the effects we found in general, and we do not address them here. Instead we selected a single representative electrode contact for all sessions to compare with the fMRI signal throughout the brain.

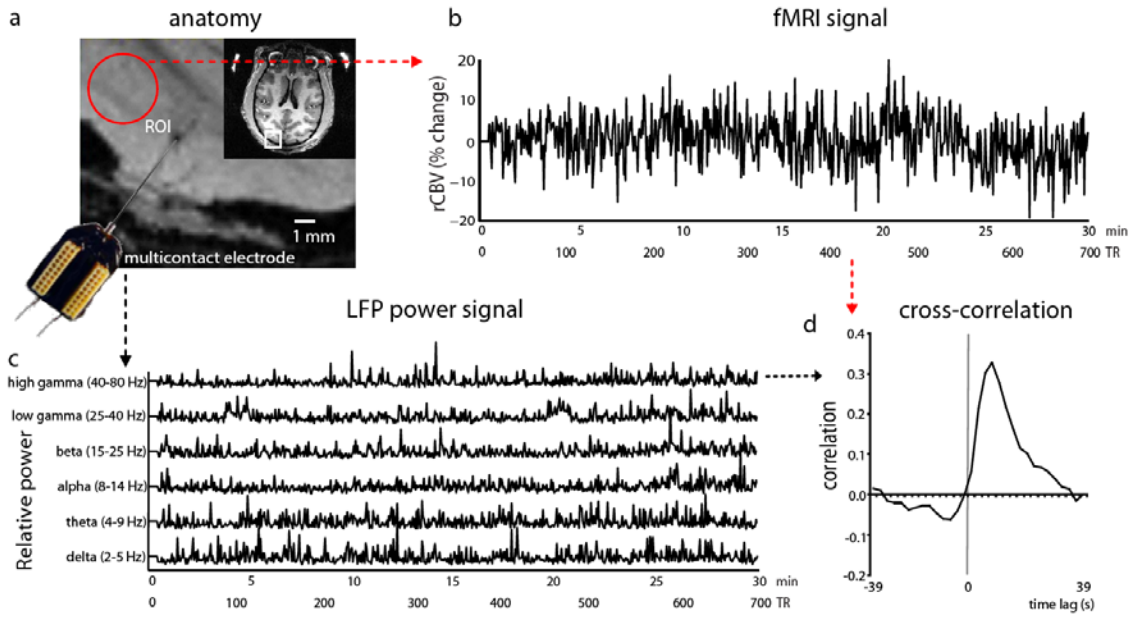

Figure 4.2 Simultaneous fMRI and electrophysiology, and data analysis. ***(a)*** *Anatomical FLASH image of the occipital cortex of monkey A, with the implanted multicontact electrode in V1 and the region of interest (in red) for panel* ***b****. White box in inset shows where the electrode was located in the brain.* ***(b)*** *Time course of rCBV signal for one run, averaged over voxels in the region of interest. The rCBV signal was acquired with a TR of 2.6 s; each run lasted for 30 mins.* ***(c)*** *Relative power traces of the LFP power during the same run as in* ***b****, for the six frequency bands: delta (2-5 Hz), theta (4-9 Hz), alpha (8-14 Hz), beta (15-25 Hz), low gamma (25-40 Hz), and high gamma (40-80 Hz). The first 10 volumes of both the rCBV signal and the LFP power traces were discarded to allow for T1 equilibration.* ***(d)*** *Cross correlation function between the high gamma (40-80 Hz) power and the fMRI signal in the ROI for the same run as a function of temporal lag.*

4.2.9 Correlation of neurophysiological and fMRI signals

The covariation between the rCBV (throughout the brain) and the neural signal (either in the form of time-varying fast Fourier transform (FFT) magnitudes or BLP estimates, but always from a single electrode position) was evaluated for each voxel by computing cross correlation functions. This analysis resembles the *seed voxel* approach often applied in fMRI functional connectivity studies (Fox et al., 2006a;Greicius et al., 2003) (see 2.3.6). Given that a certain neural event would *a priori* be likely to be associated with a haemodynamic

event occurring later in time (owing to the nature of the haemodynamic response function), we computed the cross-correlation function between the fMRI and electrophysiological signal at lags of up to ± 39 s. In other words, we artificially shifted the time courses of both signals with respect to each other and computed the cross correlation with each shifting step (see 2.4.4). Note that the electrophysiological and fMRI signals were both sampled at a rate of 2.6 s, corresponding to the TR of fMRI data acquisition. Initial analysis showed that the strongest correlation peaks (for the gamma range BLP) were found at lags between 5.2 s and 7.8 s (Fig 4.2d). The value of this peak was taken as a measure of the correspondence between the electrophysiological and (inverted) CBV signal at each voxel individually, and provided spatial maps of spontaneous activity. Unthresholded correlation coefficients were then rendered onto a 3D reconstruction of the anatomical scan for the two monkeys individually (mrVista). For the cross-correlation plots, mean voxel time courses were computed from each of three regions of interest (ROIs) in each monkey (Fig 4.3a). Each ROI consisted of 9 voxels in a sphere, corresponding to 30 mm^3 of cortex. Two ROIs were in the grey matter, with one near the electrode (ROI 1) and one in the opposite hemisphere (ROI 2). The third ROI was located in the white matter, and served as a control.

4.3 Results

4.3.1 Widespread fMRI correlation with gamma range power

For 26 of the 52 runs, there was a prominent and stereotypic cross correlation between gamma-range BLP and rCBV signals (other runs showed no such relationship, see 4.2.1). This observed positive correlation between regional CBV and gamma power from V1 electrodes (grey and blue lines in left panel of Fig 4.3b), followed a time course resembling the haemodynamic impulse-response function (Logothetis et al., 2001;Shmuel and Leopold, 2008), peaking when the fMRI signal lagged the neural signal by approximately 7-8 seconds. Note that this correlation is slightly negative before time lag = 0. For ROI 2, the cortical ROI

distant from the V1 electrode in the opposite hemisphere, a similar relationship was found between rCBV and V1 gamma LFP (Fig 4.3b, middle panel). This relationship was nearly absent, however, in the control ROI taken from the white matter (Fig 4.3b, right panel).

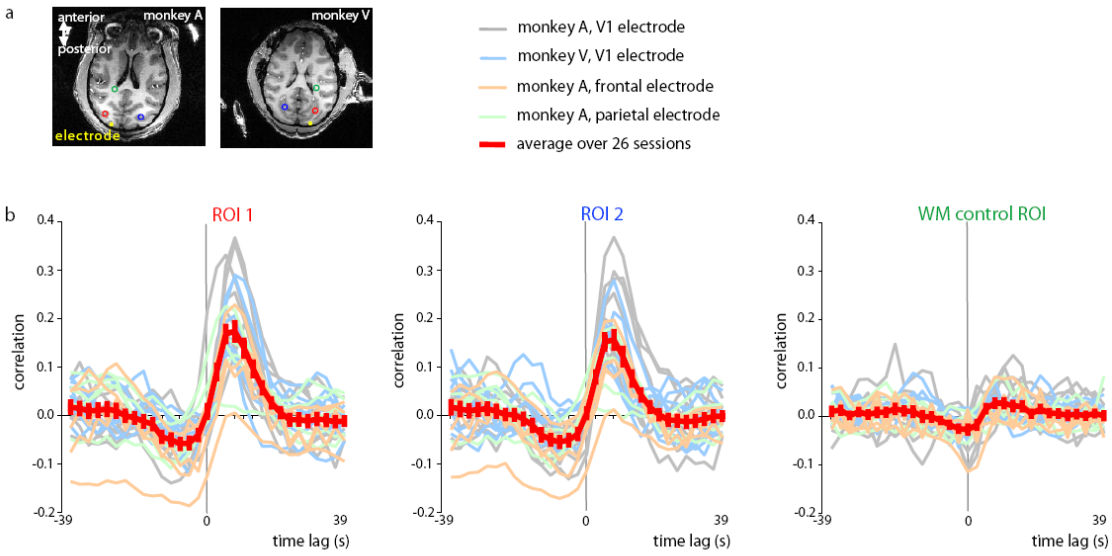

Figure 4.3 Covariation between high-gamma power fluctuations and fMRI fluctuations as a function of temporal lag. (a) *The regions of interest in monkey A (left) and monkey V (right) for which the average rCBV time course was computed. Circles show the regions of interest for panel* ***b*** *(red = ROI 1, blue = ROI 2, green = WM control ROI, yellow = electrode position).* ***(b)*** *The correlation of the average rCBV time course with the high gamma (40-80 Hz) power fluctuations is shown as a function of temporal lag. The faint curves show the correlation from each experiment (see legend for details); the red curve shows the average over 26 runs in the two different monkeys (mean ± SEM). The left panel shows the cross correlation function for ROI 1, in the ipsilateral hemisphere (same hemisphere as the electrode site), the middle panel shows the function for ROI 2, in the contralateral hemisphere, and the right panel show the cross correlation for the control ROI in the white matter.*

The similar results for nearby and distant ROIs indicated that this correlation is not restricted to the region around the electrode, but rather that it was quite widespread. Additional recordings in monkey A further indicated that this correlation was not specific to neural signals measured in area V1. In fact, very similar results were obtained from these ROIs when the gamma LFP power was recorded from electrodes in the frontal or the parietal lobe (green and orange lines in Fig 4.3b). These data suggest that widespread fluctuations in cortical gamma LFP power covary with widespread changes in the rCBV.

The spatial distribution of this correlation can be seen for the V1 electrode in monkey A and monkey V in Figs 4.4a and 4.5a, respectively. Note that the correlation coefficient is uniformly high for both monkeys in the cerebral cortex of the occipital lobe, where the V1 signal was measured, whereas it falls off in anterior parts of the brain. Interestingly, the correlation in the occipital lobe was even stronger with the gamma LFP power measured from the frontal electrode than from the V1 electrode (Fig 4.6a). This suggests that the stronger correlation in the occipital lobe is independent of electrode position, and might instead be due to the signal to noise ratio (SNR) of the radiofrequency (RF) coil, which had a posterior to anterior gradient. In all cases, the correlation was bilateral. The temporal evolution of this spatial pattern, corresponding to different lags in the cross correlation function, is shown in Figs 4.4b, 4.5b, and 4.6b. Here, the data are plotted on the surface of a 3D reconstruction of the brain for the two monkeys.

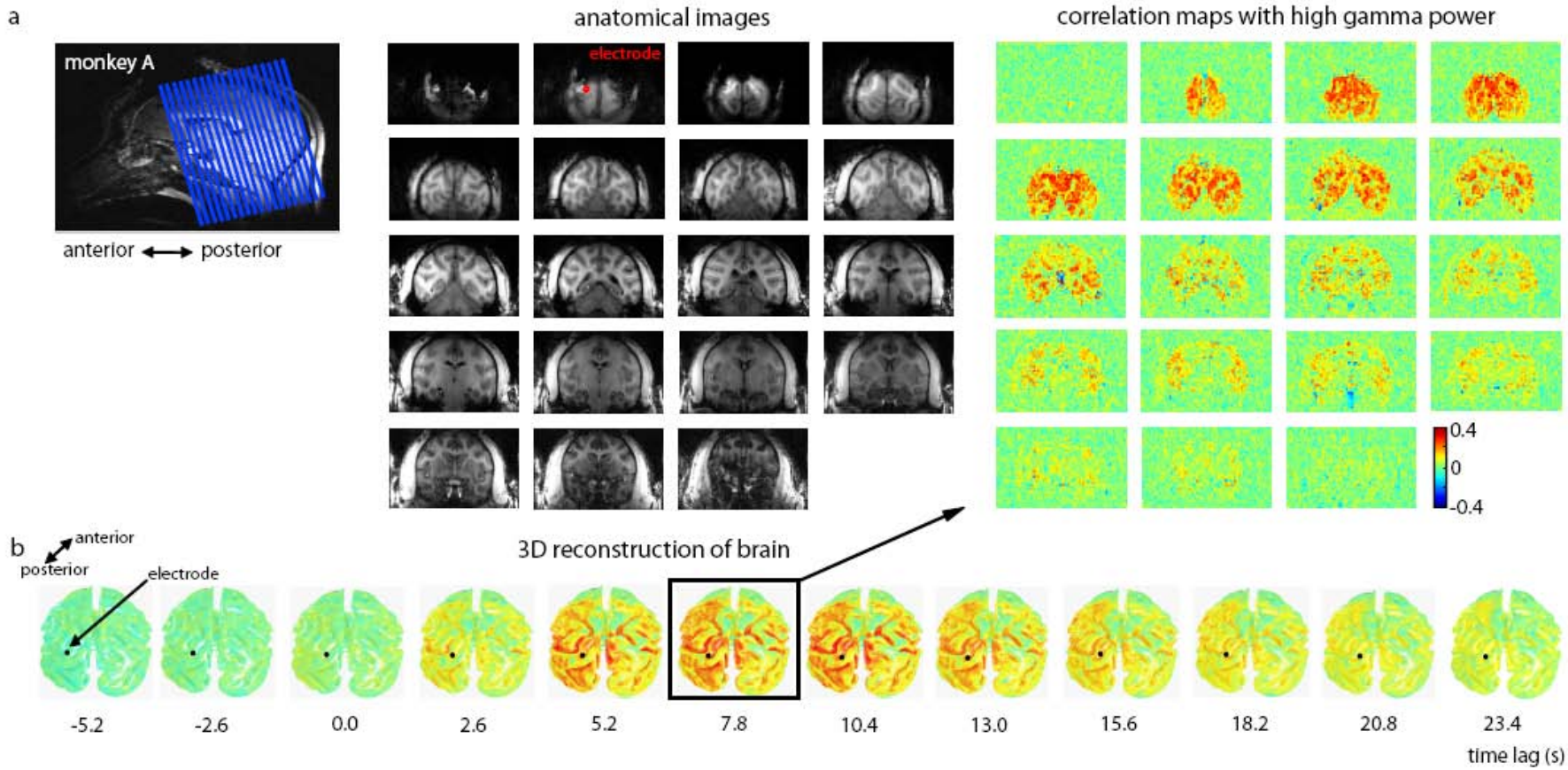

Figure 4.4 Spatial extent of the correlation between the neural signal in V1 and spontaneous fMRI fluctuations in monkey A. (a) *Correlation maps from a single run, obtained at a temporal lag of 7.8 s are shown for 19 coronal slices in monkey A. The image at the top-left corner of the grid is from the most posterior slice. The position of the electrode is shown in red on slice 2.* ***(b)*** *Correlation maps from the same run as a function of temporal lag are shown on an inflated 3D reconstruction of the monkey's brain. The boxed reconstruction shows the correlations at the same time lag as the slices in* ***a****. The temporal coupling between the two signals and the large spatial extent of the correlations are clearly visible.*

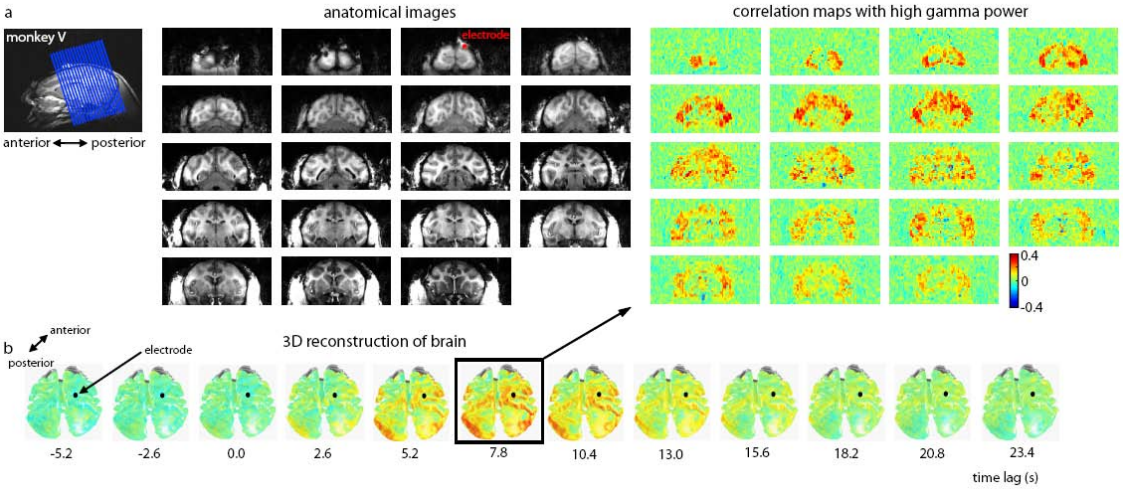

Figure 4.5 Spatial extent of the correlation between the neural signal in V1 and spontaneous fMRI fluctuations in monkey V*. For details, see Fig 4.4.*

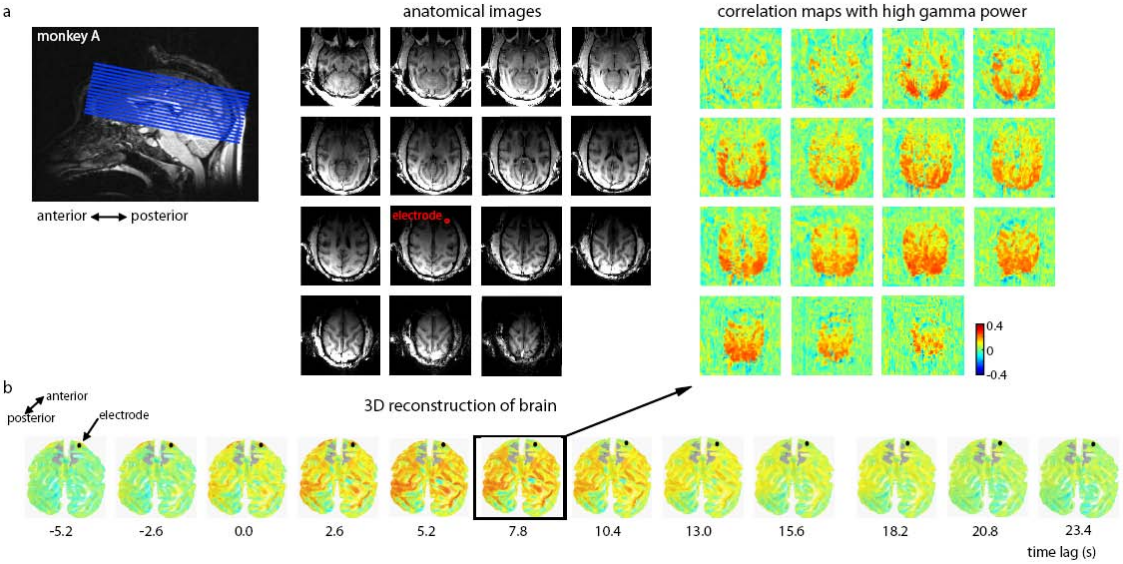

Figure 4.6 Spatial extent of the correlation between the neural signal in frontal area 6d and spontaneous fMRI fluctuations in monkey A*. Note the strong correlation in the occipital lobe. For details, see Fig 4.4.*

4.3.2 No LFP power correlation with infraslow CBV fluctuations

The resemblance of the neural/haemodynamic correlation function to a typical haemodynamic impulse-response function (Fig 4.3b) implies that shifting the fMRI and gamma power signals by more than ~40 seconds yields no correlation (since the graphs show zero correlation at < -20 s lag or > 20 s lag). This suggests that either there are no fluctuations on a slower timescale than 40 seconds present in these signals, or that these fluctuations are essentially uncorrelated. In order to examine the presence of such infraslow fluctuations, we plotted the power of the fMRI signal and the high gamma power as a function of frequency (Fig 4.7a and b). Note that neither signal type is high-pass filtered. While both signal types showed higher power at lower frequencies, the slope of drop-off for gamma power was markedly lower than for CBV. Importantly, the coherence between the two signals showed a distinct peak at approximately 0.025 Hz, which corresponds to the 40 s timescale observed in the correlation function (Fig 4.7c).

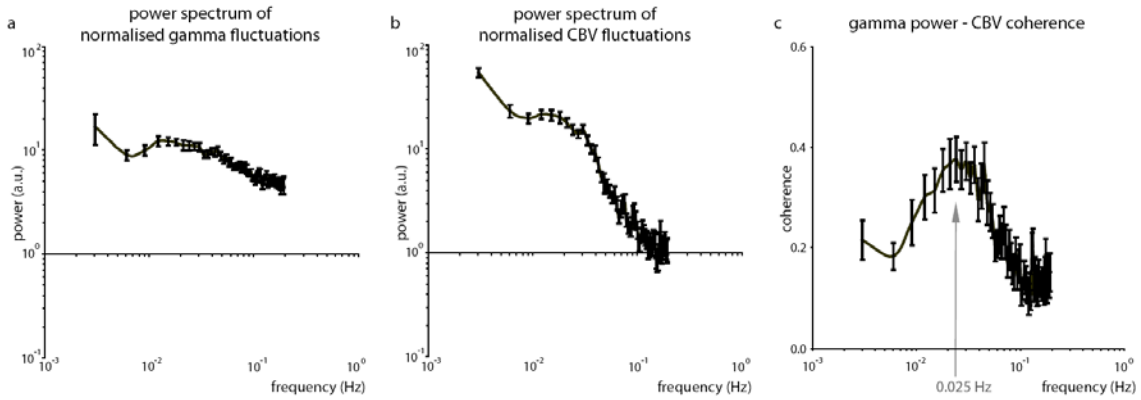

Figure 4.7 Coherence between high-gamma power and fMRI fluctuations. *Analysis of the power spectra of the gamma power signal and the fMRI signal revealed approximately constant power across frequencies for the high gamma power* ***(a)*** *and a decrease in power as a function of frequency following a characteristic 1/f shape for the fMRI signal* ***(b)****.* ***(c)*** *The correlation between these two signals as a function of frequency showed a peak in the coherence around 0.025 Hz.*

4.3.3 Correlation as a function of LFP frequency range

We performed a similar analysis for frequencies outside the gamma range, shown in Fig 4.8. The data in Fig 4.8a show the cross correlation as a function of LFP frequency and temporal lag for all sessions, computed using the fast Fourier transform (FFT) magnitude spectrum of the LFP in each gap period (see 4.2.8). This analysis provides an estimate of the root power corresponding to each fMRI time point, similar to the BLP approach, but with a high frequency resolution (but lower signal to noise ratio). The frequencies between the 40 Hz and 80 Hz dotted lines correspond to the high gamma BLP (Figs 4.3-4.7). Note that the pattern of covariation in these frequencies is consistent over a large range of the gamma signal, between approximately 32 Hz and 100 Hz. Unlike the gamma range, lower frequencies were highly variable in their relationship to the rCBV signal, as can be seen in the correlation of the other frequency ranges, shown for all sessions in Fig 4.8b. The correlation differed over sessions, between the two monkeys, and between electrode positions. This variability was present in all of the frequency ranges measured *except* the high-gamma range (Fig 4.8b). Note that other frequencies had, in some cases, very strong correlation functions (e.g. the delta and theta BLP from the frontal and parietal electrodes), which can be seen at low frequencies in Fig 4.8a; however, both the magnitude and time course of the cross correlation function was inconsistent compared to that of the high-gamma power.

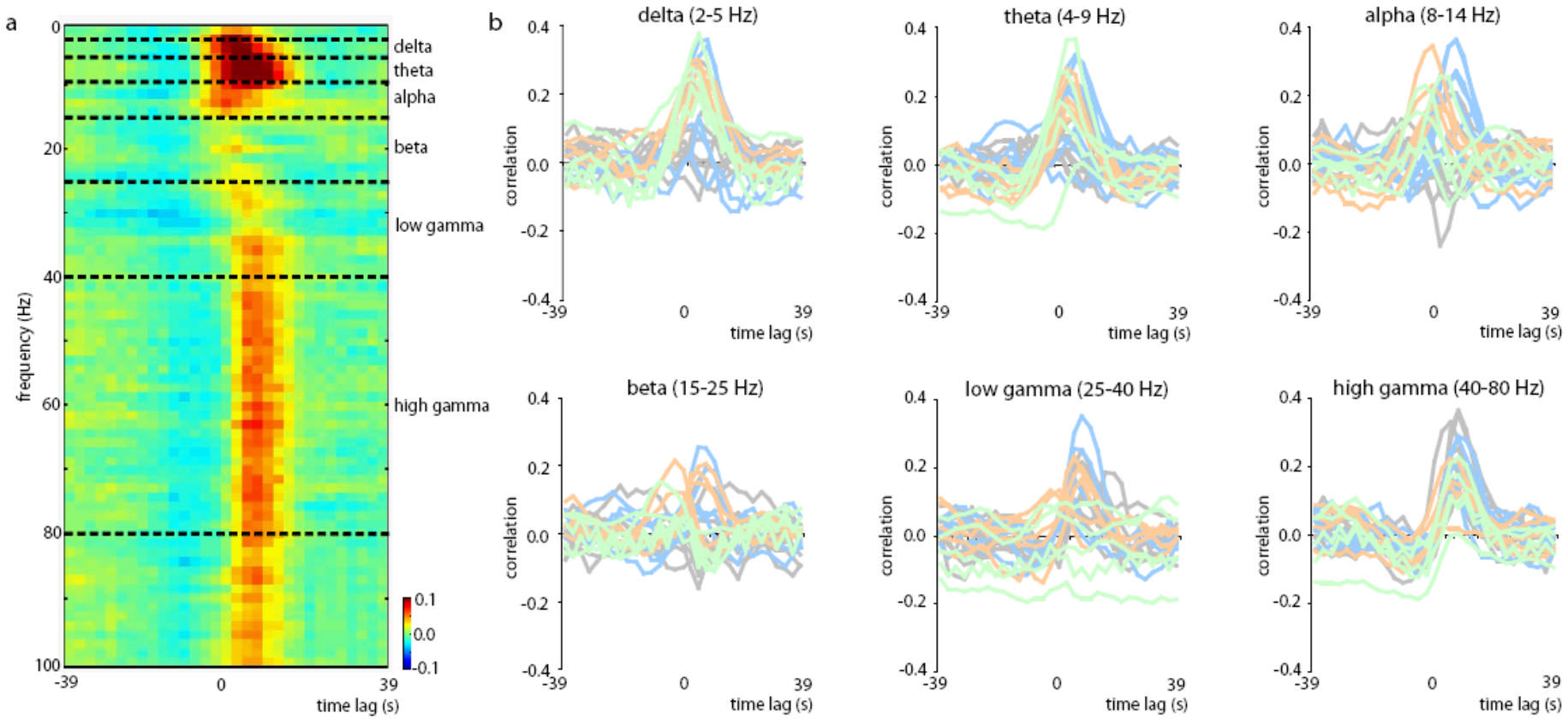

Figure 4.8 Covariation between LFP power fluctuations and fMRI fluctuations as a function of frequency and temporal lag. ***(a)*** *The correlation of all frequencies with the average rCBV time course in ROI 1 (see Fig 4.3a) as a function of temporal lag.* ***(b)*** *The correlation with the average rCBV time course as a function of temporal lag is shown for all frequency bands. The faint curves show the correlation from each session (see legend of Fig 4.3b for details).*

4.3.4 State dependence of correlation

Finally, we examined the time course of the high-gamma correlation with fMRI activity in V1, and related it to the animals' behavioural state. The animals' alertness was gauged by an infrared video camera monitoring their face throughout the experiment. We evaluated the strength of correlations within a session and between sessions, based on the level of alertness. This analysis revealed that the strength of the correlation between the fMRI and high-gamma power was not constant, but changed markedly over time.

Fig 4.9b shows a running correlation between the two signals for one session, computed between the electrode in area V1 in monkey A and the rCBV time course in ROI 1 and ROI 2, the ipsilateral and contralateral ROIs in the grey matter, respectively (Fig 4.9a). This analysis revealed that the strength of correlation can vary substantially over a period of several minutes. Further analysis in single sessions suggested that these changes were tightly linked to the monkey's behavioural state, with the highest correlation found when the eyes were closed (Fig 4.9c, top panel). These changes could not be ascribed to changes in the gamma LFP power, which remained similar throughout (Fig 4.9c, middle panel). Statistical analysis over all sessions confirmed that there was no significant difference in gamma power between periods when the eyes were open or closed ($t(21) = 1.38$, $p = .179$). The variance in the rCBV signal (Fig 4.9c, bottom panel) was slightly higher during periods when the eyes were closed ($t(21) = 2.65$, $p = .015$). Over sessions, proportion of 'eye open time' was negatively correlated with the strength of neurovascular coupling during the resting state (Fig 4.9d).

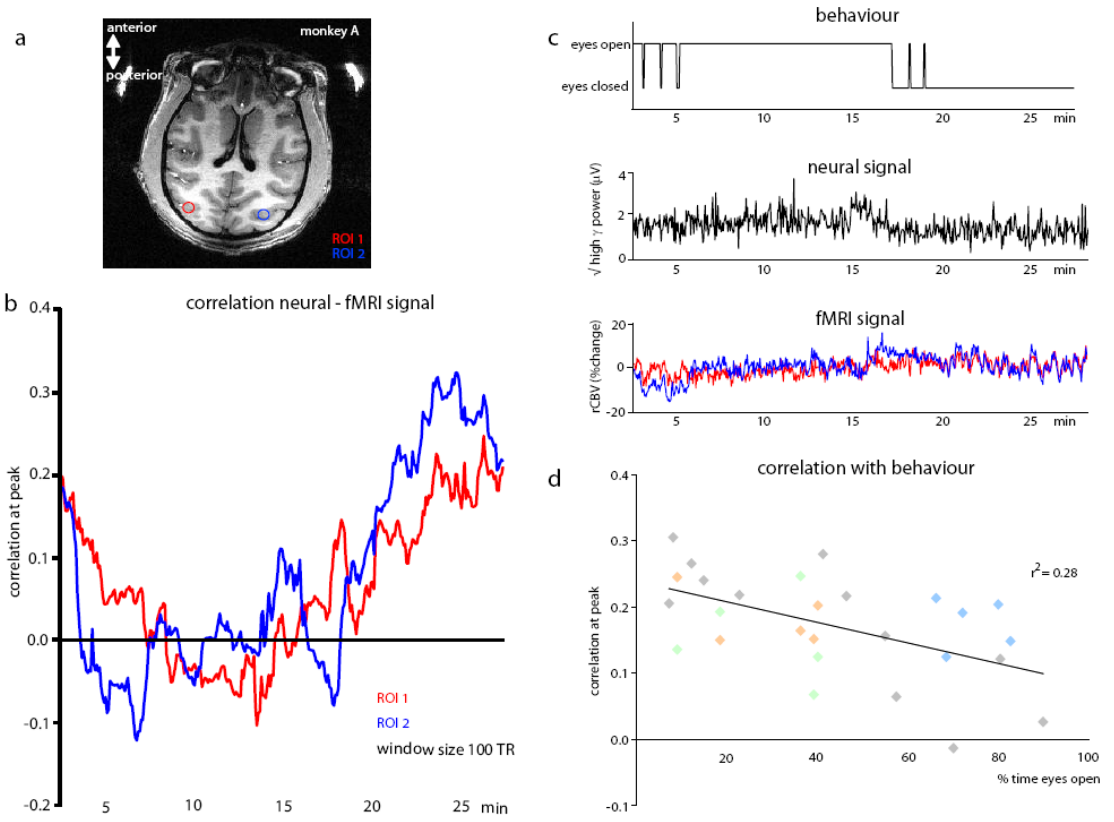

Figure 4.9 Nonstationarity of correlations. ***(a)*** *The correlation of the rCBV signal with the high gamma power was computed over time in ROI 1 and ROI 2 in monkey A (red, ROI 1 ipsilateral to the electrode; blue, ROI 2 contralateral to the electrode).* ***(b)*** *Our analysis demonstrates that this correlation (computed using a sliding 100 TR window) changed strongly over the duration of one specific run.* ***(c)*** *The strength of the correlation followed the eye openings and closures of the monkey (top panel), though high gamma (40-80 Hz) power and average raw rCBV intensity from the two ROIs did not change significantly during this run (middle and bottom panel).* ***(d)*** *Analysis of all runs from both monkeys revealed a negative correlation between the % of total time the monkeys' eyes were open and the overall strength of the correlation with high gamma power. Colours of the diamonds reflect the different sessions (see legend of Fig 4.3b for details).*

4.4 Discussion

4.4.1 Widespread, state dependent gamma correlation

Resting-state fluctuations are routinely used to study functional networks in the human brain, taking temporal correlation in fMRI activity as evidence for neural interaction between areas. Here we demonstrate widespread correlation of the grey matter rCBV signal to gamma-range LFP power sampled from a single position in the cerebral cortex. In accordance with (but not proving) a causal relationship between the neural and fMRI signal, the rCBV changes lagged behind changes in the gamma LFP by 7-8 s. Infraslow fluctuations in the gamma power and fMRI signal (< 0.025 Hz) did not contribute to this cross correlation function. The correlation between the fMRI signal and lower frequency LFP ranges was more variable. Finally, we show that the correspondence between the fMRI signal and the high-gamma power is nonstationary over time and is more robust when the monkey's eyes are closed; thus, the effective neurovascular coupling is a function of the monkey's behavioural state.

4.4.2 Global signal removal

FMRI resting-state studies routinely remove the spontaneous BOLD fluctuations common to the whole brain (the so-called global signal) in order to reveal functional networks in the data (Fox et al., 2006a;Macey et al., 2004). The assumption underlying this data processing step is that these common BOLD fluctuations are caused by physiological factors such as changes in heart rate and respiration (Fox et al., 2009). However, the widespread correlation that we observe between the LFP power and the fMRI signal throughout large swathes of the cerebral cortex suggests that some portion of the global signal that is routinely removed is closely linked to neural activity. This realisation has implications for the interpretation of functional networks found in resting-state data and especially for negative (so called anti-) correlations found between a subset of these

networks (see 2.3.5), which might be interpreted as slightly below average, yet still positive, correlations in neural activity between different networks of functionally connected brain areas (Fox et al., 2009;Murphy et al., 2009).

4.4.3 Origin of resting-state fluctuations

The widespread fMRI correlation to the gamma LFP power was observed for electrodes positioned in several different regions of the cerebral cortex (frontal, parietal, and occipital). This common correlation to the fMRI signal suggests that the gamma LFP power across distant cortical areas is also highly correlated, as has indeed been found in intracranial electrocorticography recordings in humans (Nir et al., 2008). The present data are insufficient to further investigate this possibility, but future LFP recordings from two or more of these frontal, parietal, and occipital electrode sites outside the MRI scanner environment should hopefully shed more light on this issue. Also the basis of the globally shared fMRI and neural signal is at present a matter of speculation. One possibility is that it reflects a cortex-wide modulation of neural activity from a subcortical structure, such as the ascending reticular activating system. Such a system could have a widespread, modulatory effect on neural activity over large portions of the cerebral cortex, which could lead to corresponding vascular responses via local neurovascular coupling. BOLD resting-state fluctuations in both cortical hemispheres have been shown to be strongly correlated to fluctuations in their contra- and ipsilateral thalamus (Zhang et al., 2008), thus highlighting the potential importance of thalamocortical pathways in the resting state. Alternatively, the neural and vascular response could be modulated independently by some other mechanism, such as the release or circulation of chemicals that affect both vascular and neural tone.

4.4.4 Implications for neurovascular coupling

Our observation of nonstationarity in the correspondence between the fMRI signal and the underlying neural activity has implications for the understanding of neurovascular

coupling. The neurophysiological basis of the fMRI signal has been studied almost exclusively in the context of evoked activity, that is, in the context of the response to a stimulus (Logothetis et al., 2001;Niessing et al., 2005;Viswanathan and Freeman, 2007). That work has shown that fMRI responses are tightly linked with neural activity, and particularly synaptic activity thought to be reflected in the LFP. At the same time, there is growing consensus that the relationship between the fMRI signal and the underlying neural activity is a complex one, since numerous physiological factors contribute to the modulation of microvasculature (Attwell and Iadecola, 2002). Indeed, a recent study in monkeys found that vascular responses in the primary visual cortex could be observed in the absence of significant local neural correlates (Sirotin and Das, 2009). Our findings demonstrate that observed neurovascular coupling is itself dynamic and subject to behavioural state. Recent work has shown that both fMRI (Bianciardi et al., 2009a;Moeller et al., 2009) and neural (Nir et al., 2007;Nir et al., 2008) signals independently vary as a function of behavioural state.

4.5 Conclusion

Using simultaneous LFP-fMRI measurements in awake monkeys, we demonstrated widespread correlation between high-gamma range power measured at various electrode sites and fluctuations in the fMRI signal at rest. The correlation peaked when the fMRI signal lagged behind the LFP power by 7-8 seconds, was nonstationary over time, and depended on the monkey's behavioural state. These findings have implications for the analysis as well as for the interpretation of fMRI resting-state fluctuations. The dynamic interplay between resting-state fMRI fluctuations and neural processing is explored in more detail for the visual cortex in the next chapter.

Chapter 5 Spontaneous and Evoked Activity in Visual Cortex

5.1 Introduction

Spontaneous fluctuations in the fMRI signal acquired in the resting state have been predominantly used to study networks of functionally related areas in the brain (Biswal et al., 1995;Fox et al., 2006a;Greicius et al., 2003). The fact that these resting-state fluctuations are partly vascular in origin (Birn et al., 2006;Wise et al., 2004) has complicated the interpretation of such analyses (Fox et al., 2009). However, as demonstrated in the previous chapter, there is evidence emerging that the correlated fluctuations between fMRI activity in distant brain areas reflect correlated neural activity (He et al., 2008;Nir et al., 2008;Shmuel and Leopold, 2008). This makes the existence of functional networks in resting-state activity more plausible, but more importantly, it raises the question of how these spontaneous fluctuations in neural activity impact local neuronal processing, and thereby indirectly behaviour.

In contrast to the vast body of research on resting-state functional networks, this aspect of resting-state activity has remained relatively unexplored. In the motor cortex, spontaneous fMRI activity has been shown to partly account for trial-to-trial variability in activity evoked by simple button presses (Fox et al., 2006b) as well as in motor behaviour, measured as button press force (Fox et al., 2007). In this work, the contribution of spontaneous activity to the BOLD response evoked by the button presses was determined using the spontaneous activity in the motor cortex in the opposite hemisphere as an estimate. An alternative way to assess the impact of spontaneous activity on stimulus processing is to investigate fMRI activity just prior to the stimulus. For example, the level of prestimulus activity in the right fusiform face area (FFA) influences the probability of subsequently perceiving the well-known Rubin face/vase illusion as a face or a vase (Hesselmann et al., 2008a), and

prestimulus activity in right V5/MT correlates with the probability that participants detect motion coherence in random dot displays (Hesselmann et al., 2008b).

In this chapter, I investigate the contribution of spontaneous activity to local stimulus processing in the primary visual cortex (V1). Several lines of evidence suggest that activity in V1 does not merely reflect sensory input per se, but rather the perceptual outcome of that sensory input (Ress et al., 2000;Ress and Heeger, 2003). Specifically, V1 activity is greater when participants correctly discern the presence or absence of a stimulus at perceptual threshold than when they fail to do so (Ress et al., 2000), and is also greater when participants incorrectly perceive an absent stimulus to be present (false alarm) than a present stimulus to be absent (miss) (Ress and Heeger, 2003). Using a similar task to Ress and Heeger (2003) and an improved analysis method similar to Fox et al. (2006b), I investigate whether these fluctuations in perception and corresponding V1 activity can be attributed to spontaneous fMRI fluctuations. Can spontaneous fMRI activity account for trial-to-trial variability in evoked responses? How does it interact with this stimulus-evoked activity? And does spontaneous activity influence the perceptual outcome of a stimulus?

5.2 Materials and Methods

5.2.1 Observers and stimuli

Six healthy volunteers with normal vision (22-35 years old; 3 female) gave written informed consent to participate in the experiment, which was approved by the local ethics committee. They viewed a low-contrast (luminance ~ 25.5 cd/m^2) stimulus on a uniform grey background (luminance ~ 28.4 cd/m^2) (Fig 5.1a). The stimulus was a circle composed of dark and light grey random noise, on which a low-contrast Gabor-grating (frequency: 0.93 degrees) was superimposed in half the trials. There was no detectable difference in luminance between the random noise alone and the noise plus the Gabor-grating, as

measured with a photometer. The stimulus was displayed in the upper left visual field at 7.5 degrees eccentricity (4.0 degrees up, 6.4 degrees across) and was 4.0 degrees in diameter. Observers were instructed to attend to a central fixation dot while the stimuli were presented briefly (1 second), after which the fixation dot immediately turned red to indicate that a response was required. Participants responded with their right hand using a keypad; they were required to press either the right button (grating present) or the left button (no grating present) within a one second response window. The inter-stimulus interval (ISI) was randomised to minimise anticipation; the next stimulus followed after 20 – 30 s.

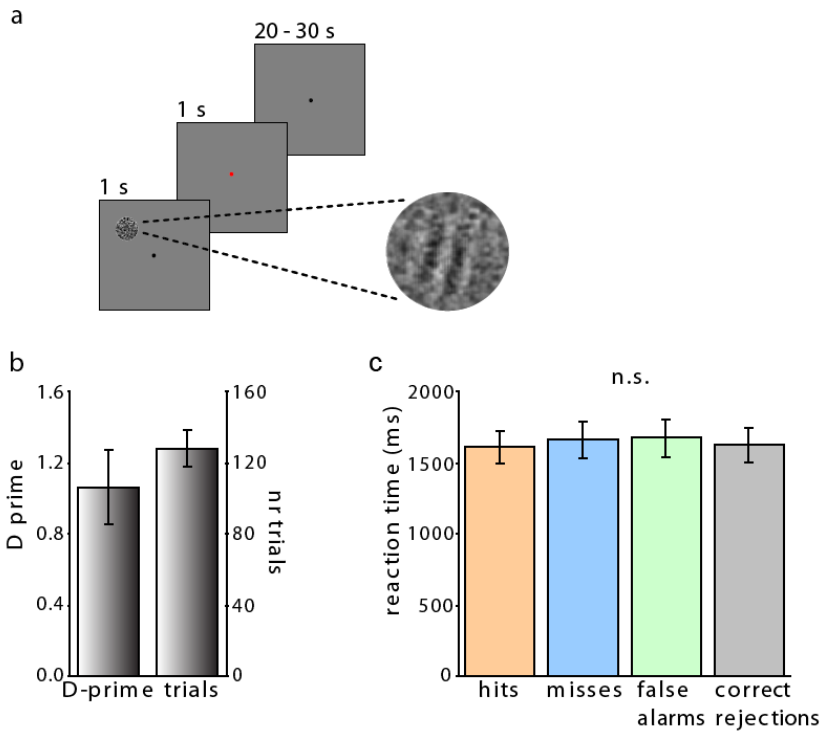

Figure 5.1 Task and behavioural data. (a) *Participants were shown a small circle in their left upper visual field, which consisted of noise or noise plus an embedded low contrast grating (shown here; grating has higher contrast than in the actual experiment for illustration purposes). The stimulus was shown for 1 s, after which participants had 1 s to respond (indicated by the fixation dot turning red). Inter-stimulus intervals were 20-30 s.* ***(b)*** *Average D-primes (left) and number of trials (right) for all participants.* ***(c)*** *Average reaction times for all participants divided into the four response categories (hits in orange, misses in blue, false alarms in green, correct rejections in grey; these colour codes are used throughout the figures in this chapter).*

5.2.2 Procedure

Participants were tested before the scanning experiment to ensure they could assign consistent responses to the different stimuli (noise and noise + grating). Their performance was held constant at 75% correct (D-prime ~1) by means of a staircase procedure. They performed another staircase block in the scanner before data recording. The contrast of the grating was individually set to the level determined by the staircase procedure. Subsequently they completed between 9 and 12 six minute runs of scanning, acquired in two separate sessions. A run started with instructions for the button presses on the screen, then a 10 second blank followed by a stimulus every 20-30 seconds. In the middle of the first session, a rest run was acquired during which the participants were instructed to close their eyes and relax for six minutes. This run was used to estimate the resting-state fluctuations (see 5.2.5). In the middle of each session, fieldmap scans were acquired (see 5.2.4). In between the functional runs, participants were given two runs of ROI localiser (see 5.2.3). Standard retinotopic (meridian) maps (see 5.2.3) and T1-weighted structural scans were acquired in a third, separate session.

5.2.3 Retinotopic mapping and ROI localiser

Each participant completed two successive scanning runs of a conventional retinotopic mapping procedure, viewing a contrast-reversing, black-and-white checkerboard stimulus presented in alternating 15 second blocks as horizontal or vertical wedges placed to cover either horizontal or vertical meridians for V1, V2, and V3 localisation (Sereno et al., 1995;Teo et al., 1997;Wandell et al., 2000). The retinotopic representation of four locations in the visual field (the stimulus location and its mirror locations in the other hemisphere and in both lower visual fields) in the early visual areas was determined by measuring brain activity while participants viewed black-and-white checkerboard stimuli flickering at 10 Hz on a grey background. The additional three locations were tagged for use in another experiment which is not described in this thesis. The checkerboard stimuli were circles of

identical size and eccentricity as the stimulus used in the actual experiment. Alternating 15 second periods of the left-upper and right-lower, versus the right-upper and left-lower stimulus, were shown for 6 minutes per run. To attract attention to the stimulus, participants were required to press a button as soon as a small red dot flashed in any stimulus throughout these runs, while they fixated on the central fixation dot.

5.2.4 fMRI data acquisition

A 3T Allegra MRI scanner (Siemens Medical Systems, Erlangen, Germany) with a standard transmit–receive head coil was used to acquire functional data with a single-shot gradient echo isotropic high-resolution echo planar imaging sequence (matrix size 64 x 72; field of view 192 x 216 mm; in-plane resolution 3 mm; 32 slices in descending acquisition order; slice thickness 2 mm with a 1 mm gap; echo time 30 ms; acquisition time per slice 60 ms; TR 1,920 ms). Each functional run comprised 180 volumes. In the middle of each session, double-echo FLASH images with TE1 10 ms, TE2 12.46 ms, 3x3x2 mm resolution, and 1 mm gap were acquired. These fieldmaps were used to correct geometric distortions in the EPI images due to field inhomogeneities. During scanning, respiration volume and heart rate were measured using a breathing belt placed round the participant's waist and an infrared clip on one finger. These data were sampled using the programme Spike (www.ced.co.uk) and used for physiological noise correction (see 5.2.5). Eye position was continually sampled at 60 Hz using an ASL 504 LRO infrared video-based MRI compatible eye tracker (Applied Science Laboratory, Bedford, MA). For four participants, half of the eye data could not be analysed due to technical difficulties. Eye movements were defined as variance round the mean (x,y) position of the eye. Statistical analysis was performed to confirm stable fixation throughout the experiment.

5.2.5 fMRI analysis of retinotopic data

Functional data were analysed using SPM5 (www.fil.ion.ucl.ac.uk/spm/software/spm5/). The first 5 images of each run were discarded from further analyses, to allow for T1 equilibration. Preprocessing of the data involved realignment of each scan to the first scan of the first experimental run, correction of slice time acquisition differences, coregistration of the functional data to the structural scan, and smoothing by a 6 mm Gaussian kernel. For the PPI analysis (see below), the data were normalised to the MNI template brain. The data were filtered with a 128-s cut-off, high-pass filter to remove low-frequency noise and adjusted for global changes in activity between runs. Physiological data (respiration and heart beat) were modelled using RETROICOR, which models the respiration volume per unit time (RVT), the respiration rate and its first 6 derivatives, and heart rate and its first 10 derivatives, as separate (confound) regressors in the design. Movement parameters in the three directions of motion and three degrees of rotation were also included as confounds.

For the ROI localiser data, the blocks of checkerboard stimuli in the left-upper and right-lower, and the right-upper and left-lower visual field were modelled as regressors. These regressors were convolved with a synthetic haemodynamic response function and entered into a General Linear Model, which produced activation maps of the four ROI localiser regions. The current analysis focused on activity in the ROI representing the stimulus location (ROI_{stim}; left upper visual field); the three other ROIs were not used in the present analysis. Retinotopic cortical areas were identified using Freesurfer (http://surfer.nmr.mgh.harvard.edu/). This yielded maps of functionally defined visual areas V1, V2, and V3 for each participant. These maps were combined with the ROI activation images to reveal retinotopic regions in V1, V2, and V3 representing the spatial location of the stimulus in the actual experiment (Fig 5.2a).

5.2.6 fMRI analysis of task data

For the task data, similar regressors modelling the stimulus, and movement and physiological parameters, were entered into a General Linear Model for each participant separately to produce activation maps of the stimulus at an FWE-corrected threshold. The preprocessed data from the task runs (i.e. the same data, but before they were entered into the GLM) and the rest run (eyes closed in darkness) were further processed in MATLAB (www.mathworks.com) using custom-made analysis tools. First, each voxel's time course was converted into units of percent change by first subtracting, and then dividing by the mean of its time course. Data were high-pass filtered at 0.005 Hz and any activity correlated with motion, cardiac and respiratory cycle (see above), and the average time course across all voxels (the 'global signal') were removed by linear regression to avoid spurious correlations in the data. The average time course of ROI_{stim} during the rest run was then used as a seed region to compute the correlation with the time courses of all other voxels in the brain (Biswal et al., 1995;Fox et al., 2006a) (Fig 5.2b). The resulting correlation map was masked with the activation map of the stimulus to exclude any voxels that were activated by the stimulus. Of those voxels that remained, the time courses of the 100 voxels with the highest correlation to the seed region during rest were multiplied by weight factors β to find the least squares estimate of the time course of the seed region (Fig 5.2c):

$$F = \beta_1 * f_1 + \beta_2 * f_2 + \ldots + \beta_{100} * f_{100} + \varepsilon \quad (5.1)$$

where F is the time course of the seed region, $f_1 \ldots f_{100}$ are the time courses of the correlated voxels, $\beta_1 \ldots \beta_{100}$ are the weight factors and ε is the error. Thus, the average time course of these 100 voxels during the rest run weighted by their respective β factors gives the best possible estimate of the spontaneous activity present in ROI_{stim}. This weighted average time course was termed $ROI_{control}$. We then turned to the task data. The individual BOLD response time courses to the stimulus, as well as the average BOLD response, were plotted for ROI_{stim} and $ROI_{control}$, and their signal power, noise power, and signal-to-noise ratio (SNR)

calculated. Signal power was computed as the mean squared deviation of the average BOLD response from baseline; noise power was computed as the mean squared deviation of the residual (individual BOLD response – average BOLD response). For each participant individually, the weighted average time course from the 100 control voxels ($ROI_{control}$) was subtracted from the ROI_{stim} time course ($ROI_{stim} - ROI_{control}$) (Fig 5.2d). This new ROI_{stim} time course was called the 'corrected' ROI_{stim} time course. The individual and average BOLD responses to the stimulus were plotted from the corrected ROI_{stim} time course and again the signal power, noise power, and SNR were calculated. These values were compared to the original values (before subtracting $ROI_{control}$). This procedure is similar to that employed by Fox et al. (2006b).

Statistical comparisons of the measures of noise power, signal power, and SNR were done at two different levels. The first level was a within subject comparison in which the noise power was computed for each individual trial. This allowed us to determine whether correcting for spontaneous activity led to a significant reduction in noise or a significant improvement in SNR for an individual participant. The second statistical analysis was at the group level. Here the noise power was averaged across trials for each individual, and it was determined whether there was a significant effect of correction for spontaneous activity on signal power, noise power, or SNR at the group level. For both within subject and group level analyses, significance was assessed using a Wilcoxon paired nonparametric test.

Similar analyses were performed for ROI_{stim} in extrastriate areas V2 and V3. As a side question to our main interest in the effect of spontaneous activity on local stimulus processing, we investigated the degree of coupling present between the spontaneous activity in the stimulus region in V1, V2, and V3. The coupling between these retinotopic regions under rest and task conditions was assessed by cross-correlating their time courses obtained in the rest run and the task runs.

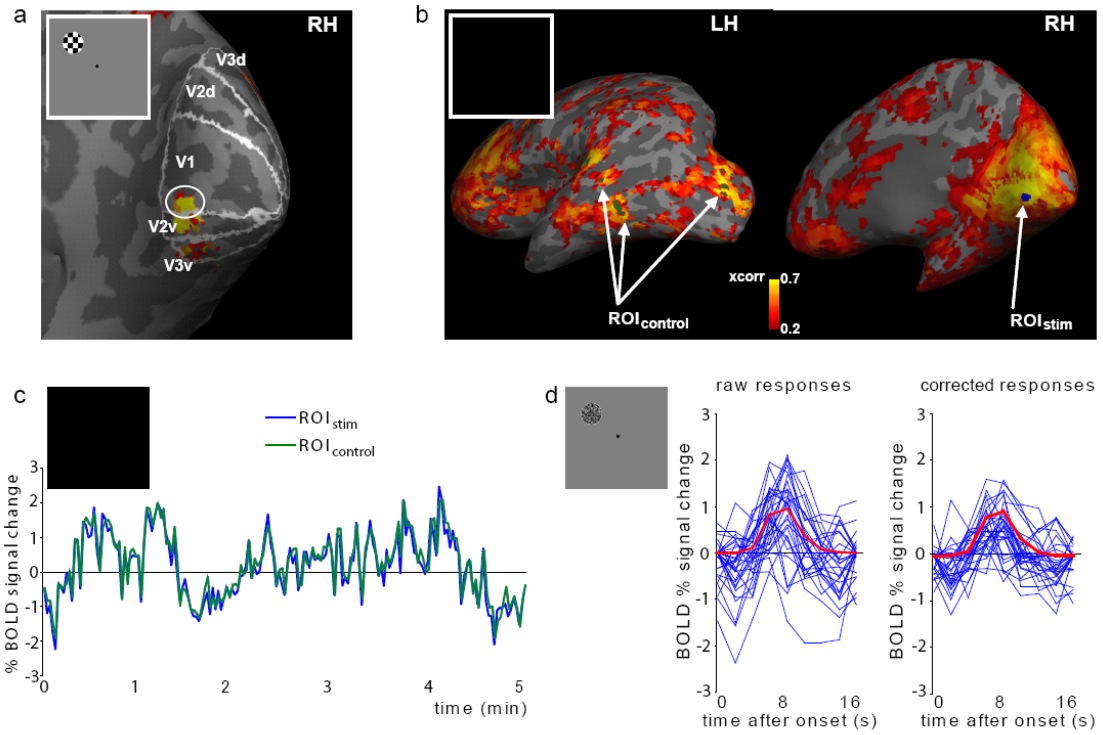

Figure 5.2 fMRI analysis. (a) *Combining activity evoked by a stimulus localiser (inset) with borders of the visual areas revealed by retinotopic mapping yielded retinotopic regions in V1, V2, and V3 representing the spatial location of the stimulus. The stimulus location in V1 (encircled) was chosen as* ROI_{stim}*. RH, right hemisphere.* ***(b)*** *The time course of* ROI_{stim} *(blue) during the rest run (inset) was correlated with all other voxels in the brain, and the 100 most correlated voxels were collectively termed the* $ROI_{control}$*, shown here in green.* ***(c)*** *The time courses of the 100 voxels in* $ROI_{control}$ *(green) were weighted by* β *values to arrive at the best possible estimate of the time course of* ROI_{stim} *(blue) during the rest run (inset).* ***(d)*** *Raw time courses of* ROI_{stim} *in response to the stimulus (inset) in the task runs were plotted (left; individual responses are shown in blue, the average response in red). The weighted average* $ROI_{control}$ *time course was then subtracted from the* ROI_{stim} *time course and the BOLD responses to the stimulus plotted again (right).*

5.2.7 PPI analysis

In order to investigate whether spontaneous and evoked BOLD activity are linearly superimposed (Fox et al., 2006b;Bianciardi et al., 2009a), or whether they interact in a nonlinear way (Hesselmann et al., 2008a;Hesselmann et al., 2008b), a psychophysiological interaction (PPI) was conducted, which took the form of the following GLM:

$$Y = \beta_1*E + \beta_2*S + \beta_3*(E*S) + \varepsilon \quad (5.2)$$

Activity evoked by the stimulus (E) and spontaneous brain activity (S) are modelled by the first two terms; the combination of (β_1*E + β_2*S) models brain activity that can be explained either by the stimulus alone (β_2 = 0), spontaneous activity alone (β_1 = 0), or a linear combination of the two. By excluding the first two possibilities with the use of masks, any brain activity explained by a linear combination of spontaneous and evoked brain activity can be revealed. The third term, on the other hand, specifically models brain activity explained by a nonlinear interaction between evoked and spontaneous brain activity.

5.2.8 fMRI analysis of behaviour

The effect of spontaneous BOLD activity on stimulus visibility was evaluated by averaging the evoked BOLD responses by response category (hits – misses – false alarms – correct rejections) and subtracting the estimate of the spontaneous activity provided by $ROI_{control}$. Differences in BOLD responses depending on response type were evaluated before and after this correction for spontaneous activity. In a cruder analysis, all trials were pooled into correct trials and incorrect trials and a similar analysis performed. The trials were then divided into two equally sized groups; those with high, and those with low spontaneous activity. In signal detection theory, two independent measures of stimulus visibility are given by D-prime and criterion; D-prime is a measure of discriminability, whereas criterion is a measure of the response bias of the subject (Macmillan and Creelman, 2005). D-primes and criterion values were separately calculated for the low and high spontaneous activity groups and statistically compared. If spontaneous activity affects the probability of perceiving the stimulus, then D-primes will be different between trials with low and high spontaneous activity. Alternatively, the level of spontaneous activity might influence the criterion value, which would lead to a criterion shift between low and high spontaneous activity levels.

5.3 Results

5.3.1 Behavioural data

On average, participants completed 128 trials over the two separate sessions. Their average D-prime was 1.06, which indicates that the grating embedded in the noise stimulus was at their perceptual threshold for detection (Fig 5.1b). The average reaction time to the stimulus was 1643 ms measured from stimulus onset; since participants were allowed to respond only after termination of the 1-second long stimulus, this RT is relatively long. The reaction times were not significantly different for the four response categories (hits – misses – false alarms – correct rejections) (Fig 5.1c). For individual participant data, see Table 5.1.

participant	nr trials	D-prime	RT hits	RT misses	RT false ala	RT corr reject
s1	119	1.11	1469 ms	1460 ms	1490 ms	1446 ms
s2	117	0.83	1744 ms	1744 ms	1770 ms	1703 ms
s3	141	1.22	1675 ms	1761 ms	1847 ms	1755 ms
s4	130	1.21	1595 ms	1715 ms	1684 ms	1666 ms
s5	139	1.25	1496 ms	1533 ms	1559 ms	1511 ms
s6	122	0.76	1673 ms	1747 ms	1697 ms	1682 ms

Table 5.1 Individual participants' behaviour. *For each participant, the total number of trials, D-prime, and reaction time for the four response types (hits – misses – false alarms – correct rejections) are shown.*

5.3.2 Spontaneous activity contributes to response variability

BOLD responses in V1 evoked by the stimulus exhibited considerable variation within participants (Fig 5.3a). These BOLD responses are a mixture of stimulus-evoked activity and underlying spontaneous activity. Subtracting the estimate of spontaneous activity provided by $ROI_{control}$ reduced the variability in the BOLD responses (Fig 5.3b). For this representative participant, the reduction in variability ('noise') was 25.4%; this decrease in variability was

highly significant (p<.0001). The average response (shown in red in Fig 5.3a,b) did not change when the contribution of spontaneous activity was subtracted, as demonstrated by a change in signal power of 0.0% for this particular participant. The resulting change in signal to noise ratio (SNR) was 34.0%; again, this increase in SNR was highly significant (p=.001). Note that the average response to the stimulus in $ROI_{control}$ is essentially zero (Fig 5.3c); this implies that $ROI_{control}$ was itself not activated by the stimulus, as was indeed ensured by masking the correlation map obtained for the rest run with the stimulus activation map (see 5.2.5).

Similar reductions in noise and corresponding increases in SNR were obtained for all participants (Table 5.2). Overall, variability in responses decreased by 25.5%, whereas the average response to the stimulus decreased by 1.7%, which resulted in a 32.2% increase in SNR. This decrease in variability was significant (p=.028), whereas the corresponding increase in SNR approached significance (p=.075).

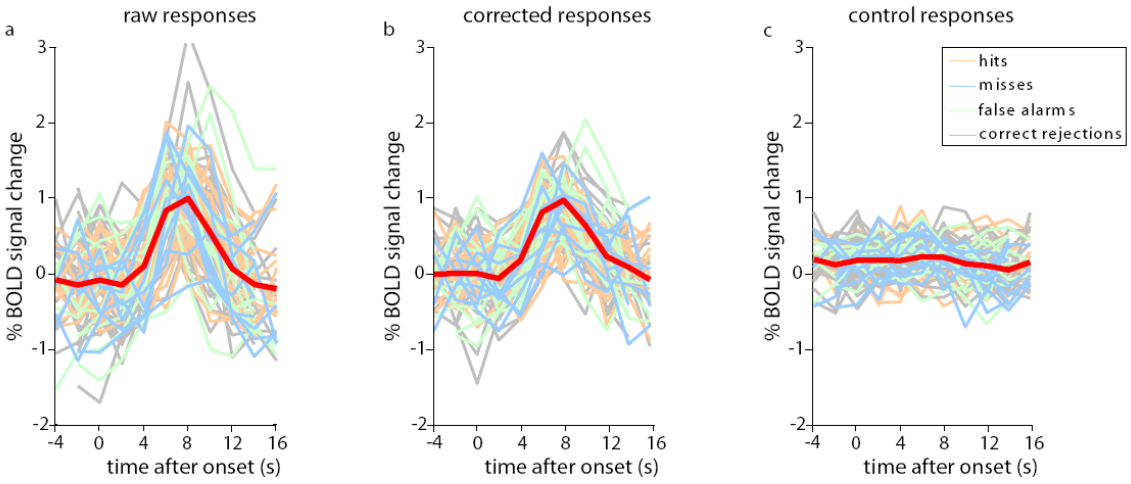

Figure 5.3 Effect of spontaneous activity on BOLD response variability in V1. (a) *The raw BOLD response is plotted for all trials of a representative participant. Individual trials are shown in thin lines (colour code: see legend); thick red line shows the average.* ***(b)*** *Subtracting the spontaneous activity reduces the variability in the evoked BOLD responses.* ***(c)*** *BOLD responses to the stimulus in $ROI_{control}$; the average was essentially flat, indicating that activity in $ROI_{control}$ is a true measure of spontaneous activity.*

participant	change in signal (%)	change in noise (%)	change in SNR (%)
s1	-2.0	-25.5*	31.5
s2	9.2	-20.3*	37.0*
s3	-1.2	-16.0	17.6
s4	0.0	-25.4*	34.0*
s5	-18.0	-33.9	24.0
s6	1.6	-31.8	48.9
ALL	**-1.7**	**-25.5***	**32.2**

Table 5.2 Changes in signal power, noise power, and SNR per participant. *Asterisks indicate significance. Note that the change in signal power (for individual participants) represents a single value and can therefore not be statistically assessed.*

5.3.3 Linear superposition of spontaneous and evoked activity

The above analysis demonstrates that spontaneous activity fluctuations in visual cortex account for a substantial fraction of the variability found in evoked BOLD signals in response to a visual stimulus. It does not reveal, however, whether spontaneous activity combines additively with the activity evoked by the stimulus, or instead interacts with this activity to produce the BOLD response that is observed. We therefore conducted a psycho-physiological interaction (PPI) analysis to assess the capability of stimulus-evoked activity and spontaneous activity to explain the observed BOLD responses. This analysis revealed expected activations in ROI_{stim} and motor cortex in response to the stimulus (Fig 5.4a). More importantly, it clearly showed that a linear combination of stimulus-evoked and spontaneous activity could explain the activity in large regions of visual cortex that could not be explained by the stimulus alone (Fig 5.4b). Further inspection of the data demonstrated that the average relative contributions of evoked and spontaneous activity in these visual areas were 74.8% and 25.2%, respectively. Note the similarity between this relative contribution of the spontaneous activity of 25.2%, and the amount of variability in the evoked BOLD

response accounted for by spontaneous activity (25.5%; see 5.3.2). A linear combination of evoked and spontaneous activity explained the data better than a nonlinear interaction between the two (Fig 5.4c).

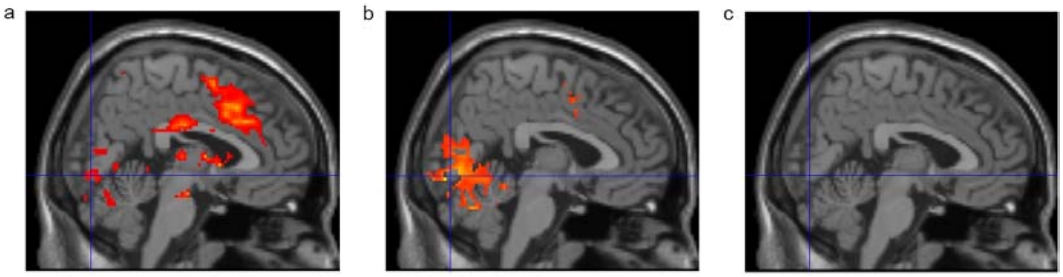

Figure 5.4 Linear superposition of spontaneous and evoked activity. (a) *Brain activity explained by the stimulus.* ***(b)*** *Brain activity explained by a linear combination of evoked and spontaneous activity.* ***(c)*** *Brain activity explained by a nonlinear interaction between evoked and spontaneous brain activity. A linear combination explains the data better than a nonlinear interaction. All maps are thresholded at p<0.05, FDR corrected. Cross-hairs intersect at the location of* ROI_{stim} *in V1.*

5.3.4 Extrastriate areas

The stimulus-evoked BOLD responses in areas V2 and V3 exhibited a similar degree of variability, although the overall response was slightly lower than in the primary visual cortex (Fig 5.5a,d). Similar to V1, subtracting the spontaneous activity (approximated by a $ROI_{control}$ optimised for V2 and V3, respectively) substantially reduced the variability in the evoked response (Fig 5.5b,e), resulting in an increase in SNR. Again, the average response to the stimulus in $ROI_{control}$ was essentially zero (Fig 5.5c,f). These results are for the same representative participant as the results in Fig 5.3; similar results were obtained in the other participants (data not shown). Overall, variability in responses decreased by 28.8% in V2 and 20.3% in V3, which resulted in an increase in SNR of 37.4% in V2 and 27.6% in V3.

The coupling between the three retinotopic stimulus regions in V1, V2, and V3 was assessed using cross correlation. Under rest conditions (eyes closed in darkness), the coupling between the three regions was significantly stronger than during task conditions (p=.010) (Table 5.3). Since these correlation coefficients were not corrected for cortical

distance between the three retinotopic regions, no definitive conclusions can be drawn about differential coupling between, for instance, V1-V2 and V1-V3.

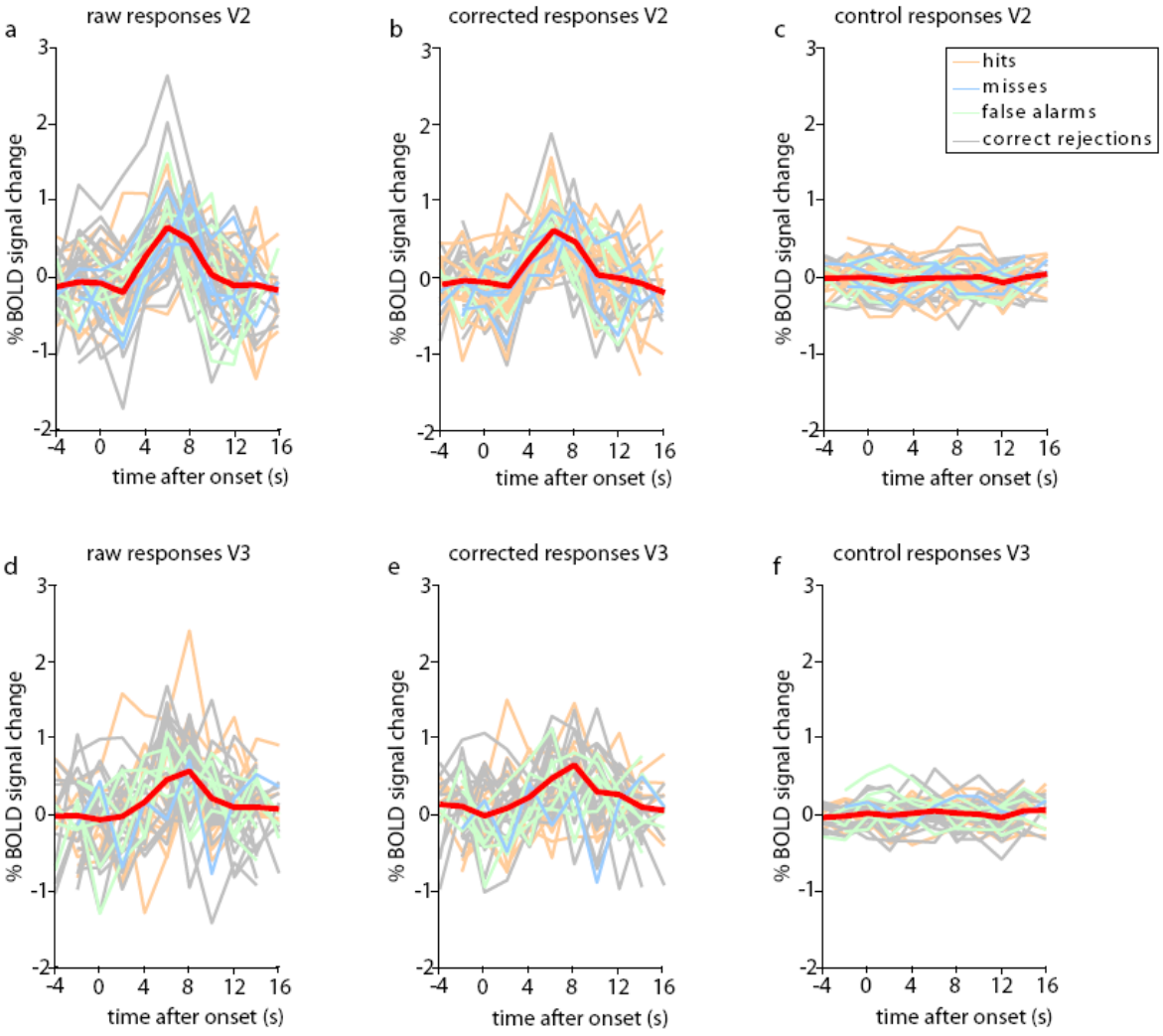

Figure 5.5 Effect of spontaneous activity on BOLD response variability in V2 and V3. (a,d) *The raw BOLD response is plotted for all trials of the same representative participant as in Figure 5.3.* ***(b,e)*** *Subtracting the spontaneous activity reduces the variability in the evoked BOLD responses.* ***(c,f)*** *BOLD responses to the stimulus in* $ROI_{control}$*. For details, see Fig 5.3.*

	V1	V2v	V3v
V1	1.00	0.67	0.31
V2v	0.74	1.00	0.47
V3v	0.47	0.66	1.00

Table 5.3 Correlation values between visual areas. *The average cross correlation coefficients between the retinotopic location of the stimulus in V1, V2, and V3 are shown under rest conditions (dark grey cells) and task conditions (light grey cells). The correlation coefficients are stronger under rest than under task conditions (p=.010).*

5.3.5 Effect of spontaneous activity on stimulus visibility

In order to investigate the potential role of spontaneous fluctuations on stimulus perception, we classified the BOLD responses based on perceptual outcome (hits – misses – false alarms – correct rejections). The average BOLD responses for the four response types were not significantly different (Fig 5.6a), in contrast to previous results obtained using a similar paradigm (Ress and Heeger, 2003). Our failure to detect any significant differences between the BOLD responses might have been due to a much lower number of trials in the present study. Likewise, subtracting the spontaneous activity from the raw responses (Fig 5.6b) or the spontaneous activity itself (Fig 5.6c) did not show any differences between the four response categories.

A cruder analysis, in which all correct (hits and correct rejections) and incorrect (misses and false alarms) trials were pooled, revealed slightly higher activity for correct trials compared to incorrect trials in the peak of the BOLD response (Fig 5.6d). This difference was diminished when the evoked responses were corrected for the contribution of spontaneous activity (Fig 5.6e); however, the same difference was not visible in the spontaneous activity itself (Fig 5.6f). Thus, we can conclude that spontaneous activity has a modest effect on perception, although it must be noted that this effect is very small and possibly obscured by the low number of trials per participant in our study.

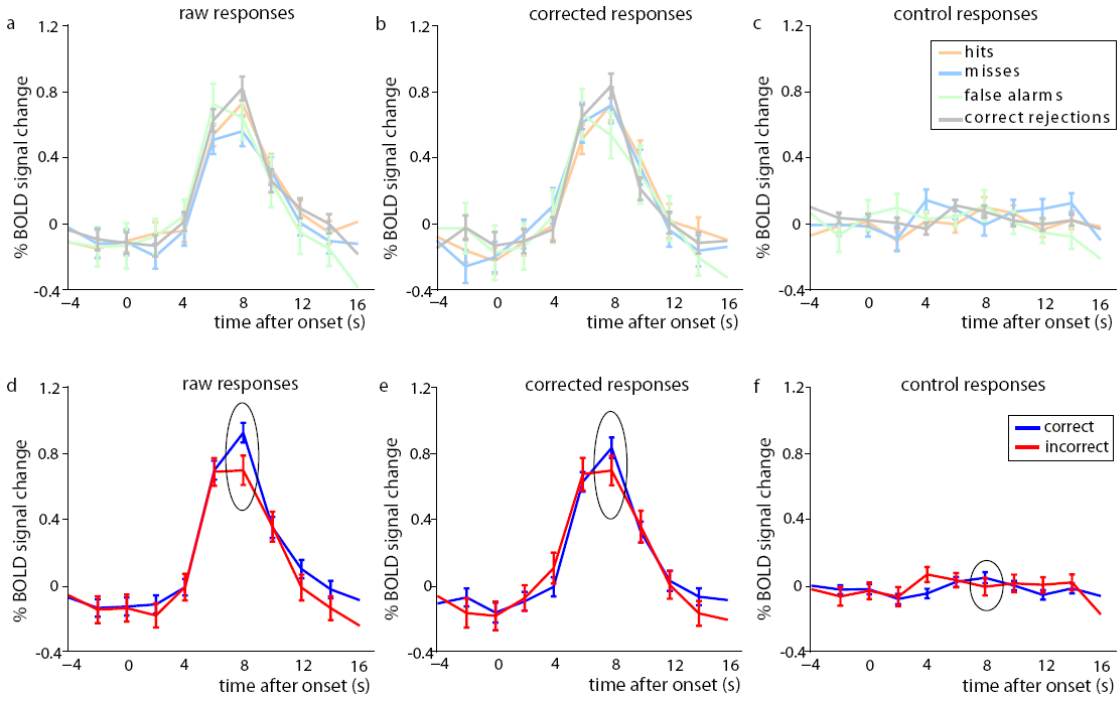

Figure 5.6 Effect of spontaneous activity on stimulus visibility. *BOLD responses in V1 were not significantly different for hits, misses, false alarms, and correct rejections, neither in the raw responses* ***(a)*** *nor in responses corrected for the spontaneous activity* ***(b)****.* ***(c)*** *Also the estimates of the spontaneous activity sorted by response category did not show any differences for the four response types.* ***(d)*** *A cruder division into correct and incorrect trials revealed slightly higher peak activity for correct versus incorrect trials (circle). This difference diminished when correcting for spontaneous activity* ***(e)****, though the same difference was hardly visible in the spontaneous activity itself* ***(f)****.*

Dividing all trials per participant into low and high spontaneous activity trials and separately calculating D-primes and criterion values for each group (see 5.2.5) did not yield any significant differences in D-prime or criterion shifts that depended on the level of spontaneous activity.

5.3.6 Other influencing factors

Spontaneous activity is partly responsible for the variability observed in evoked BOLD responses and to a slight degree responsible for differences in perception. Are there any other factors that can account for variability in brain activity or behaviour? We considered four

confounding factors: reaction time, eye position and variance, inter-stimulus interval, and response history. For each of these factors, we determined their influence on the BOLD activity in ROI_{stim} and participants' behaviour. Reaction time differences can neither account for differences in perceptual outcome (Fig 5.1c), nor for differences in peak activity of the evoked BOLD responses (Fig 5.7a); this lack of correlation between peak activity and reaction times speaks against attentional influences on the variability in the BOLD response.

Also eye position and eye movement are not significantly different for the four response types, and overall eye position was very stable during presentation of the stimulus (Fig 5.7b). It is therefore unlikely that differences in eye position and hence, retinal input, cause the substantial variability in the BOLD response. Inter-stimulus interval length did not correlate with the peak of the BOLD response (Fig 5.7c) or with reaction time (r^2=0.01), nor did it affect the perceptual outcome (hits – misses – false alarms – correct rejections) of the subsequent trial (p=.260).

The only factor having a clear influence on perceptual outcome, was the cumulative response history. As can be seen in the entire response history over all runs of one representative participant (Fig 5.7d), the response types were far from randomly distributed. Instead, this participant experienced slow fluctuations in performance, with sessions where a lot of mistakes were made (box 1 in Fig 5.7d) and sessions where a correct response was given in almost all trials (box 2 in Fig 5.7d). Indeed, when the number of 'runs' (a run being defined as two or more correct or incorrect trials in succession) was calculated for all participants and compared to random data (generated by shuffling the data 1000 times), the number of 'runs' in the real data was significantly lower (21.2 for real data vs 28.8 for random data) and the average length of the runs longer (125.1 s for real data vs 79.6 s for random data). This implies that the data were clustered into periods when only correct responses, and periods when only incorrect responses were given. The influence of response history on variability in the BOLD signal could not be assessed, since the data were acquired in 9-12 separate scanning runs (see 5.2.2).

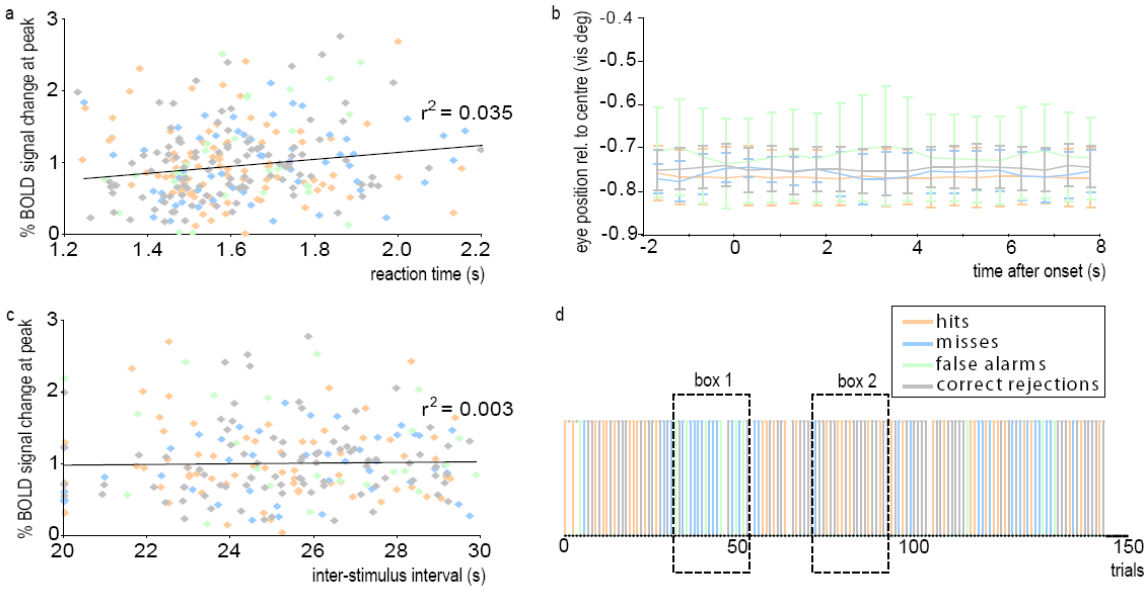

Figure 5.7 Other factors influencing perception and response variability. (a) *Reaction time did not correlate with the peak activity of the evoked BOLD responses. Neither did it differ between response categories (Fig 5.1c).* ***(b)*** *Eye position and variance were not significantly different between the four response categories.* ***(c)*** *Inter-stimulus interval length did not correlate with the peak activity of the evoked BOLD responses.* ***(d)*** *The response history for a representative participant shows that correct and incorrect trials are not randomly distributed, but that performance fluctuates over long timescales. Box 1; period of almost only incorrect trials. Box 2; period of almost only correct trials.*

5.4 Discussion

5.4.1 Spontaneous activity and neuronal response variability

The influence of spontaneous fluctuations in the fMRI BOLD signal on local stimulus processing has remained largely unknown to date. Here, we show that spontaneous activity accounts for a large portion of the variability in the BOLD signal in response to a visual stimulus, in both striate and extrastriate areas. This result is in agreement with findings in the motor cortex, where spontaneous activity contributes substantially to the variability in fMRI

activity in response to a button press (Fox et al., 2006b;Fox et al., 2007). Taken together, these results suggest that spontaneous activity has similar effects throughout the cerebral cortex, and therefore that these findings are of general relevance.

Our estimate of the fraction of the variability in the BOLD response explained by spontaneous activity is slightly lower than the previous estimates in the motor cortex (25% in the present findings, versus 40% (Fox et al., 2006b) to 60% (Fox et al., 2007) in motor cortex). We also found slight differences for the spontaneous activity between visual areas. However, these different fractions are probably the result of differences in effectiveness of the $ROI_{control}$ in estimating the spontaneous activity in the stimulus region, rather than reflecting a fundamental difference between cortical areas.

It is well-known that the characteristics of spontaneous activity in the visual cortex change depending on behavioural state (Bianciardi et al., 2009a;McAvoy et al., 2008;Nir et al., 2006;Yang et al., 2007). More specifically, the amplitude of the spontaneous fluctuations is significantly reduced under eyes-open conditions compared to when the participant's eyes are closed (Bianciardi et al., 2009a;McAvoy et al., 2008), an effect which has been attributed to the generation of visual imagery when the eyes are closed (Wang et al., 2008). Moreover, visual areas that are functionally unrelated exhibit a high degree of correlation during rest, but become spatially decoupled during visual stimulation (Nir et al., 2006). Indeed, our own data show that retinotopically related areas in V1, V2, and V3 are significantly more decoupled under task than under rest conditions. Our main analysis uses correlations between voxels obtained when the eyes were closed as an estimate of the spontaneous activity during our task and thereby assumes that the spatial coherence of the spontaneous fluctuations stays the same under eyes-closed and task conditions. Although the success of our analysis proves the validity of this assumption, it remains a concern that the obtained correlations might change with behavioural state. We therefore repeated the analysis using resting-state data from a run where the participants fixated on a small fixation cross in the centre of a blank (grey) screen. When subtracting the estimates of the spontaneous activity

based on these resting-state data from the task data, similar reductions in variability of the BOLD response were found (data not shown).

Subtracting the spontaneous activity that is responsible for a large part of the variability in BOLD responses to a stimulus has been proposed as a tool for improving the SNR in fMRI analyses (Bianciardi et al., 2009c;De Zwart et al., 2008) (see also 2.3.7). Our method of determining $ROI_{control}$, by masking for stimulus-related activation, then selecting the 100 best correlated voxels to ROI_{stim} and weighting their contribution, rather than selecting an arbitrary group of voxels, might be used to improve these analyses.

5.4.2 Linear superposition of spontaneous and evoked activity

In contrast to the clear effect of spontaneous activity on stimulus response variability, there is conflicting evidence regarding the interaction of this spontaneous activity with the activity evoked by the stimulus. Previous work on the interaction between spontaneous and task-related neuronal activity has been conducted in the visual cortex of the anaesthetised cat (Arieli et al., 1996). Using a combination of optical imaging and electrophysiological recordings, an approximately linear superposition between spontaneous and task-evoked neuronal activity was found (Arieli et al., 1996). Subsequent fMRI investigations in motor cortex (Fox et al., 2006b) and visual cortex (Bianciardi et al., 2009a) supported these findings. However, based on quantitative differences in the BOLD responses associated with the two perceptual outcomes in Rubin's ambiguous face/vase illusion (Hesselmann et al., 2008a) or moving random dot stimuli at coherence threshold (Hesselmann et al., 2008b), it was argued that prestimulus baseline activity in FFA and V5/MT interacts with activity evoked by the stimulus in a nonlinear way. The findings from our PPI analysis support the former view of a linear superposition of spontaneous and evoked activity, with respective contributions of around 25% and 75%. It is difficult to reconcile our negative finding of no interaction between spontaneous and evoked activity with the findings in FFA and V5/MT. However, the observed differences might stem from the brain areas studied; it might be

possible that no interaction is observed in the cortex of anaesthetised animals (Arieli et al., 1996) or low-level sensory areas such as M1 (Fox et al., 2006b) and V1 (Bianciardi et al., 2009a; present findings), but that spontaneous and task-related activity interact in a nonlinear way in higher-level areas such as the FFA (Hesselmann et al., 2008a) and V5/MT (Hesselmann et al., 2008b).

5.4.3 Spontaneous activity and perception

Activity in V1 reflected our participants' performance; the BOLD response to the stimulus was slightly larger to correct than to incorrect trials, in agreement with previous findings (Ress et al., 2000). We found very modest evidence for an effect of spontaneous activity on this difference in activity. Subtracting the spontaneous activity from the evoked BOLD responses diminished the difference associated with incorrect and correct trials; however, the same relative activity difference was not clearly visible in the spontaneous activity itself. Given that such small activity differences between correct and incorrect trials are usually found after averaging over no fewer than several hundred trials (Ress et al., 2000), or several thousand trials to find differences between hits, misses, false alarms, and correct rejections (Ress and Heeger, 2003), the absence of a clear difference in the spontaneous activity in the present study could be due to a lack of statistical power.

The slight influence of spontaneous activity on behaviour is consistent with the role of spontaneous activity in previously observed BOLD-behaviour relationships. For example, 74% of the variability in force that is normally observed when participants are required to press a button repeatedly, can be accounted for by spontaneous activity in the motor cortex (Fox et al., 2007). Similarly, the perceptual outcome of the ambiguous Rubin's face/vase illusion or randomly moving dots at coherence threshold, depends on prestimulus 'baseline' activity in the FFA and V5/MT, respectively (Hesselmann et al., 2008a;Hesselmann et al., 2008b).

The influence of spontaneous neuronal activity on subsequent stimulus perception has also been demonstrated using EEG. Especially neural activity in the alpha frequency band (8-14 Hz) has an effect on stimulus detectability (Mathewson et al., 2009;Romei et al., 2008;Thut et al., 2006). The amplitude of posterior alpha band activity correlates negatively with behavioural performance in target detection (Thut et al., 2006), and also the phase of prestimulus alpha oscillations strongly affects detection probability of visual stimuli that are presented near threshold (Busch et al., 2009). Spontaneous EEG activity in the alpha band thus has a direct influence on stimulus perception.

5.4.4 Attentional mechanisms

FMRI activity in visual cortex is not a direct reflection of the retinal input, but is influenced by many factors, an important one being attention. The enhancement of neuronal activity in parts of the visual cortex corresponding to an attended location relative to unattended regions is called the 'spotlight of attention' (Brefczynski and DeYoe, 1999;Kastner et al., 1999). This attentional modulation can be observed prior to and independent of the stimulus (Kastner et al., 1999;Sapir et al., 2005). Attention also influences participants' reaction times and accuracy, as is demonstrated in the classic Posner paradigm (Posner, 1980). It is not surprising, therefore, that many BOLD-behaviour relationships have been attributed to fluctuations in attention (Pessoa et al., 2002;Ress et al., 2000;Sapir et al., 2005).

Hence, the question arises whether the fluctuations in the BOLD signal that we observed during our task runs and which accounted for a substantial part of the variability in evoked responses, are truly spontaneous in nature. There are several lines of evidence that speak against attention as the main mechanism responsible for the observed variability in BOLD activity. First of all, reaction times, which can be used as a marker for attention (Posner, 1980), did not correlate with the peak amplitude of the BOLD response. Neither was there a significant relationship between inter-stimulus interval length and the peak of the BOLD

response, arguing against increased stimulus expectancy (reflected in a larger BOLD response) for long inter-stimulus intervals. Finally, our $ROI_{control}$ was composed of distributed voxels throughout the entire brain and is therefore highly unlikely to be under the influence of an attentional spotlight, yet was still able to account for a substantial fraction of the variance in the BOLD signal.

The potential influence of attention on our participants' behaviour is another matter. Although the elimination of the difference in peak activity between correct and incorrect trials after correction for the spontaneous activity speaks for a role for spontaneous activity in behavioural variability rather than fluctuations in attention, the absence of this difference in the spontaneous activity itself calls for caution. Several factors, however, argue against fluctuations in attention having a major influence on the perception of the stimulus in our paradigm. The spatial location of the stimulus was easily discernible and always the same, allowing participants to allocate spatial attention to the correct stimulus location on every trial. Although inter-stimulus intervals were variable, their length did not have an effect on task performance, neither for accuracy nor for reaction time, which suggests participants maintained their attention quite steadily. Yet the influence of attention on task performance in our paradigm cannot be completely eliminated.

5.4.5 Timescale of spontaneous activity

As we have seen, the influence of spontaneous activity on perception is very modest on a trial-by-trial basis. However, the fluctuations in spontaneous activity typically follow a 1/f pattern, with the largest power in the lowest frequencies (Cordes et al., 2001). Also human behaviour is well-known to exhibit 1/f like fluctuations (Farrell et al., 2006;Gilden et al., 1995). The response patterns of our participants over the course of the entire experiment (Fig 5.7d) are reminiscent of such 1/f like behaviour. We hypothesise that these slow fluctuations in response behaviour might be correlated with the slow fluctuations in spontaneous activity; such a correlation might be more indicative of the role of spontaneous activity in behaviour

than the influence of spontaneous activity on single trials. Indeed, the phase of ultraslow EEG fluctuations has been shown to correlate well with performance (Monto et al., 2009). Unfortunately it is not possible to test this hypothesis in the present dataset, however, since the BOLD and behavioural data were acquired in separate scanning runs and are therefore not continuous. Future experiments, in which similar performance fluctuations are induced within one run, are needed to investigate the possible correlation of these fluctuations in performance with spontaneous activity fluctuations.

5.5 Conclusion

In this chapter, we investigated the contribution of spontaneous activity to local stimulus processing in visual cortex. Spontaneous activity accounts for a large fraction of the variability in the BOLD response evoked by a stimulus, by being linearly superimposed on the activity evoked by the stimulus per se. Conversely, the influence of spontaneous activity on the perceptual outcome of the stimulus is very modest. In order to investigate the role of spontaneous activity for perception in more detail, in the next chapter we therefore use a stimulus which fluctuates much more drastically in its perceptual outcome: a bistable stimulus.

Chapter 6 Neural Correlates of Motion-Induced Blindness

6.1 Introduction

As we have seen in the previous chapter, spontaneous BOLD fluctuations in visual cortex have a modest effect on the perceptual outcome of a low-contrast stimulus; that is, they slightly influence whether a repeatedly presented stimulus will be correctly or incorrectly perceived to contain a certain feature. A much more striking example of how spontaneous activity interacts with perceptual outcome is provided by bistable perception, in which fluctuations in internal brain state lead to very different percepts of identical retinal input. Where in the brain these fluctuations in brain state are initiated has been the topic of intense investigation; currently, a hybrid model, with low-level visual areas such as the primary visual cortex and high-level association areas such as the prefrontal cortex interacting, has gained consensus (Blake and Logothetis, 2001;Sterzer et al., 2009).

An interesting model system of bistable perception in this respect is motion-induced blindness (MIB). MIB is a striking phenomenon in which a perceptually salient stationary visual target repeatedly disappears (and subsequently reappears) when superimposed on a field of moving distracters (Bonneh et al., 2001). Although this paradigm has been studied extensively in a number of behavioural studies, the neural mechanisms underlying this phenomenon have remained less well investigated.

One possibility is that MIB is similar to other types of perceptual fading such as Troxler fading (Troxler, 1804) and reflects neural activity in low-level visual cortex. Consistent with this, target disappearance in MIB is influenced by the target's saliency. For example, the target disappears more often at increased eccentricity (Hsu et al., 2004) and when it is smaller (Bonneh et al., 2001). Furthermore, MIB is indirectly influenced by boundary adaptation, consisting of the fading of the boundaries of the target, followed by interpolation

of the surrounding distracter elements (Hsu et al., 2006). Importantly, the properties of the target in relation to the background and the moving distracters are also important; MIB is impaired at equiluminance of the target, background and distracters (Wallis and Arnold, 2009). Moreover, reducing the contrast between the target and the distracters (Hsu et al., 2004), and paradoxically, increasing the contrast between the target and the background (Bonneh et al., 2001), both enhance disappearance of the target.

Other evidence points to the involvement of higher-level areas. Behavioural results suggest that MIB is not likely to reflect only local adaptation, as it persists for targets that are moving or flickering or when distracters and targets are spatially separated (Bonneh et al., 2001). Disappearance of the target is subject to gestalt-like grouping effects; several targets tend to disappear together rather than separately when they form good gestalts. More specifically, when two Gabor patches are presented as targets, they tend to disappear together when they are collinear, and in alternation when their orientation is orthogonal (Bonneh et al., 2001). Finally, MIB is sensitive to the depth relations between target and distracters (Graf et al., 2002).

Lastly, MIB displays interesting dynamics compared to other types of perceptual fading, which might also provide clues to the nature and locus of the spontaneous fluctuations leading to perceptual switches. In contrast to, for example, Troxler fading and filling-in of an artificial scotoma, MIB can occur following very brief observation periods and disappearance of the target is rapid (i.e. there is no intermediate stage at which the target is dimly perceived, before full disappearance occurs).

Taken together, these purely behavioural findings suggest that MIB might reflect processes at the earliest stages of visual processing (e.g. primary visual cortex) as well as in extrastriate or nonsensory association areas. As a step towards investigating these different possibilities, we used functional MRI to investigate activity changes in the cortex that were time-locked to perceptual fluctuations in target visibility during MIB in human participants. Whole-brain analysis together with standard retinotopic mapping of visual cortex was used to characterise activity related to reported visibility of the target. To anticipate our findings,

activity in low-level visual cortex (V1, V2), plus V5/MT, depended on the visibility of the target reported by our participants. Specifically, invisibility of the target was associated with increased activity in retinotopic regions of V1 and V2 representing the target, plus a broader modulation of activity in V2 and area V5/MT. No activity differences depending on target visibility were found in nonsensory association cortex. These findings reinforce the notion that activity in low-level visual cortex is strongly associated with fluctuations in perceptual awareness (Lee et al., 2005;Mendola et al., 2006;Polonsky et al., 2000), generalising this notion to the phenomenon of motion-induced blindness.

6.2 Materials and Methods

6.2.1 Observers and stimuli

Eight healthy volunteers with normal vision (20-30 years old; 6 female) gave written informed consent to participate in the experiment, which was approved by the local ethics committee. They viewed a yellow dot in their left upper visual field amidst a grid of blue distracter crosses rotating at 5.5 deg/s round a central fixation dot (Fig 6.1a). This type of display configuration is known to invoke MIB (Bonneh et al., 2001;Caetta et al., 2007;Graf et al., 2002). The grid (luminance 8.81 cd/m^2) was superimposed on a black background (luminance 0.10 cd/m^2). The yellow dot (luminance 11.23 cd/m^2) of diameter 0.8 degrees at 5.8 degrees eccentricity (5 degrees across and 3 degrees up) was flickering at 15 Hz to enhance its salience and avoid adaptation after-effects. The upper left visual field was chosen as MIB has been shown to be most robust at this location (Bonneh et al., 2001).

Observers were instructed to attend to the central fixation dot and count the number of times it flashed red per run of scanning, while simultaneously reporting the disappearance and reappearance of the target by pressing one of two buttons with their right hand. The central fixation task was designed to reduce eye movements while not requiring further

button presses. Furthermore, we reasoned that this dual task situation (MIB task and central fixation task) might direct attention away from the MIB target and might therefore minimise any potential fluctuations in attention associated with perception of the target.

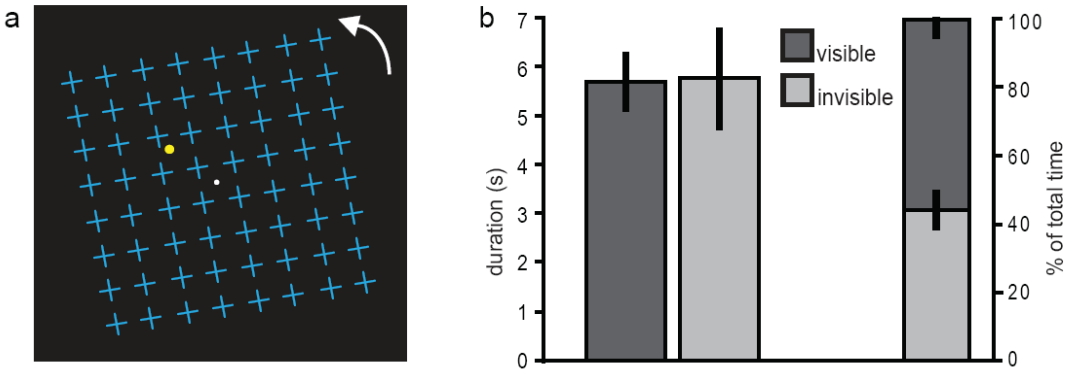

Figure 6.1 Stimulus configuration and behavioural data. (a) *Participants fixated centrally (white dot) and viewed a yellow flickering dot placed in the left upper quadrant and surrounded by blue crosses. In the dynamic display, the entire field of cross distracters rotated clockwise or anticlockwise about the fixation point. Participants were required to indicate by button presses when the yellow flickering dot became visible or invisible to them.* ***(b)*** *Durations and percent total time of visibility and invisibility of the target are shown for the scanning experiment, averaged across participants. Error bars represent the standard error of the mean.*

6.2.2 Procedure

Participants were tested extensively before the scanning experiment to ensure they could experience MIB and assign consistent responses to the different perceptual states. They performed a further practice block in the scanner before data recording. Subsequently they completed nine 6 minute runs of scanning. A run started with 10 seconds when only the field of rotating blue crosses was presented (*target absent*), after which the yellow flashing dot appeared. Participants then indicated continuously by button presses when the target either became visible (*target visible*) or became invisible (*target invisible*). In addition, during periods while the participant had indicated that the target was visible, the target would be physically removed from the display for periods of ten seconds five more times during the

scanning run at random intervals. These extra absent periods were included to determine that participants were correctly following instructions; upon subsequent debriefing, all participants declared that they had not realised that the target was sometimes not only perceptually, but also physically absent. Theoretically, during these absent periods subjects could perceive the target as being visible (fourth condition); however, analysis of their button presses showed that this was never the case. The button presses made by participants were thus used to divide the viewing epochs into the remaining three conditions (target visible, target invisible, and target absent). As the target was flickering, there were no target-contingent after-effects. Halfway through each run, the rotation direction of the distracter field was reversed to prevent a strong after-effect from the rotating crosses.

Every three runs of task were followed by a run of ROI localiser (see 6.2.3). Standard retinotopic maps (see 6.2.3) and T1-weighted structural scans were acquired in a separate session.

6.2.3 Retinotopic mapping and ROI localiser

Each participant completed two successive scanning runs of a conventional retinotopic mapping procedure, viewing a contrast-reversing, black-and-white checkerboard stimulus presented in alternating 15 second blocks as horizontal or vertical wedges placed to cover either horizontal or vertical meridians for V1, V2, and V3 localisation (Sereno et al., 1995;Teo et al., 1997;Wandell et al., 2000). V5/MT was localised using expanding and contracting rings of dots (Rees et al., 1997). Finally, the retinotopic location of the target representation in low-level visual areas was determined by measuring brain activity while participants viewed a white dot on a black background (luminance 13.64 cd/m^2 and 0.10 cd/m^2) flickering at 15 Hz, of identical size and location as the dot used in the actual experiment. This was shown for three 5 minute runs, each consisting of alternating 15 second periods of the flickering dot and a blank screen. To ensure stable fixation,

participants were required to press a button as soon as a small red dot flashed on either side of the fixation cross throughout these runs.

6.2.4 fMRI data acquisition and analysis

A 3T Allegra MRI scanner (Siemens Medical Systems, Erlangen, Germany) with a standard transmit–receive head coil was used to acquire functional data with a single-shot gradient echo isotropic high-resolution echo planar imaging sequence (matrix size 128 x 128; field of view 192 mm; in-plane resolution 1.5 mm; 32 slices with interleaved acquisition; slice thickness 3 mm; echo time 30 ms; acquisition time per slice 102 ms; TR 2,040 ms). During scanning, eye position was continually sampled at 60 Hz using an ASL 504 LRO infrared video-based MRI compatible eye tracker (Applied Science Laboratory, Bedford, MA).

Functional data were analysed using SPM5 (www.fil.ion.ucl.ac.uk/spm/software/spm5/). The first 5 images of each series were discarded from further analyses, to allow for T1 equilibration effects. Preprocessing of the data involved realignment of each scan to the first scan of the first experimental run and coregistration of the functional data to the structural scan. Data were normalised to an EPI template in MNI stereotactic space and smoothed by a 6 mm kernel for whole brain analysis; the ROI localiser, and individual retinotopic and V5/MT analyses were carried out on non-normalised, unsmoothed data. Data were not smoothed because of the small size of the ROI localiser regions. The data were filtered with a 128-s cut-off, high-pass filter to remove low-frequency noise and adjusted for global changes in activity. The timing of button presses for each participant individually was used to construct three participant-specific regressors that represented hypothesised brain activity associated with each of the three behaviourally defined conditions (target visible; target invisible due to MIB; target absent due to physical removal). In an additional analysis, participants' individual average reaction time was calculated from the reaction times of their button presses to the 'target absent' condition; this average reaction time was then subtracted

from the time of all button presses to arrive at a better estimate of the 'real' time of the perceptual switches. These corrected times were then used as regressors in the analysis. In a second additional analysis, variance associated with eye blinks was modelled and removed as an extra regressor of no interest. In all analyses, movement parameters in the three directions of motion and three degrees of rotation were included as confounds. The three regressors (target visible, target invisible, and target absent) were convolved with a synthetic haemodynamic response function and entered into a General Linear Model. Parameter values for each regressor were estimated for each participant independently. In the group analysis, these estimates were entered treating participants as a random factor, using a one-sample t-test across participants.

For two participants, eye data could not be analysed due to technical difficulties. Eye movements were defined as variance round the mean x and y position of the eye, eye blinks as an absence of signal. Statistical analysis was done to examine differences in eye movements and blinks between the various experimental conditions.

6.2.5 Retinotopic analysis

Retinotopic cortical areas were identified using MrGray (Teo et al., 1997;Wandell et al., 2000). This yielded maps of functionally defined visual areas V1, V2, and V3 for each participant. These maps were combined with activation images of the ROI localiser to reveal retinotopic regions in V1 and V2 representing the spatial location of the target. Retinotopic regions in V3 corresponding to the target location could not be identified in all subjects, as the target was small and eccentrically placed, making it more difficult to localise in higher visual areas (Dougherty et al., 2003). This process thus yielded ROIs representing the spatial location of the target in V1 and V2 for each participant. We then used these ROIs to extract estimates of activity in each of the three experimental conditions of interest (target visible, target invisible, and target absent) obtained from the multiple linear regression analysis described above. Activity estimates were averaged across the voxels within the ROI and

subjected to repeated measures ANOVAs and subsequent planned paired t-tests to test for differences between conditions.

In order to compare activation in these ROI localiser regions with activation in regions of comparable size and eccentricity that did not represent the spatial location of the target, regions of the same size (spatial extent) at a corresponding eccentricity (based on visual inspection of the retinotopic maps) were sampled from the left dorsal V1 and V2 (representing the lower right visual quadrant, diagonally opposite the visual field location of the target) for each participant individually. Activity associated with each of the three experimental conditions in these control ROIs was assessed in a similar fashion as for the target ROI. We further examined additional, larger control regions in which activity was extracted and averaged across the whole of right and left V1 and V2 (i.e. regions contralateral and ipsilateral to the visual field location of the MIB target).

The location of V5/MT was determined for each participant by subtracting activation during the static dots from activation during the expanding and contracting dots (Rees et al., 1997), taking the peak voxel in the regions closest to where V5/MT has commonly been reported (Morrone et al., 2000), and taking all grey matter voxels in a sphere of 8 mm round these peak voxels. These spheres were used as masks for all voxels activated by our stimulus (distracters and target) (F contrast of all our conditions versus the rest period) to reveal voxels in right and left V5/MT that were activated in our experiment.

6.3 Results

6.3.1 Behavioural data

On average across all scanning runs, periods where the target was invisible to participants due to MIB lasted for a mean duration of 5.81 s (s.e. ± 0.98 s) and those where the target was visible for a mean duration of 5.74 s (s.e. ± 0.55 s) (Fig 6.1b; individual

participant data are shown in Table 6.1). In total, the target was invisible due to MIB (excluding target absent periods) for 44.3 % (s.e. ± 5.0 %) of the time (Fig 6.1b). For each participant, we estimated their reaction time to a perceptual disappearance or appearance due to MIB by measuring their reaction time to respond to actual physical removal of the target. Their average reaction time was 1.67 s (s.e. ± 0.17 s); the flicker and peripheral location of the target, a conservative response strategy, and engagement of participants in the simultaneous central fixation task are all consistent with this relatively long reaction time.

participant	*duration (sec)*		*percentage of total time*	
	visible ± SEM	invisible ± SEM	visible	invisible
s1	4.26 ± 0.20	2.57 ± 0.08	65	35
s2	6.23 ± 0.48	3.78 ± 0.19	66	34
s3	5.63 ± 0.40	4.85 ± 0.24	58	42
s4	5.81 ± 0.34	8.71 ± 0.32	46	54
s5	5.73 ± 0.19	5.52 ± 0.20	56	44
s6	4.00 ± 0.22	10.77 ± 0.54	31	69
s7	9.06 ± 0.55	3.67 ± 0.17	76	24
s8	5.20 ± 0.47	6.62 ± 0.39	48	52

Table 6.1 Individual participants' behavioural data. *Average duration and percentage of total time of the experiment that the target was visible and invisible are shown for each participant. SEM, standard error of the mean.*

6.3.2 Neural activity associated with MIB in retinotopic target locations

We investigated whether there were any differences in activation in the localiser ROIs (Fig 6.2a) comparing the experimental conditions (target visible, target invisible, and target absent). Repeated measures ANOVAs (Greenhouse–Geisser corrected) on measures of the BOLD activity within these ROIs (Fig 6.2b) showed significant differences between the

three experimental conditions in both V1 and V2 ROI locations ($F(2,14) = 22.121$, $p = .001$ and $F(2,14) = 11.659$, $p = .008$ for V1 and V2, respectively). These differences were obtained from mean-corrected data; raw BOLD data are shown in Fig 6.3a. Planned t-tests revealed that these differences reflected a significant increase in activity when the target was physically present and reported as visible compared to when it was physically absent (and reported as 'invisible') ($t(7) = 4.583$, $p = .003$ for V1 and $t(7) = 3.923$, $p = .006$ for V2) (Fig 6.2b). More importantly, activity was also significantly elevated when the target was physically present but invisible due to MIB compared to the visible condition ($t(7) = 3.804$, $p = .007$ for V1 and $t(7) = 2.654$, $p = .033$ for V2) (Fig 6.2b). Activity in this invisible condition was also increased compared to the absent condition ($t(7) = 5.125$, $p = .001$ for V1 and $t(7) = 3.523$, $p = .010$ for V2) (Fig 6.2b). Such a pattern was highly consistent across our participants, being observed in 7 out of 8 participants. Qualitatively, visual inspection of time courses (Fig 6.2c) from the three conditions time-locked to reports of perceptual transitions show that these significant differences were associated with a large initial decrease and a slightly smaller initial increase in the absent and invisible condition, respectively.

Both the V1 and the V2 localiser ROIs showed a similar pattern of activity (Fig 6.2b) associated with the experimental conditions, and this pattern persisted in a subsequent control analysis when the timing of the three experimental conditions defined by button presses was corrected for the individual reaction times of each participant assessed from physical disappearances of the target (see 6.2.4; data not shown).

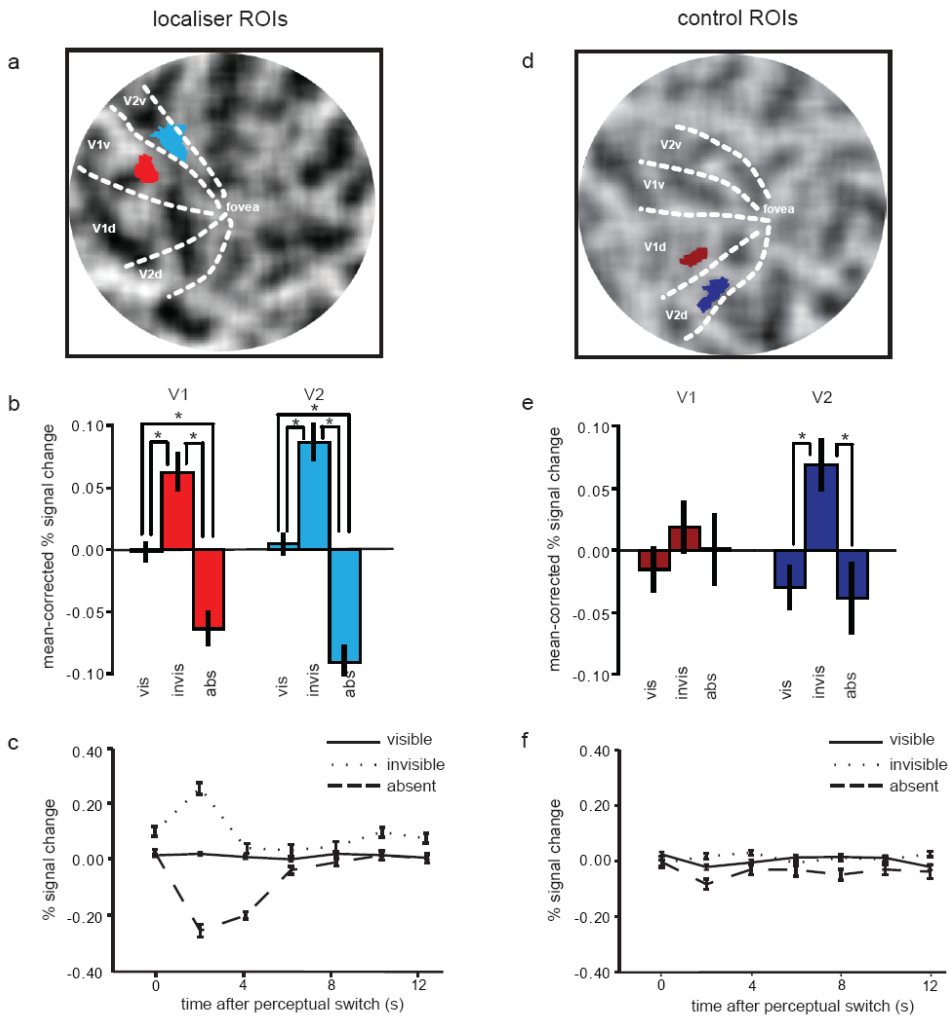

Figure 6.2 BOLD signal in localiser and control ROIs. (a) *The retinotopic regions in visual cortex (localiser ROIs) representing the spatial location of the target for a representative participant are shown on a flattened representation of the right (contralateral) visual cortex (V1 is bright red, V2 is bright blue).* ***(b)*** *Mean percent BOLD signal change (mean-corrected) in these regions for the three conditions (vis: target visible – invis: target invisible – abs: target absent); bright red bars represent the V1 localiser ROI, bright blue bars represent the V2 localiser ROI. Error bars represent the group standard error of the mean.* ***(c)*** *Time courses of these three conditions for the localiser region in V1. Time zero signals the time of the button press signalling the perceptual switch; time courses for the visible, invisible, and absent condition are shown in a straight, dotted, and dashed line respectively.* ***(d)*** *Retinotopic regions of the same size but representing the right lower visual quadrant (control ROIs) are shown on a flattened representation of the left visual cortex for the same representative participant (V1 is dark red, V2 is dark blue).* ***(e)*** *Mean percent BOLD signal change (mean-corrected) for the three conditions (target visible – invisible – absent); dark red bars represent the V1 control ROI, dark blue bars represent the V2 control ROI.* ***(f)*** *Time courses of the three conditions for the control ROI in V1; conventions are the same as in* ***c****.*

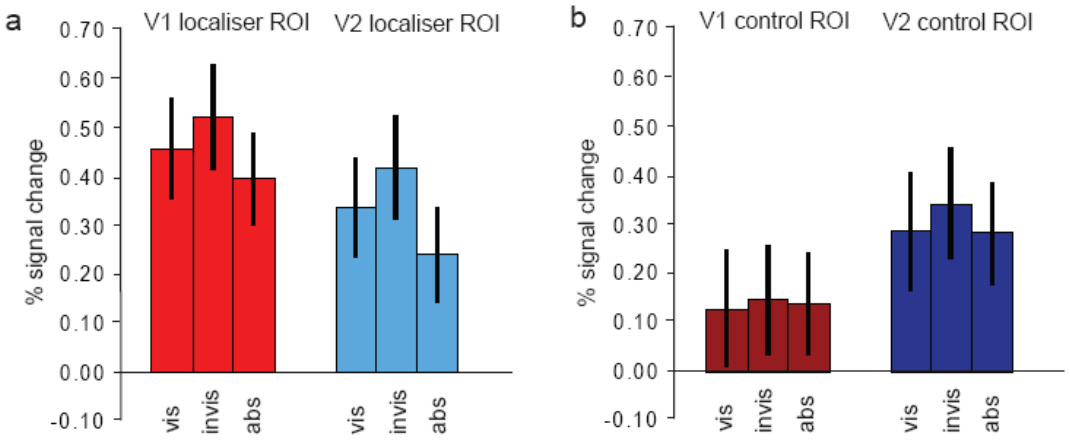

Figure 6.3 Raw BOLD signal in V1 and V2. *The raw BOLD signal is shown for the V1 and V2 localiser ROIs* ***(a)*** *and for the V1 and V2 control ROIs* ***(b)****. V1 is bright/dark red; V2 is bright/dark blue. Error bars represent the group standard error of the mean.*

6.3.3 Activity in other regions of visual cortex

In order to determine whether these activity differences were retinotopically specific, or whether they reflected more general activity differences in visual cortex, we investigated BOLD activity in a number of control regions: the (similarly sized) control ROIs in V1 and V2 ipsilateral to the stimulus, the whole of ipsilateral V1 and V2 activated by the stimulus (target and distracters), and contralateral and ipsilateral V5/MT.

Activity in the control ROIs in V1 and V2 (Fig 6.2d) qualitatively showed a similar pattern, but of much lower amplitude, as for the localiser regions. However, these qualitative differences between conditions were not significant in V1 ($F(2,14) = .681$, $p = .497$) though they trended towards significance in V2 ($F(2,14) = 3.541$, $p = .078$; Fig 6.2e). Post-hoc planned t-tests also showed no significant differences between any of the conditions (all $t(7) < 1.886$, all $p > .101$), apart from the differences between the invisible and visible, and the invisible and absent conditions in V2 ($t(7) = 2.462$, $p = .043$). Raw BOLD data are shown in Fig 6.3b. Time courses for the three conditions in these control ROIs were qualitatively very similar to each other (Fig 6.2f).

As these small changes in activity associated with the experimental conditions were present in these control ROIs, we explicitly tested whether the activity differences we observed in localiser ROIs were significantly different from control ROIs. Critically, the interaction between condition (visible, invisible, absent) and region (localiser, control) was significant in V1 and trended towards significance in V2 ($F(2,14) = 9.510$, $p = .003$ and $F(2,14) = 3.582$, $p = .087$ for V1 and V2, respectively). Hence, MIB-associated modulation of activity in retinotopic regions representing the target was significantly greater than in control ROIs in V1, but not in V2.

Activity in the whole of ipsilateral V1 and V2 showed a similar pattern of activity that was non-significant in V1 and almost significant in V2 ($F(2,14) = 2.584$, $p = .136$ and $F(2,14) = 4.515$, $p = .052$ for V1 and V2, respectively, see Fig 6.4a and c). However, post-hoc planned t-tests showed a significant difference between the visible and invisible condition in both regions ($t(7) = 2.761$, $p = .028$ and $t(7) = 3.378$, $p = .012$ for V1 and V2, respectively, see Fig 6.4a and c). Activity in contralateral V5/MT showed a similar pattern to the ROI localiser regions in V1 and V2. There was a significant difference between the three experimental conditions ($F(2,14) = 10.791$, $p = .010$), which was due to greater activity in the target invisible condition compared to the target visible condition ($t(7) = 6.085$, $p < .001$) or compared to the target absent condition ($t(7) = 4.677$, $p = .002$) (Fig 6.4b and d). There were no significant differences between the target visible and the target absent condition where (in both conditions) the distracters were always present ($t(7) = 0.924$, $p = .386$). Activity in ipsilateral V5/MT showed no significant difference between any of the conditions ($F(2,14) = 2.476$, $p = .128$) (Fig 6.4b and d).

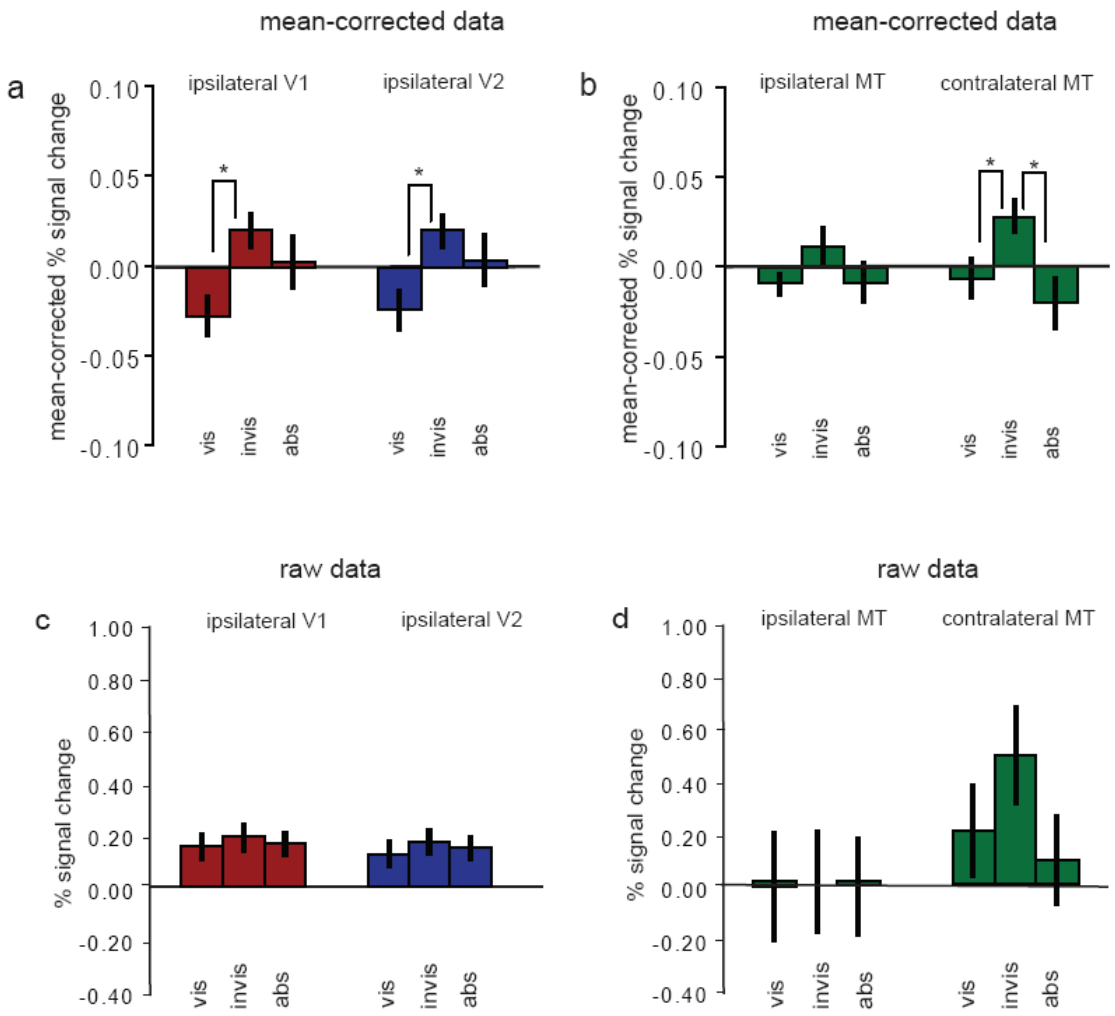

Figure 6.4 BOLD signal in other control regions. ***(a)*** *Mean percent BOLD signal change (mean-corrected and compared to resting baseline) is shown for the three conditions (vis: target visible – invis: target invisible – abs: target absent) for the whole of ipsilateral V1and V2.* ***(b)*** *Same data are shown for ipsilateral and contralateral V5/MT. Raw BOLD data for the same areas are shown in* ***(c)*** *and* ***(d)****. V1 is dark red, V2 is dark blue, V5/MT is dark green. Error bars represent the group standard error of the mean.*

6.3.4 Whole brain analysis

For completeness, we also performed a whole brain analysis to identify any areas outside low-level visual cortex that might show modulation by perceptual state during MIB. It should be noted that such an analysis necessarily has lower sensitivity due to the much larger number of multiple comparisons and absence of a prior hypothesis. Outside occipital cortex

and at a statistical threshold of $p < 0.05$ (FDR-corrected for multiple comparisons across the whole brain), neither the comparison of the invisible versus visible condition nor the comparison of the visible versus absent condition yielded any suprathreshold clusters of voxels. When the threshold was dropped to $p < 0.0001$ uncorrected, the location in V1 corresponding to the target was significantly activated in all expected conditions (invisible > visible, invisible > absent, visible > absent), MNI coordinates [12 -78 -3], 13 voxels, $Z > 4.97$, $p < 0.0001$. These conditions also showed significant activation in right and left parietal cortex at this threshold (MNI coordinates [30 -42 54] and [-30 -42 54], ~ 15 voxels, $Z > 5.52$, $p < 0.0001$). When looking specifically at perceptual switches, the left frontal cortex was activated (MNI coordinates [-15 -6 66], 15 voxels, $Z = 5.33$, $p < 0.0001$). However, as these areas were not hypothesised *a priori* to be involved in MIB and the activations were obtained at quite a liberal threshold, these results will not be discussed any further.

6.3.5 Fixation and eye blink data

Repeated measures ANOVAs of eye position and average number of eye blinks/sec revealed that there were no significant differences between the three conditions ($F(2,10) = 1.916$, $p = .222$ and $F(2,10) = .352$, $p = .675$, respectively). In addition, modelling eye blinks as an additional regressor of no interest did not qualitatively alter our findings (data not shown). Hence, the differences in activity we observed in low-level visual cortex cannot be explained by differences in retinal input caused by larger eye movements or blinks. However, the resolution of our eye tracker was too low to rule out any potential effects by microsaccades, the rate of which has been shown to change around the time of perceptual switches in MIB (Hsieh and Tse, 2009).

6.4 Discussion

6.4.1 Activity increases associated with target invisibility

In this chapter, we have shown that disappearance of a target in MIB was associated with an increase in activity in low-level visual cortex, which was largest in retinotopic regions of V1 and V2 corresponding to the cortical representation of the target, plus in V5/MT contralateral to the target. Much smaller, and mostly insignificant, activity increases were observed for both V1 and V2 in control ROIs distant from the target representation. In contrast, activity in retinotopic regions corresponding to the target location in V1 and V2 was reduced when the target was physically removed from the display. The striking differences in activity associated with the perceptually comparable situations of the target being invisible through MIB and through physical removal suggest that the neural processes underlying perceptual disappearances may reflect not merely target absence, but also an additional mechanism that is specific to this state of target invisibility.

6.4.2 Local neuronal competition

It has been suggested that MIB might reflect the disruption of attentional switching mechanisms, thus implying a global interaction between higher and lower cortical areas (Bonneh et al., 2001). Others have argued that MIB results from surface completion associated with the moving distracters (Graf et al., 2002), which implies local neural competition between representations of the moving distracters and the target (Keysers and Perrett, 2002;Libedinsky et al., 2009). The small size of the target in our study and the inherently limited spatial resolution of fMRI make it difficult to disentangle distracter from target activation in our localiser regions. We can therefore not isolate the separate contributions of target- and distracter-related activity in our results. One way to distinguish between target- and distracter-related activity in a future experiment would be frequency-

tagged MEG, which has been used successfully to distinguish between target- and background-related activity in perceptual completion (Weil et al., 2007).

Nevertheless, such proposed neural competition between target and distracters (Keysers and Perrett, 2002;Libedinsky et al., 2009) could account for the enhanced activations correlated with invisibility that we observe; the activations could reflect an active process of completion of the perceived field of distracters into a perceptual surface occluding the target (Graf et al., 2002). There is physiological evidence for surface representation early in visual processing; V1 neurons show responses to the presence of contextual lines parallel and in close proximity to a line within their receptive field (Kapadia et al., 1995), and V2 neurons use local depth information to integrate contours and segment the visual input into surfaces (Bakin et al., 2000). Interestingly, V1 and V2 neurons also show increased activity when an illusory contour is perceived in their receptive field (Lee and Nguyen, 2001), consistent with an active contour-completion mechanism giving rise to an increase in population activity. Thus, the increases in activity that we observe might result from local completion of the distracter field in the target region.

Interesting in this respect is the fact that although behavioural evidence suggests that MIB and perceptual completion associated with artificial scotomas (Ramachandran and Gregory, 1991) are susceptible to similar factors (Hsu et al., 2006), the retinotopic increase in population-level neural activity we found associated with MIB contrasts with reports of decreases in activity associated with perceptual completion of an artificial scotoma (Mendola et al., 2006;Weil et al., 2007;Weil et al., 2008). The resolution of functional MRI in humans is relatively low; so one possibility is that differences in population activity indexed by the BOLD signal reflect a combination of signals from different neural processes. For example, in perceptual completion associated with an artificial scotoma it is hypothesised that a more rapid process of surface completion may follow a slow process of neural adaptation at the border between a target and its surround. Functional MRI, even at high spatial resolution, would be expected to conflate the two signals from the relatively small target, and so differences between MIB and other paradigms might not reflect different underlying

mechanisms (e.g. surface completion) but instead a different balance or combination of individual neuronal properties underlying the phenomena. Future work will need to carefully manipulate stimulus properties in order to dissect out potential components of the underlying neural mechanisms.

6.4.3 Global modulations

Strikingly, perceptual invisibility during MIB was also associated with modulation of activity in ipsilateral control ROIs, consistent with earlier findings (Donner et al., 2008;Hsieh and Tse, 2009). While statistically not significant in V1, in V2 the changes were more pronounced and reached statistical significance. Importantly, this modulation was observed in regions of visual cortex that do not represent the same visual field as where the MIB target was shown. Consistent with this, these regions showed only significant differences in activity when the visibility of the target changed, and no significant difference between the physical presence versus absence of the target. Also, the invisible and the absent condition required the same response behaviour. This indicates that these ipsilateral control regions do not respond to the physical presence of the target or to the detection of its disappearances, but only to changes in visibility associated with MIB, which are therefore associated to some extent with a more generalised non-retinotopic modulation of activity. This is reminiscent of the global modulation of activity observed in low-level visual areas in a similar study investigating MIB (Donner et al., 2008), though our pattern of activity is opposite in sign. One possibility is that our increases in activity reflect a general arousal associated with perceptual invisibility of the target. However, this cannot account for why the changes are most prominent in V2, nor why similar elevation in activity for invisible versus visible is not also seen for the perceptually comparable situations of target absent versus visible. Another possibility is the differences in distracters used; the distracters in the present study formed a structured field of similarly oriented lines organised into crosses,

whereas Donner et al. (2008) used an unstructured cloud of dots. These differences might result in differences in neural processing, resulting in qualitatively different results.

The work presented in this chapter failed to find strong evidence for the involvement of higher level areas in MIB. As noted above, this might be due to the small number of subjects used in this study or the small size of the target. If higher level areas were involved, though, they might influence the activity changes in low-level visual cortex through a feedback mechanism. Perceptual switches in bistable perception paradigms have been suggested to rely at least partly on feedback from higher level areas to low-level visual cortex (Blake and Logothetis, 2001;Lumer et al., 1998;Windmann et al., 2006). Indeed, a possible role of feedback in MIB seems to be supported by the modulation of activity in visual areas V4 and the intraparietal sulcus by subjective target disappearances (Donner et al., 2008). Alternatively, the activity changes in low-level visual cortex that we observe might be the result of long-range horizontal connections within V1 that play a role in contour integration (Stettler et al., 2002), that is, they might result from local processing in low-level visual cortex. This notion must be treated with caution, however, because several electrophysiological studies have revealed an apparent discrepancy between the BOLD signal and local neuronal activity in V1 during perceptual suppression (Maier et al., 2008;Wilke et al., 2006).

6.4.4 Spatial attention

One key process that can exert influences on activity in low-level visual cortex through feedback is spatial attention (Brefczynski and DeYoe, 1999;Ghandi et al., 1999;Somers et al., 1999). However, voluntary direction of spatial attention cannot easily account for our findings of increased activity in retinotopic regions representing the target associated with invisibility during MIB. First of all, participants were continuously involved in dividing their attention between a demanding task at fixation and reporting the MIB target, thus leaving less attentional resources for the MIB target per se. Moreover, there were also strong

differences in activity between the perceptually comparable (and so equally likely to lead to voluntary shifts of attention) situations of the target being invisible due to MIB versus the target being invisible due to physical removal. However, it is important to note that although these findings indicate that voluntary attention may not play a role in MIB per se, they do not rule out the fact that attention can influence the timing of the perceptual disappearances and reappearances, as will be demonstrated in the next chapter.

6.5 Conclusion

In conclusion, we present evidence for an involvement of low-level visual areas in MIB. We show that perceptual, but not physical, disappearance of the target is coupled to an increase in activity in retinotopic locations in V1 and V2 representing the target, plus motion area V5/MT contralateral to the target. We hypothesise that these findings are consistent with a local active process of completion of the field of distracters underlying MIB, but also point out the more general involvement of large regions of visual cortex. The spontaneous fluctuations in internal brain state that underlie MIB can thus be explained by local neuronal processes that act alongside fluctuations at a more global level. The next chapter will demonstrate how this account fits in with the effect of endogenous attention on these fluctuations in internal brain state.

Chapter 7 Attentional Effects on Motion-Induced Blindness

7.1 Introduction

Bistable perception can be considered as the behavioural outcome of spontaneous fluctuations in internal brain state while the retinal input remains constant. These fluctuations can be the result of local competition processes, as well as global mechanisms, as we have seen in the last chapter. Another factor having an impact on these fluctuations in brain state is endogenous attention. Attention has been shown to influence both the rate of perceptual switching (Van Ee et al., 2005) as well as the awareness (Meng and Tong, 2004) of bistable stimuli.

In the context of motion-induced blindness (MIB), it has been proposed that switches in attention play a role in visibility of the target. Specifically, disappearance of the target in MIB is thought to reflect a disruption of the commonly assumed, but usually unnoticed, fast attentional switching between objects in a visual scene (Bonneh et al., 2001). With such disruption, the objects (i.e. the target and the distracters) are perceived one at a time, resulting in the target fluctuating in and out of awareness. In line with this proposal, it has been shown that focusing attention on one MIB target versus dividing attention among several targets facilitates MIB (HaiYan et al., 2007). This study, however, did not dissociate any spatial attention effects from general task difficulty differences (keeping track of only one target is easier and might have been reported more reliably than reporting disappearances of several targets simultaneously) and therefore the influence of attention on target disappearance and other aspects of MIB remains elusive.

To investigate this issue, in this chapter I present two behavioural experiments to characterise how attention affects the dynamics of MIB. In the first experiment, we manipulated the voluntary allocation of spatial attention to one of two MIB targets placed on

a field of moving distracters. This allowed us to examine how directing attention towards versus withdrawing attention away from one target might alter the competitive interactions between that target and the distracters believed to underlie MIB. In a second experiment, we manipulated attentional load in a task entirely unrelated to the MIB target or moving distracters (Lavie et al., 2004;Lavie, 2005). By increasing the attentional demands in an unrelated task, we could now examine the effects of withdrawing attentional resources from the entire MIB display, both targets and moving distracters. Briefly, we found that directing spatial attention to the MIB target led to an increased probability of its disappearance, while withdrawing attention from both target and distracters led to a decrease in perceptual switches and prolonged periods of target invisibility.

7.2 Materials and Methods

7.2.1 Observers and stimuli

Six healthy volunteers (27-31 years old) with normal or corrected-to-normal vision gave informed consent to take part in Experiment 1, nine other healthy volunteers (26-36 years old) with normal vision agreed to take part in Experiment 2. Participants fixated centrally while viewing an MIB display consisting of yellow dots (the targets) of 0.6 degrees in diameter, amidst a grid of blue crosses (the distracters) rotating at 5.5 deg/s round a central fixation dot (Bonneh et al., 2001;Graf et al., 2002;Caetta et al., 2007). In Experiment 1, two targets were shown, which were placed in the left and right upper visual quadrants at 5.8 degrees eccentricity (5 degrees lateral and 3 degrees superior to central fixation) (Fig 7.1a); in Experiment 2, only the left upper target was shown (Fig 7.2a). The upper visual field was chosen for target placement as MIB is most robust at this location (Bonneh et al., 2001). The blue distracter grid (luminance 8.81 cd/m^2) and yellow targets (luminance 11.23 cd/m^2) were displayed on a black background (luminance 0.10 cd/m^2). In Experiment 2, a continuous

stream of coloured crosses (0.250 degrees wide and 0.375 degrees high) was presented at fixation, with each cross appearing for 250 ms with a 500 ms blank period between subsequent crosses. Each individual cross could appear in any of six colours (red, green, yellow, blue, cyan, and purple) and two orientations (upright or inverted; the horizontal line of the cross was placed 0.25 degrees above or below the centre of the vertical line) (Fig 7.2a). Stimuli were created in Cogent 2000 (www.vislab.ucl.ac.uk/cogent.php) under MATLAB 7.1.0 (www.mathworks.com) and presented on a CRT display (21" Sony GDM-F520) that was set at 600 by 800 pixel resolution and an 88 Hz refresh rate.

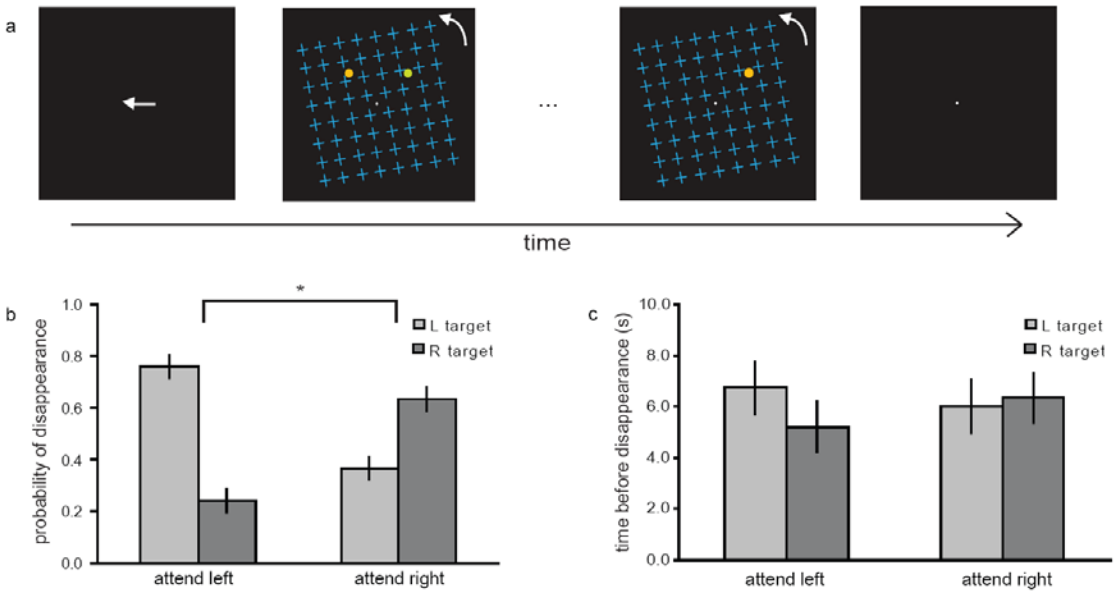

Figure 7.1 Experiment 1. (a) *Participants viewed an MIB display of two dots in their upper visual field amidst a grid of rotating blue crosses and reported hue changes and disappearances. Each trial started with an arrow reminding the participant of the target to attend to (left or right), followed by the MIB display. Participants reported hue changes (from reddish yellow to greenish yellow) in the attended target. As soon as one (in this case the left) target perceptually disappeared, they responded using a key press upon which the screen turned black, followed by a key press indicating which target had disappeared. This signalled the start of the next trial. The probability of* ***(b)*** *and time required until* ***(c)*** *disappearance of either target is shown for each attended side separately. Light grey bars represent disappearance of the left target, dark grey bars represent disappearance of the right target. Error bars represent the standard error of the mean. Significant differences are indicated by asterisks.*

7.2.2 General procedure

Both experiments lasted about an hour, including practice trials and breaks, and were carried out in a darkened room. Participants were tested extensively before the experiments to ensure they could experience MIB and assign consistent responses to the different perceptual states. To ensure a fixed viewing distance of 57 cm, a chin rest supported their head. They responded by use of a keyboard. Eye position and pupil diameter were continually sampled at 300 Hz using a CRS infrared video-based eye tracker (Cambridge Research Systems Ltd, Kent, England). Eye position was defined as the mean horizontal and vertical position of the eye, eye movements were defined as variance round the eye position, and eye blinks as an absence of signal. Statistical analyses were performed to examine differences in eye movements and blinks between the various experimental conditions. For one (Experiment 1) and four (Experiment 2) participants, eye data could not be analysed due to technical difficulties. Procedures specific to each experiment are described below.

7.2.3 Experiment 1 procedure

Experiment 1 tested the effect of directed spatial attention on MIB. In separate blocks, participants were instructed to fixate centrally while attending either the left or the right yellow target. Each target subtly changed hue between reddish-yellow and greenish-yellow at random intervals every 1-3 seconds. Both dots changed hue at random times (though never simultaneously), so changes to the attended and unattended target were perceptually equivalent. Participants were required to report hue changes of the attended target while ignoring hue changes of the unattended target by pressing either the left or the right arrow on the keyboard with their right index finger, depending which side was attended. At the same time as reporting hue changes for the attended side, observers monitored both target dots for perceptual disappearance. As soon as they saw either target disappear, they were required to press the up arrow, upon which the screen turned completely black. They then had 3 seconds to indicate which target (left, right or both) had disappeared using a key press (left, right, or

up arrow respectively). This second key press signalled the start of the next trial, which was preceded by an arrow on the screen pointing leftward or rightward to remind participants whether they were required to attend the left or right visual field target. Each visual field target was attended for 8 blocks of 3 minutes; thus, there were 16 blocks in total, each block consisting of a variable number of trials (depending on the time it took for a target to disappear), but always with the same attended side throughout. Participants could take breaks in between the blocks.

In addition, during one trial in each block, one of the targets (the attended targets in half these trials) was physically removed from the screen after 5 seconds. The latency with which observers responded to the physical disappearance of this target served as an estimate of their reaction times to the perceptual disappearance of the targets. After the experiment, trials were divided into those where the attended target perceptually disappeared first, and those where the unattended target perceptually disappeared first. These trial 'categories' were used to arrive at an estimate of the probability with which a target disappeared; for instance, the probability that the left target disappeared whilst being attended was defined as the number of trials the left target disappeared while attending to the left side, divided by the number of trials that any target disappeared while attending to the left side.

7.2.4 Experiment 2 procedure

Experiment 2 tested the effect of attentional load in an unrelated task at fixation on MIB in three different conditions; no, low, and high attentional load. For each condition, identical physical stimuli were presented at fixation while an MIB target was presented in the periphery; but the nature of the central task changed. The central task has been extensively described elsewhere (Schwartz et al., 2005).

Under no attentional load, participants fixated the central stream of crosses but were not required to perform any task on these stimuli. To avoid involuntary responses to the stimuli, all crosses in this condition were of the same colour which was random, though not one of

the target colours in the other two conditions (red, green, or yellow). At the same time, participants were required to monitor the peripheral MIB target and to indicate its disappearance by pressing a key down with their right index finger when it was invisible, and releasing the key when it was visible. In the low attentional load condition, in addition to monitoring the peripheral MIB target for disappearances and reappearances, participants performed a simple feature-detection task on the stream of crosses presented at fixation. Specifically, they were required to monitor the stream of crosses and press a key with their left index finger whenever they saw a red cross. In the high attentional load condition, in addition to monitoring the peripheral MIB target for disappearances and reappearances, participants performed a more challenging conjunction-detection task on the stream of crosses presented at fixation. Specifically, they were required to monitor the stream of crosses and press a key with their left index finger when either an upright yellow or an inverted green cross was displayed.

In all three conditions, participants were encouraged to respond as quickly and accurately as possible. Each of the three conditions was tested in 8 blocks of 2 minutes, giving 24 blocks in total; their order was randomised and they were preceded by a written instruction specifying the load condition beforehand. Participants could take a break after every fourth block. In addition, during each block, the yellow target was physically removed from the screen once for 7.5 seconds approximately halfway through the block, yet always at a time when it was being reported by the participants as perceptually visible. Upon debriefing, participants declared they could not distinguish between instances where the target disappeared due to MIB or due to physical removal. Their key presses to the physical disappearance and reappearance of the target in these instances served as an estimate of their reaction times to the switches in perception.

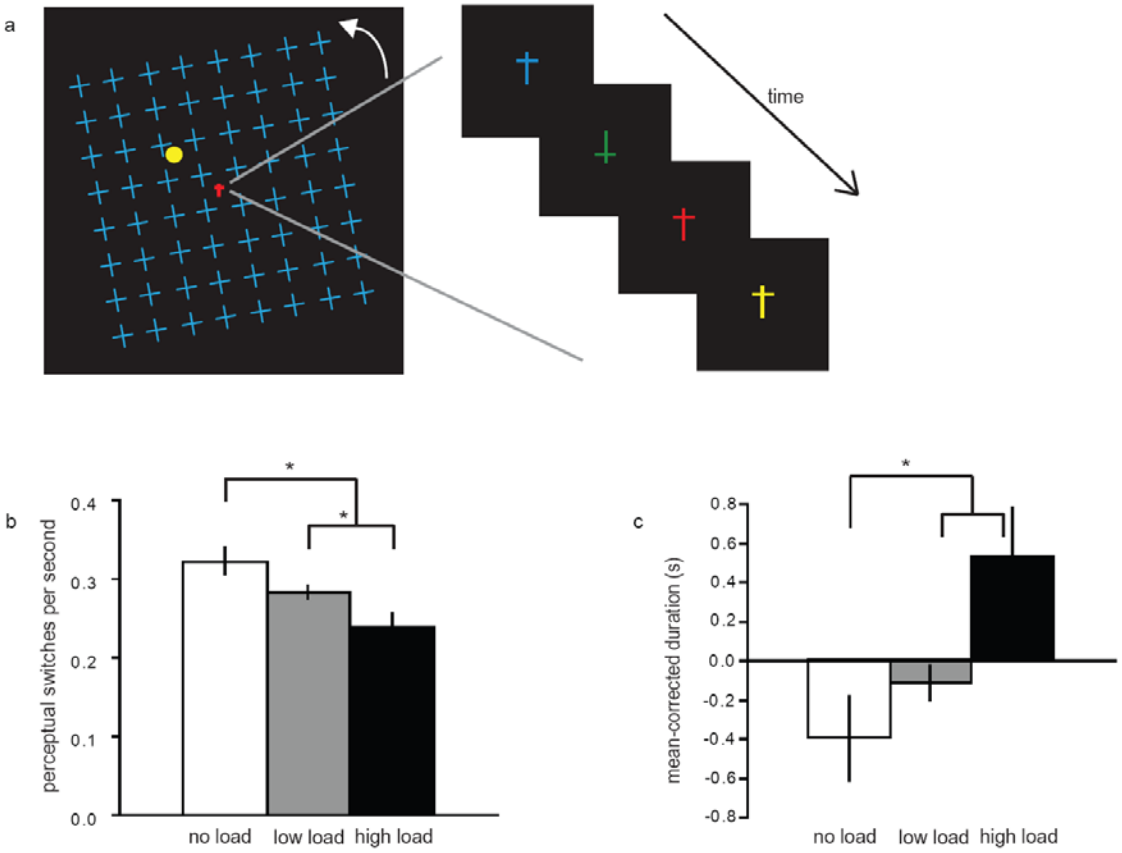

Figure 7.2 Experiment 2. (a) *Participants viewed an MIB display of one yellow dot in their left upper visual field amidst a grid of rotating blue crosses, whilst maintaining fixation at a central stream of crosses of different colour and orientation (enlargement of centre). They indicated by pressing or releasing a button when the target dot was visible or invisible, while simultaneously performing an attentional task involving the central crosses (see 7.2.4).* ***(b)*** *The average number of perceptual disappearances and reappearances of the target (taken together as perceptual switches per second) are shown; the average durations of the target invisibility are shown in* ***(c)****. Since invisibility durations were highly variable across participants (2616 ± 2724 ms, 2894 ± 2391 ms, and 3526 ± 4298 ms for the no, low, and high load conditions) and the difference between the conditions within participants was the variable of importance, durations were individually mean-corrected to the average of the three conditions. White bars represent the no load condition, grey bars the low load condition, and black bars the high load condition in both graphs. Error bars represent the standard error of the mean-corrected average of participants. Significant differences are indicated by asterisks.*

7.3 Results

7.3.1 Experiment 1

In Experiment 1, spatial attention was directed towards one of two targets by requiring participants to report hue changes of this target; they also reported perceptual disappearances of both targets. The first disappearance of either target signalled the end of the trial. Trials where both targets disappeared simultaneously were excluded from the analysis. On average, participants completed 154 and 146 trials while attending to the left and the right visual field target, respectively. Their reaction times to the hue changes of the attended target did not differ significantly between visual field ($t(5) = .135$, $p = .898$; 961 ms and 968 ms for the left and right target, respectively).

Directing attention to the left visual field target strongly increased the probability of that left target disappearing first (compared to the unattended right visual field target), and vice versa (Fig 7.1b). This striking effect of attention was confirmed by the significant interaction between perceptually disappearing target (right or left) and attended side (right or left) ($F(1,5) = 58.357$, $p = .001$), as revealed by repeated-measures ANOVA. There were no main effects of target ($F(1,5) = 2.853$, $p = .152$) or attended side ($F(1,5) = 1.107$, $p = .319$). A χ^2 test on the probability of the attended target disappearing first showed that this effect was highly significant across all 6 participants (all p values below 0.0001). In contrast, the direction of attention had no effect on the time from the start of a trial until a target perceptually disappeared (Fig 7.1c). The interaction between required time and attended side was not significant ($F(1,5) = 2.679$, $p = .163$) and there was no main effect of attended side ($F(1,5) = .036$, $p = .857$). There was a main effect of target ($F(1,5) = 23.432$, $p = .005$), with the right target perceptually disappearing quicker than the left target, regardless of whether it was attended to or not.

The observed differences in probability of disappearance between the attended and the unattended target could be caused by a failure to notice disappearance of the unattended

target. In order to account for this, the targets were periodically removed from the screen and reaction times to these disappearances were measured. Surprisingly, the reaction times to report physical disappearance of the unattended target were slightly shorter compared to the reaction times to the attended target (1126 ms and 1267 ms respectively; $t(5) = 2.319$, $p = .068$, values more than 2 std. from the mean excluded). Our results can therefore not be explained by a failure to keep track of the unattended target. The peripheral location of the targets, participants' division of attention between the two targets, and their engagement in the hue change detection task are all consistent with these relatively long reaction times. The probability of disappearance might also be influenced by small eye movements or blinks round the time of the perceptual switch (Hsieh and Tse, 2009;Martinez-Conde et al., 2006). However, paired t-tests of eye position, eye movements and average number of eye blinks / sec (see 7.2.2) showed that these did not differ significantly in the 1.5 s leading up to the button press signalling the disappearance of the attended or unattended target ($t(4) = .885$, $p = .426$, $t(4) = 1.716$, $p = .161$, and $t(4) = 2.152$, $p = .098$, respectively). Thus, the increased probability of disappearance of the target can reliably be attributed to an attentional effect.

One possible attentional mechanism which could have contributed to the increased probability of disappearance for the attended target is prior entry into awareness, which is the notion that an attended stimulus or event will be experienced sooner than a physically simultaneous unattended stimulus or event (Schneider and Bavelier, 2003). Thus, maybe the targets disappeared simultaneously, but the disappearance of the target on the attended side was detected first. In order to control for this possibility, we conducted a control experiment in three subjects who had also participated in the original experiment. We introduced a short delay of 750 ms between the time of the first button press (indicating that one of the targets had disappeared) to erasing the stimulus from the screen, thus allowing the detection of a possible disappearance of the unattended target as well. If there had been a prior entry effect of attention, more 'simultaneous disappearance' button presses would be expected in this manipulation than when the stimulus was removed immediately. However, the number of 'simultaneous disappearance' button presses did not increase (1 vs 0, 7 vs 5, and 26 vs 14 for

the previous vs present number of button presses, respectively, for the three subjects) as compared to the condition where the stimulus was removed from the screen immediately. We therefore conclude that the increased probability of the attended target to disappear first was not due to a prior entry of this target into awareness.

7.3.2 Experiment 2

In Experiment 2, attention was progressively directed away from the target and distracters by introducing an unrelated task at fixation at increasing levels of attentional demand. Participants' performance on the central task showed that the manipulation of attentional load was successful. Mean reaction times were shorter and the percentage of correctly detected central targets higher in the low load compared to the high load condition (623 and 753 ms, 96% and 85%, respectively). These differences were significant ($t(8) = 9.118$, $p < .001$ for RTs; $t(8) = 5.004$, $p = .001$ for accuracy). This replicates previous findings (e.g. Schwartz et al., 2005) and confirms that attentional demands were indeed higher under high compared to low attentional load.

Behaviour on the motion-induced blindness task was captured by two variables: the average number of disappearances and reappearances of the target (together called 'perceptual switches') and the average duration that the MIB target was invisible. Assessing the probability and time it took for the target to disappear, as calculated in Experiment 1, was not possible due to the use of a continuous MIB display instead of discrete trials. To assess the influence of the unrelated attentional task on the normal MIB behaviour of our participants, we first computed an attention index (AI), using the formula AI = (average of the number of perceptual switches under low and high load conditions together) / (average number of perceptual switches under the no load condition). This AI for switches equalled .81, corresponding to a significant decrease in number of perceptual switches under the load (versus the no load) conditions ($t(8) = 3.664$, $p = .007$). Using the same attentional index formula but now using average durations that the target was invisible rather than switches,

the attention index for durations equalled 1.23 for the load (versus the no load) conditions, corresponding to a small but significant increase in duration of the invisible periods ($t(8) = 2.340$, $p = .047$). Thus, while the duration that the target was invisible increased with attentional load, the number of switches decreased. Independent of this, the percentage of total time of the experiment that the target was invisible slightly decreased as a function of load (38.5%, 36.8%, and 35.6% for the no, low, and high load conditions respectively), though this measure did not reach significance ($F(1,8) = .334$, $p = .645$). Thus, adding an unrelated task to MIB decreases the number of perceptual switches and increases the duration that the target is invisible, whilst not significantly influencing the total proportion of time that the target is invisible.

The average number of perceptual switches decreased even more for the high attentional load compared to the low attentional load condition ($t(8) = 4.458$, $p = .002$) (Fig 7.2b). Also the effect of attention on duration was further increased; the target was invisible for longer under high attentional load compared to low attentional load (Fig 7.2c). This pattern could be observed in 6 out of 9 participants, although it was not significant ($t(8) = 2.080$, $p = .071$). These observed duration differences between the three conditions could be due to shorter reaction times to a disappearance of the target, or longer reaction times to a reappearance of the target under high attentional load. To examine this possibility, we examined reaction times to the periodic physical removals and reappearances of the target. Mean reaction times to these target disappearances were 780 ms, 771 ms, and 1067 ms for the no, low, and high attentional load condition, respectively; for the reappearances of the target on the screen the mean reaction times were 1164 ms, 1378 ms, and 1463 ms. The peripheral location of the target and participants' engagement in the simultaneous central task can account for these relatively long reaction times. The effect of condition was not significant for either disappearances or reappearances ($F(1,8) = 2.082$, $p = .171$ and $F(1,8) = 0.954$, $p = .370$, respectively); moreover, both reaction time sets tended in the same general direction (higher reaction times under the high attentional load condition).

Any effect on reaction times to physical reappearances of the target could in principle be masked by the fixed interval of physical removal (7.5 seconds; see 7.2.4) which might conceivably have made anticipation possible (though participants were not informed about the physical removals). To rule out this possibility we therefore conducted a control experiment in two subjects, which followed an identical procedure but now with physical removals of variable duration (5-10 seconds). Mean reaction times to the target removals in this control experiment were 568 ms, 627 ms, and 679 ms for the no, low, and high attentional load condition, respectively; for the reappearances of the target on the screen the mean reaction times were 814 ms, 1497 ms, and 1190 ms. In both subjects, the effect of load (no, low, and high) was not significant for either physical disappearances or reappearances ($F(1,7) = 3.293$, $p = .100$ and $F(1,7) = 0.566$, $p = .503$). Also their reaction times did not differ significantly from their reaction times in the original experiment in any condition ($t(5) < 2.184$, $p > .065$). We therefore conclude that the regularity in duration of the physical removal of the target in the original experiment cannot account for our findings.

The observed differences in number of perceptual switches and average duration of MIB can therefore not be attributed to differences in reaction times. Alternatively, the differences in duration might have been due to differences in small eye movements or blinks (Hsieh and Tse, 2009;Martinez-Conde et al., 2006). Repeated measures ANOVA of eye position, eye movements, and average number of eye blinks / sec (see 7.2.2) revealed no significant differences between the three conditions ($F(1,4) = 1.141$, $p = .352$, $F(1,4) = 2.762$, $p = .155$, and $F(1,4) = 3.497$, $p = .129$, respectively). Hence, the differences we observed in number of perceptual switches and duration cannot be caused by differences in eye movements (although the precision of our eye tracker does not rule out potential differences in microsaccades). We therefore conclude that placing attentional demands on an unrelated central task decreases the number of perceptual switches and increases the duration of perceptual invisibility of the target.

7.4 Discussion

7.4.1 Effects of attention on stimulus awareness

The influence of high-level factors, such as endogenous attention, on the dynamics of motion-induced blindness has not been studied extensively. Here we showed that directing spatial attention to an MIB target directly increased its probability of disappearance (compared to an unattended MIB target), whilst not interfering with the time it took the target to disappear. Conversely, increasing the attentional load in a central task unrelated to MIB decreased the number of disappearances and reappearances of the target and prolonged the periods of its perceived visibility and invisibility.

It is well established that spatial attention can modify processing in local regions of the visual field, and this is associated with corresponding retinotopically-specific modulations of activity in primary and extrastriate visual cortex (Brefczynski and DeYoe, 1999;Ghandi et al., 1999;Somers et al., 1999). Typically, the effect of spatial attention is characterised as strengthening the representation of a stimulus, enhancing its salience and potency in competitive interactions with cortical representations of other stimuli in the visual environment (Kastner et al., 2009). Here, we found that spatial attention directed to an MIB target increased the probability of it disappearing. This appears counter-intuitive given the characterisation of spatial attention as increasing the salience of a target; why should a more salient target be more likely to disappear? However, previous behavioural work suggests that increasing target salience increases the duration of MIB (Bonneh et al., 2001). Specifically, disappearance of the target occurs for longer when the contrast between target and distracters is greater, presumably hampering the grouping of target and distracters (Hsu et al., 2004). These findings have led to the proposal that MIB is unlikely to be caused by local adaptation, but rather that higher level attentional and grouping mechanisms play a role (Bonneh et al., 2001). Thus, our findings of increased probability of disappearance with spatial attention are

consistent with the notion that increased salience of the target (relative to distracters) is associated with enhanced disappearance.

While Experiment 1 tested the effects of increasing attention directed specifically to the MIB target, Experiment 2 tested the effects of globally withdrawing attention from both MIB target and MIB distracters using attentional load in an unrelated central task. Attentional load theory (Lavie, 2005) proposes that at any one time the attentional capacity of participants is limited. After capacity is voluntarily allocated to the task at hand, any spare capacity results in processing of task-irrelevant stimuli. Thus, the extent to which task-irrelevant stimuli are processed depends on the degree to which attentional load in the relevant task has withdrawn resources from processing them. Processing of irrelevant distracters can be inferred either by measuring brain activity associated with their presence (Rees et al., 1997;Rees et al., 1999), or their behavioural interference on the central task (Lavie, 1995). Here, we explicitly required participants to monitor the peripheral MIB target at all times and so even under high load in the central task, attention by definition was not fully withdrawn but always remained to some extent divided. Moreover, the MIB target was not task-irrelevant, but rather associated with a different task. Nevertheless, the changes in performance in the central task replicate previous findings (Schwartz et al., 2005) and suggest that attention was progressively withdrawn from the MIB display under no, low and high load respectively. We found that such allocation of attention to the central task leads to a decrease in number of perceptual switches reported. Following load theory, this implies that perceptual alternations require some allocation of attentional resources.

7.4.2 Attention in the neural competition model

How do the findings from both experiments relate to existing explanations of motion-induced blindness? Bonneh et al. (2001) speculated that MIB might be caused by a disruption of usually unnoticed, fast attentional switching. This disruption might result from an inability to divide attention between dissociated elements (i.e. the target and distracters)

of the visual scene. On such an account, directing attention towards the target location would predict increased disappearance of the target since it is incompatible with the distracters. This is in line with our first experiment. However, directing attention away from the target would predict diminished attentional disruption and therefore more, naturally occurring, perceptual switches. This is not in agreement with our findings of a 'slow-down' of perceptual fluctuations in the second experiment. MIB has more recently been described in terms of a process of completion of the distracters into one homogeneous field, thus hiding the target from view (Graf et al., 2002). Such a completion process implies local neuronal competition between target and distracters. This process might be likely to occur in regions in early visual cortex, corresponding retinotopically to the target location, as we have demonstrated in the previous chapter. Local neural competition is also assumed to underlie other completion processes such as perceptual filling-in (Mendola et al., 2006;Weil et al., 2008), neon colour spreading (Sasaki and Watanabe 2004), and filling-in of a visual phantom (Meng et al., 2005). Such neural interpolation mechanisms are facilitated by attention (Hol et al., 2003;De Weerd et al., 2006). Thus, directing attention to the MIB target should favour the distracters in the neural competition by enhancing distracter field completion and inducing target disappearance, which agrees with our findings. Conversely, directing attention away from both target and distracters should hamper the competition between target and distracters, thus slowing down the alternations of target visibility and invisibility.

7.4.3 Attention and bistable perception

Most studies investigating the effect of attention on bistable perception have focused on voluntary control over the perceptual alternation rate of the bistable stimuli. For example, voluntary attention can influence the rate of alternations in perception of apparent motion (Kohler et al., 2008). Attentional control over perceptual reversals of ambiguous figures is associated with activity in both frontal (Windmann et al., 2006) and posterior parietal (Pitts et al., 2008;Slotnick and Yantis, 2005) areas. Selective attentional control over perceptual

alternations in binocular rivalry is considerably weaker than control over alternations in other forms of bistable perception, such as Necker cube or face/house reversals (Meng and Tong, 2004;Van Ee et al., 2005).

More relevant to the present findings are several recent studies that have begun to investigate the effects of directing attention towards versus away from a bistable stimulus. In one study employing a continuous MIB display with two targets, attention to a target was manipulated by asking subjects to respond to the two targets simultaneously versus to only one of them (HaiYan et al., 2007). When attention is focused on one target only, it disappears more frequently and for longer than in the divided attention condition. Similar enhancement of disappearance by attention has also been reported for Troxler fading (Lou, 1999), and perceptual filling-in, a phenomenon related to MIB (Hsu et al., 2004;Hsu et al., 2006), is likewise affected by attention (De Weerd et al., 2006). All these results are consistent with our findings from Experiment 1. Another study showed that disengaging attention from a binocular rivalry stimulus by using a demanding, unrelated task reduces the rate of rivalry alternations (Paffen et al., 2006), and recently less disappearance of an MIB target has been reported under similar conditions (Carter et al., 2008). Thus, the results from both our experiments seem to be in agreement with the emerging literature on spatial attention and bistable perception.

7.5 Conclusion

We have shown that appearances and disappearances of the target in motion-induced blindness are influenced by endogenous attention. It has been hypothesised that the neural processes underlying motion-induced blindness reflect the completion of the distracters into a homogeneous field (Graf et al., 2002). Our present results support this account, by demonstrating that directing attention away from the target (and distracters) by an unrelated task elsewhere hampers this process, by impeding competition between target and

distracters, while directing attention towards the MIB target enhances such a process, by enhancing competition between MIB target and MIB distracters. Together, these results demonstrate that endogenous attention can indeed influence fluctuations in internal brain state leading to bistable perception.

Chapter 8 General Discussion

8.1 Overview of findings

At any point in time, the brain's activity constitutes a complex interplay between activity evoked by sensory stimuli and cognitive processes, and ongoing, spontaneous activity that is unrelated to such processes. This spontaneous activity is in fact the dominant component of the brain's total activity. This thesis has explored the nature of spontaneous brain activity, focusing on several of its aspects and using several methodologies.

Using a theoretical approach, I first demonstrated that the large contribution of spontaneous activity to the brain's total activity is reflected in cortical energy use. Calculations based on monkey electrophysiology data revealed that conscious perception of a stimulus in three modalities (vision, touch, and hearing) was associated with a minute increase in total cortical activity and therefore, energy use. This very small increase in energy use might well translate into a very small increase in blood flow; so small that it might not even be detected in the fMRI BOLD signal.

The relationship between the BOLD signal and cortical activity changes was explored further in the context of purely spontaneous activity, i.e. in situations where no stimulus is present at all. Under such conditions, the fMRI signal exhibits slow fluctuations that are spatially coherent over the entire brain, so-called resting-state activity. Using simultaneous LFP-fMRI measurements in awake monkeys, I demonstrated widespread correlation between gamma power in the LFP signal and fMRI resting-state activity. The correlation peaked when the fMRI signal lagged behind the LFP power by 7-8 seconds and depended on the monkey's level of drowsiness. Thus, the coherent fluctuations observed in the fMRI signal in the resting state are reflected in fluctuations in correlated neuronal activity, while the strength of this relationship depends on behavioural state.

Having shown that spontaneous activity measured by fMRI is directly related to spontaneous neural activity, I then used fMRI to explore the influence of spontaneous activity on local stimulus processing in visual cortex. Presenting a stimulus at perceptual threshold, I showed that spontaneous activity accounted for a large fraction of the variability in the BOLD response that this stimulus evoked. Conversely, the influence of spontaneous activity on the behavioural outcome of the stimulus (perceiving or failing to perceive the stimulus at threshold) was very modest.

In order to investigate the influence of spontaneous activity on more drastic changes in perceptual outcome, I decided to use a bistable stimulus instead of a stimulus at perceptual threshold. I used motion-induced blindness (MIB) as a model system for studying the effect of spontaneous activity on bistable perception. Using fMRI, I showed that perceptual disappearance of the stimulus in MIB is coupled to an increase in activity in retinotopic locations representing the stimulus in early visual cortex. Local fluctuations in spontaneous activity thus have a direct effect on the perceptual awareness of the bistable stimulus.

Finally, I investigated the influence of other factors such as endogenous attention on fluctuations in spontaneous activity itself. Again using motion-induced blindness as a model system, I demonstrated in two behavioural experiments that the dynamics of the perceptual appearances and disappearances of the stimulus, which are underlied by fluctuations in internal brain state, are influenced by attention.

In conclusion, therefore, I have demonstrated that spontaneous activity makes up the dominant component of the brain's total activity and energy use. I have revealed a direct relationship between spontaneous activity measured by fMRI and spontaneous neuronal activity. Using fMRI, I have then explored the influence of spontaneous activity on stimulus-evoked activity and behaviour. I have shown that spontaneous activity partly accounts for variability in the response evoked by a stimulus, as well as variability in the perceptual outcome of a stimulus, such as awareness of a bistable stimulus. Spontaneous activity itself might be under the influence of other factors such as attention.

8.2 Implications of this research

The work presented in this thesis has contributed to the study of spontaneous brain activity. Since the main experimental method used in this work was fMRI, this contribution has been mainly in the domain of fMRI resting-state activity. In particular, it has advanced our understanding of two aspects of fMRI resting-state activity; its relation to the underlying neural activity and its effect on local stimulus processing.

8.2.1 Neurovascular coupling in the resting state

The relationship between the fMRI signal and the underlying neural activity has been studied almost exclusively in the context of a stimulus-evoked response (Logothetis et al., 2001;Niessing et al., 2005;Viswanathan and Freeman, 2007). That work has shown that fMRI responses are tightly linked with neural responses to a stimulus, particularly synaptic activity reflected in the local field potential. The work described in Chapter 4 presents the most direct evidence to date that this tight relationship between fMRI activity and local field potential also holds true for spontaneous activity. This conclusion is important for the interpretation of fMRI studies of resting-state activity; the large-scale, coherent fluctuations commonly observed in the resting-state fMRI signal are not an artefact of fluctuations in heart rate or respiration, but are genuinely associated with large-scale fluctuations in neural activity. Quantifying the relationship between these large-scale fluctuations in neural and fMRI activity will be difficult, however, since numerous physiological factors contribute to the modulation of microvasculature (Attwell and Iadecola, 2002). Moreover, our data show that the relationship between resting-state fMRI activity and spontaneous neural activity depends on the behavioural state of the subject; the fMRI and the neural signal were more tightly coupled when the monkey was in a more drowsy state than when the monkey was alert. Our data therefore also provide a word of warning to fMRI research in general; ‘fMRI activity’ does not linearly translate into ‘neural activity’.

8.2.2 Spontaneous activity and local stimulus processing

To date, the effects of resting-state activity on stimulus-evoked activity and behaviour have not been studied in great detail. The main findings on this topic were obtained in motor cortex, where the effects of spontaneous activity on BOLD activity evoked by a button press (Fox et al., 2006b) and button press force (Fox et al., 2007) were assessed. The work presented in Chapter 5 generalises these findings to the visual cortex. A similar effect of spontaneous activity on BOLD response variability was found; in contrast, the effect of spontaneous activity on the behavioural outcome associated with stimulus presentation was modest. Spontaneous activity studied in the context of bistable perception (Chapter 6) showed a clearer correspondence between internal brain state and perception; robust fluctuations in visual perception (awareness of the stimulus) were associated with clear changes in activity in stimulus-specific retinotopic locations in early visual cortex. This work contributes to the literature concerning perceptual awareness (Blake and Logothetis, 2001;Sterzer et al., 2009) and further elucidates the role of early visual areas in bistable perception.

8.2.3 Practical implications

Finally, the work on spontaneous activity presented here has some practical implications for the analysis of resting-state activity measured using BOLD fMRI. As outlined in 2.3.5, fMRI resting-state studies routinely remove the spontaneous BOLD fluctuations common to the whole brain (the so-called global signal) in order to reveal functional networks in the data (Fox et al., 2006a;Macey et al., 2004). The work presented in Chapter 4, however, demonstrates widespread correlation between neural activity and the fMRI signal throughout large parts of the cerebral cortex. This suggests that some portion of the global signal that is routinely removed in fMRI resting-state studies is closely linked to neural activity. We therefore advocate the use of a region that is unlikely to be influenced by neuronal activity

(such as the ventricles), rather than the global signal from the entire brain, to obtain a reference time course from in order to remove spurious correlations from the data.

The data presented in Chapter 5 demonstrate that spontaneous activity accounts for a large portion of the variability in stimulus-evoked responses in the fMRI signal. Removing this contribution of spontaneous activity by means of a control region resulted in a substantial increase in signal to noise ratio (SNR). In order to achieve a similar increase in SNR in any task-related fMRI study, a short resting-state scan can be acquired alongside with the task data, which can be used to extract a control region; the spontaneous activity in this control region during acquisition of the task-related data can then be included as an extra regressor in the design. This method has already begun to be used (Bianciardi et al., 2009c;De Zwart et al., 2008) (see also 2.3.7). Our optimised method for extracting a suitable control region, by using a weighted average of the activity in the 100 best correlated voxels as an estimate of the 'true' spontaneous activity in a stimulus region (see 5.2.5), can potentially help the implementation of this analysis step into many task-related designs.

8.3 Experimental shortcomings

In hindsight, several aspects of the design and analysis of some of the described experiments could have been improved. These shortcomings in the experiments do not invalidate the results presented in this thesis, but pose some limitations on their interpretation and implications.

8.3.1 Controlling electrode position and behavioural state

In order to gain an even better understanding of the neural basis of fMRI resting-state fluctuations, the permanent electrodes that were implanted in the brains of our monkeys (Chapter 4) could have been placed more strategically. For present purposes, they were implanted at rather arbitrary locations in frontal, parietal, and occipital cortex. Had they been

carefully placed in, for instance, areas that are part of the so-called default mode network (Greicius et al., 2003), then correlating their activity with the fMRI activity in all voxels in the brain (the 'seed region' approach) might have revealed more specific networks in the data. Also, having electrode pairs within the same functional network as well as in opposing networks might have given a better insight into the spatial specificity of the fMRI/neural correlation. Secondly, no heart rate and respiration data were collected for the monkeys, even though this can be effected relatively easily using a pulse oximeter and by monitoring exhaled CO_2. These physiological data could have provided complementary information on the correlation between the fMRI and the neural signal, by providing a quantitative estimate on how much of the fMRI activity is explained not by fluctuations in neural activity, but instead by heart rate and respiration. Finally, the behavioural states ('awake' and 'asleep') for which we make differential claims about neurovascular coupling (see 4.3.4) are not very well defined. In particular, they comprise spontaneous opening and closure of the monkeys' eyes and are therefore not well balanced across monkeys and sessions. Future experiments in which 'alert' and 'relaxed' states are experimentally controlled (for instance by a simple fixation task), will allow us to investigate neurovascular coupling in the resting state in a more rigorous manner.

8.3.2 Protection zone and control ROIs

The experiment into the neural correlates of motion-induced blindness (Chapter 6) would have benefitted from a slightly improved task design. First of all, the target stimulus (the yellow dot, see Fig 6.1a) was not surrounded by a blank 'protection zone' in which no distracters were present (Bonneh et al., 2001). At present, the activity increase in the retinotopic location of the target in V1 (see 6.3.2) can be attributed to either target-related activity, distracter-related activity, or a combination of both. Despite the limited spatial resolution of fMRI in relation to the size of the target, the presence of a protection zone without distracters could have aided in the disentanglement of target- and distracter-related

activity. Secondly, the control region in the hemisphere opposite from the target representation, which was used to check for spatial specificity of the observed activity increase for perceptual invisibility (the 'control ROI', see 6.2.5), could have been chosen more carefully, for instance by localising this region of visual space (the 'diagonal' from the target location) together with the stimulus localiser (see 6.2.3). Alternatively, a number of control regions throughout the visual cortex could have been selected more or less at random, and activity differences between the three perceptual states ('target visible', 'target invisible', and 'target absent') could have been examined in each of them. Both methods would have provided a more rigorous control measurement of the activity increase associated with perceptual disappearance of the target. Finally, the experimental design was not optimised for finding differences associated with perceptual switches in higher level areas, such as prefrontal cortex. Transient fMRI signal increases associated with perceptual transitions have been previously found in frontal regions (Kleinschmidt et al., 1998;Lumer et al., 1998), but were not observed in our study. This might have been due to the low number of participants in our experiment (eight), and including more participants in the study might have allowed us to detect activity differences in extra-visual areas.

8.3.3 Controlling for attention

It is well known that even in the absence of a stimulus, spatial attention can increase both fMRI activity (Kastner et al., 1999;Sapir et al., 2005) and neuronal firing rates (Colby et al., 1996;Luck et al., 1997). This increased baseline activity has been interpreted as a direct demonstration of top-down feedback, biasing neurons with receptive fields overlapping the attended location and thereby favouring stimuli that will subsequently appear there at the expense of those appearing at unattended locations (Kastner and Ungerleider, 2000). It is a reasonable concern, therefore, that the effect of spontaneous fMRI activity on participants' behaviour during the grating detection task at threshold (Chapter 5) and motion-induced blindness (Chapter 6) might have been confounded by attention.

For instance, the variability in the evoked BOLD response and the behavioural variability in the responses to the low-contrast Gabor grating (Chapter 5) could conceivably have been due to fluctuations in attention rather than purely spontaneous fluctuations in the fMRI BOLD signal. Although several lines of evidence, such as the absence of any relationship between reaction times and magnitude of the evoked BOLD response or inter-trial interval length, speak against the presence of a big attentional component in the data, the possible influence of attention cannot be completely eliminated. In order to control for a potentially confounding effect of attention even more rigorously, we could have shown 'catch' stimuli at unpredictable locations in the visual field. This would have eliminated a potential contribution of spatial attention, yet would have made the experiment even longer due to the addition of these catch stimuli.

The activity increases associated with target invisibility in the motion-induced blindness task (Chapter 6) could also potentially be explained by involuntary, transient shifts in attention to the disappearing target, an effect termed attentional capture (Lee et al., 2007;Pastukhov and Braun, 2007). This is especially likely given that directed spatial attention has a direct effect on target disappearance (Chapter 7). We attempted to keep such confounding fluctuations in attention to a minimum by introducing a secondary task at fixation and having a control condition of 'real' target disappearance (which is perceptually indistinguishable from perceptual target disappearance). It is difficult to rule out the attentional capture effect any further. In order to estimate the effect of attentional capture on the data, long periods (>10 seconds) of stimulus invisibility could be taken and the level of activity in relation to stimulus visibility estimated for the first half of these periods (just after the perceptual switch) as well as for the second half (when the stimulus percept is stable).

8.4 Outstanding issues

Several chapters in this thesis have touched upon outstanding issues in the study of spontaneous brain activity, which call for new experiments and will hopefully shape the themes around which the research field will evolve in the near future.

8.4.1 Interaction between spontaneous and evoked activity

In Chapter 5, the interaction between spontaneous and stimulus-evoked brain activity was examined for the stimulus used in the experiment, a low contrast Gabor grating at perceptual threshold superimposed on a patch composed of random noise. This interaction was assessed in a psycho-physiological interaction (PPI) analysis. Spontaneous BOLD activity and BOLD activity evoked by the stimulus were found to be linearly additive; no evidence for a nonlinear interaction was found (Fig 5.4). This result is in agreement with findings in motor cortex, where the magnitude of the response to a button press did not depend on whether the response occurred during a peak or a trough in the underlying spontaneous activity (Fox et al., 2006b). Conflicting evidence has been reported for the FFA and V5/MT, however, where the shape of the BOLD response to a visual stimulus depended on the activity prior to that stimulus, leading to the conclusion that prestimulus 'spontaneous' activity interacted with the activity evoked by the stimulus (Hesselmann et al., 2008a;Hesselmann et al., 2008b). One explanation for the apparent inconsistency in the findings might lie in the way spontaneous brain activity was measured; when an estimate of the spontaneous activity in the area of interest by means of another brain area was used, no interaction between the spontaneous and evoked activity was found, whereas when prestimulus activity was used as a measure of spontaneous activity, an interaction was found.

Both methods of measuring spontaneous brain activity (using an estimate versus using prestimulus activity) yield inaccurate accounts of the veridical spontaneous activity in the area of interest while the stimulus is presented. Therefore settling this apparent inconsistency in the findings to date might benefit from electrophysiological methods, which can measure

the spontaneous neural activity directly and have much better spatial resolution than fMRI. The interaction between spontaneous and stimulus-evoked neural activity has been studied in one of the earliest, seminal electrophysiology studies on spontaneous neuronal activity (Arieli et al., 1996). Measuring the effect of a very simple visual stimulus on the visual cortex of anaesthetised cats, this study proposed that the stimulus evoked a constant amount of neuronal activity that was linearly superimposed on a variable amount of ongoing, spontaneous activity. This experiment can be repeated in awake animals, so that the spontaneous neuronal activity is not compromised by the anaesthesia (Vincent et al., 2007) and more complicated stimuli can be used. In addition, doing this experiment in awake animals allows for the option of requiring a behavioural choice of the animal based on the stimulus. In this way, the effect of spontaneous activity on the behaviour of the animal itself can be studied and compared to the findings in humans (Fox et al., 2006b;Thut et al., 2006).

8.4.2 Origins of spontaneous activity

In our simultaneous LFP-fMRI recordings in monkeys (Chapter 4), we found widespread correlation between the gamma LFP power and the fMRI signal, irrespective of where the LFP signal was sampled from, be it the occipital (Fig 4.4), frontal (Fig 4.6), or parietal cortex. This suggests that across the entire cortex, correlated spontaneous fMRI activity is coupled to correlated spontaneous neural activity. The correlation between spontaneous fMRI activity in distant cortical areas has been studied extensively (Biswal et al., 1995;Fox et al., 2006a;Greicius et al., 2003). Correlation in spontaneous neural activity has been less well investigated to date. Intracranial electrocorticography (ECoG) recordings in humans have revealed significant interhemispheric correlations in gamma power between functionally similar areas, such as the auditory cortices (Nir et al., 2008) and the sensorimotor network (He et al., 2008). These correlations were enhanced during rapid eye movement and stage 2 sleep (Nir et al., 2008). Only one of the two monkeys used in the experiment described in Chapter 4 had more than one functioning implanted electrode in the

brain at any point in time. Additional simultaneous recordings from these electrodes outside the scanner environment, when the LFP signal is not being polluted by the switching of the gradients, could confirm and extend the findings from human data (Nir et al., 2008).

The basis of the widespread correlation between the fMRI signal and the gamma LFP power fluctuations is at present a matter of speculation. One possibility is that modulations in both the neural and the haemodynamic signals share a common, perhaps subcortical origin. BOLD resting state fluctuations in both cortical hemispheres have been shown to be strongly correlated to fluctuations in their contra- and ipsilateral thalamus (Zhang et al., 2008), thus highlighting the potential importance of thalamocortical pathways in the resting state. Activity in thalamocortical loops could have a widespread, modulatory effect on neural activity over large portions of the cerebral cortex, which could lead to corresponding vascular responses via local neurovascular coupling. Simultaneous recordings of spontaneous LFP fluctuations from these potential subcortical loci and the cerebral cortex in future studies might shed more light on the origin of resting state fluctuations.

8.4.3 Scale at which spontaneous activity operates

In this thesis, I have focused mainly on the ultra-slow fluctuations in spontaneous activity across the entire cerebral cortex that can be detected with BOLD contrast fMRI. These spontaneous fluctuations are dominated by very low temporal frequencies, following a 1/f –like power distribution (Cordes et al., 2001). The data presented in Chapter 4 show that these ultra-slow fluctuations in BOLD signals are also present in electrophysiological signals, especially in gamma-band local field potential power. The brain-wide coverage of BOLD signals has led to the uncovering of widespread correlations at the spatial scale of the entire cerebral cortex, a fact which has been exploited in the choice of a control region in Chapter 5.

FMRI inherently offers a limited spatial resolution (in the order of mm^3) and a very limited temporal resolution (in the order of seconds), and can therefore detect only a subset

of the spontaneous activity that is potentially present. Electrophysiological data show that the spontaneous activity of single neurons can shape network activity on much smaller temporal and spatial scales. The spontaneous firing of single neurons is strongly correlated to the instantaneous spatial pattern of ongoing population activity in its neighbours, and these spatial patterns remain very similar when the single neurons are driven by their optimal stimulus instead of firing spontaneously (Tsodyks et al., 1999). Such spontaneously emerging spatial patterns in the population activity in visual cortex often closely resemble orientation maps (Kenet et al., 2003). This suggests that orientation maps are largely determined by intra-cortical connectivity, and that the response of neurons in visual cortex is affected to a large degree by spontaneously emerging 'cortical states' rather than being a direct reflection of the visual input. These studies therefore show that spontaneous activity on the level of single neurons has a highly stable and coherent spatio-temporal structure.

Spontaneous activity in the brain is therefore present at multiple temporal and spatial scales. What, if any, is the connection between the fast switching spontaneous cortical states measured with electrophysiology, and the very slow, global fluctuations detectable with fMRI? Do they share a common origin? Attempts to answer such questions would benefit greatly from electrophysiological measurements at the scale of the entire brain. The properties of the spontaneous activity recorded in this way would be directly comparable to resting-state fMRI data, since the data could contain arbitrarily low frequencies (depending on the length of continuous data collection) and have brain-wide coverage just like fMRI data, yet would contain much more precise temporal and spatial information.

8.4.4 Function of spontaneous activity

The influence of spontaneous brain activity on stimulus-evoked activity and behaviour, as was studied in Chapters 5, 6, and 7, touches upon a much more fundamental issue; namely, what function spontaneous cortical activity serves. Why does the brain spend so much energy on neuronal activity without a clear purpose, and comparatively so little on

neuronal activity that is clearly linked to sensory and cognitive processing? The role of spontaneous activity in brain function is currently unknown, but several suggestions have been made.

One possibility is that spontaneous activity resembles a memory trace, with correlated spontaneous activity between areas or neurons revealing common activation by recent sensory experiences or cognitive tasks. For example, optical imaging in rat visual cortex has shown that following repetitive presentation of a visual stimulus, spatiotemporal activity patterns resembling the evoked response appear more frequently in the spontaneous activity than prior to the stimulus (Han et al., 2008). Such immediate 'replay' of sensory experience has also been reported in rat hippocampus (Foster and Wilson, 2006). This reverberation of recent sensory experiences in subsequent spontaneous activity could contribute to short-term memory by helping to consolidate these experiences into stable cortical modifications.

Another possibility is that spontaneous activity serves to organise and coordinate neuronal activity by supporting cortical network structures (Buzsaki and Draguhn, 2004;Salinas and Sejnowski, 2001). A myriad of self-governed oscillations at various spatial and temporal scales can be detected in the sleeping brain (Steriade et al., 1993;Steriade and Timofeev, 2003). These spontaneous network oscillations temporally link neurons into assemblies, which might, for example, be responsible for the binding of separately processed visual attributes into a coherent visual percept (Gray et al., 1989). Another example of spontaneous activity shaping cortical structures is given by the spontaneous and synchronous firing of ganglion cells, which generates waves of activity that help the formation of eye-specific layers in the retina and thereby structures the precise visual pathway from the retina to the lateral geniculate nucleus (Shatz, 1996).

A final possibility is that spontaneous activity represents dynamic predictions about future sensory events (Engel et al., 2001;Pouget et al., 2003) (see also 1.3.3). Experimental support for this 'predictive coding' notion comes both from optical imaging (Kenet et al., 2003) and fMRI (Hesselmann et al., 2008a) studies. Electrophysiological recordings in cat visual cortex even show that spontaneous activity has predictive power for the subsequent

neural response to that stimulus; synchronous fluctuations between pairs of neurons before stimulus onset predict their response latency to be correlated (Fries et al., 2001a).

These possibilities are not mutually exclusive and all of them may be important in understanding the role of spontaneous activity in brain function. Whatever its precise role may be, the presence and properties of spontaneous activity are already altering the traditional views on brain function and will likely continue to do so in the future.

8.5 Conclusion

In this thesis, I have explored the nature of the brain's spontaneous activity, with an emphasis on its interaction with brain activity devoted to visual perception. Using a variety of complementary neuroscientific methods, I provided converging evidence to demonstrate that the large contribution of spontaneous activity to the brain's total activity is reflected in energy use; that spontaneous brain activity measured with fMRI is widely correlated with spontaneous neural activity; that spontaneous activity in visual cortex partly accounts for the variability in fMRI responses to a stimulus; that local fluctuations in the spontaneous activity in visual cortex have a direct effect on the perceptual awareness of a bistable stimulus; and that spontaneous activity itself is influenced by endogenous attention.

This work has advanced our understanding of the neurovascular coupling between spontaneous neural and fMRI activity under different behavioural conditions, as well as our understanding of the effect of spontaneous activity on local stimulus processing. In addition, it has a number of practical implications for the study of resting-state fMRI.

There are many 'big' questions that remain to be answered about spontaneous brain activity, including its origins, the temporal and spatial scale at which it operates, and its significance for brain function. This thesis has hopefully made a small contribution towards addressing these issues, and convinced the reader that understanding the brain's spontaneous activity will ultimately provide a deeper insight into the functioning of the brain as a whole.

References

Aguirre GK, Zarahn E, D'Esposito M (1998a) The inferential impact of global signal covariates in functional neuroimaging analyses. Neuroimage 8:302-306.

Aguirre GK, Zarahn E, D'Esposito M (1998b) The variability of human, BOLD hemodynamic responses. Neuroimage 8:360-369.

Albright TD, Desimone R, Gross CG (1984) Columnar organization of directionally selective cells in visual area MT of the macaque. J Neurophysiol 51:16-31.

Allen PJ, Josephs O, Turner R (2000) A method for removing imaging artifact from continuous EEG recorded during functional MRI. Neuroimage 12:230-239.

Anami K, Mori T, Tanaka F, Kawagoe Y, Okamoto J, Yarita M, Ohnishi T, Yumoto M, Matsuda H, Saitoh O (2003) Stepping stone sampling for retrieving artifact-free electroencephalogram during functional magnetic resonance imaging. Neuroimage 19:281-295.

Andrews TJ, Schluppeck D, Homfray D, Matthews P, Blakemore C (2002) Activity in the fusiform gyrus predicts conscious perception of Rubin's vase-face illusion. Neuroimage 17:890-901.

Arieli A, Sterkin A, Grinvald A, Aertsen A (1996) Dynamics of ongoing activity: explanation of the large variability in evoked cortical responses. Science 273:1868-1871.

Attwell D, Iadecola C (2002) The neural basis of functional brain imaging signals. Trends Neurosci 25:621-625.

Attwell D, Laughlin SB (2001) An energy budget for signaling in the grey matter of the brain. J Cereb Blood Flow Metab 21:1133-1145.

Azouz R, Gray CM (1999) Cellular mechanisms contributing to response variability of cortical neurons *in vivo*. J Neurosci 19:2209-2223.

Bakin JS, Nakayama K, Gilbert CD (2000) Visual responses in monkey areas V1 and V2 to three-dimensional surface configurations. J Neurosci 20:8188-8198.

Barlow HB (1957) Increment thresholds at low intensities considered as signal/noise discriminations. J Physiol 136:469-488.

Beckmann CF, DeLuca M, Devlin JT, Smith SM (2005) Investigations into resting-state connectivity using independent component analysis. Philos Trans R Soc Lond B Biol Sci 360:1001-1013.

Berger H (1929) Über das Elektroenzephalogramm des Menschen: 1. Mitteilung. Arch Psychiatr Nervenkr 87:527-528.

Bianciardi M, Fukunaga M, Van Gelderen P, Horovitz SG, De Zwart JA, Duyn JH (2009a) Modulation of spontaneous fMRI activity in human visual cortex by behavioral state. Neuroimage 45:160-168.

Bianciardi M, Fukunaga M, Van Gelderen P, Horovitz SG, De Zwart JA, Shmueli K, Duyn JH (2009b) Sources of functional magnetic resonance imaging signal fluctuations in the human brain at rest: a 7 T study. Magn Res Imag 27:1019-1029.

Bianciardi M, Van Gelderen P, Duyn JH, Fukunaga M, De Zwart JA (2009c) Making the most of fMRI at 7 T by suppressing spontaneous signal fluctuations. Neuroimage 44:448-454.

Birn RM, Diamond JB, Smith MA, Bandettini PA (2006) Separating respiratory variation-related fluctuations from neuronal-activity-related fluctuations in fMRI. Neuroimage 31:1536-1548.

Birn RM, Smith MA, Jones TB, Bandettini PA (2008) The respiration response function: The temporal dynamics of fMRI signal fluctuations related to changes in respiration. Neuroimage 40:644-654.

Biswal B, Yetkin FZ, Haughton VM, Hyde JS (1995) Functional connectivity in the motor cortex of resting human brain using echo-planar MRI. Magn Res Med 34:537-541.

Blake R, Logothetis NK (2001) Visual competition. Nat Rev Neurosci 3:1-11.

Boly M, Balteau E, Schnakers C, Degueldre C, Moonen G, Luxen A, Phillips C, Peigneux P, Maquet P, Laureys S (2007) Baseline brain activity fluctuations predict somatosensory perception in humans. Proc Natl Acad Sci USA 104:12187-12192.

Boly M, Phillips C, Tshibanda L, Vanhaudenhuyse A, Schabus M, Dang-Vu TT, Moonen G, Hustinx R, Maquet P, Laureys S (2008) Intrinsic brain activity in altered states of consciousness: how conscious is the default mode of brain function? Ann NY Acad Sci 1129:119-129.

Bonneh YS, Cooperman A, Sagi D (2001) Motion-induced blindness in normal observers. Nature 411:798-801.

Brefczynski JA, DeYoe EA (1999) A physiological correlate of the 'spotlight' of visual attention. Nat Neurosci 2:370-374.

Bregman AS, Campbell J (1971) Primary auditory stream segregation and perception of order in rapid sequences of tones. J Exp Psychol 89:244-249.

Britten KH, Newsome WT (1998) Tuning bandwidths for near-threshold stimuli in area MT. J Neurophysiol 80:762-770.

Britten KH, Shadlen MN, Newsome WT, Movshon JA (1992) The analysis of visual motion: a comparison of neuronal and psychophysical performance. J Neurosci 12:4745-4765.

Britten KH, Shadlen MN, Newsome WT, Movshon JA (1993) Responses of neurons in macaque MT to stochastic motion signals. Vis Neurosci 10:1157-1169.

Brouwer GJ, Van Ee R (2007) Visual cortex allows prediction of perceptual states during ambiguous structure-from-motion. J Neurosci 27:1015-1023.

Buckner RL, Andrews-Hanna JR, Schacter DL (2008) The brain default network: anatomy, function, and relevance to disease. Ann NY Acad Sci 1124:1-38.

Busch NA, Dubois J, VanRullen R (2009) The phase of ongoing EEG oscillations predicts visual perception. J Neurosci 29:7869-7876.

Buzsaki G, Draguhn A (2004) Neuronal oscillations in cortical networks. Science 304:1926-1929.

Caetta F, Gorea A, Bonneh YS (2007) Sensory and decisional factors in motion-induced blindness. J Vision 7:4.1-4.12.

Carter O, Lüdeman R, Mitroff S, Nakayama K (2008) Motion induced blindness: The more you attend the less you see. Abstract at Vision Sciences Society: 237.

Castelo-Branco M, Formisano E, Backes W, Zanella F, Neuenschwander S, Singer W, Goebel R (2002) Activity patterns in human motion-sensitive areas depend on the interpretation of global motion. Proc Natl Acad Sci USA 99:13914-13919.

Chen JJ, Pike GB (2009) Origins of the BOLD post-stimulus undershoot. Neuroimage 46:559-568.

Clark DD, Sokoloff L (1999) In: Basic Neurochemistry. Molecular, Cellular, and Medical Aspects (Siegel GJ, Agranoff BW, Albers RW, Fisher SK, Uhler MD, eds), pp 637-670. Philadelphia: Lippincott-Raven.

Colby CL, Duhamel JR, Goldberg ME (1996) Visual, presaccadic, and cognitive activation of single neurons in monkey lateral intraparietal area. J Neurophysiol 76:2841-2852.

Cordes D, Haughton VM, Arfanakis K, Carew JD, Turski PA, Moritz CH, Quigley MA, Meyerand ME (2001) Frequencies contributing to functional connectivity in the cerebral cortex in 'resting-state' data. Am J Neuroradiol 22:1326-1333.

Cordes D, Haughton VM, Arfanakis K, Wendt GJ, Turski PA, Moritz CH, Quigley MA, Meyerand ME (2000) Mapping functionally related regions of brain with functional connectivity MR imaging. Am J Neuroradiol 21:1636-1644.

Cusack R (2005) The intraparietal sulcus and perceptual organization. J Cogn Neurosci 17:641-651.

Damoiseaux JS, Rombouts SARB, Barkhof F, Scheltens P, Stam CJ, Smith SM, Beckmann CF (2006) Consistent resting-state networks across healthy subjects. Proc Natl Acad Sci USA 103:13848-13853.

De Weerd P, Smith E, Greenberg P (2006) Effects of selective attention on perceptual filling-in. J Cogn Neurosci 18:335-347.

De Zwart JA, Van Gelderen P, Fukunaga M, Duyn JH (2008) Reducing correlated noise in fMRI data. Magn Res Med 59:939-945.

Di Martino A, Scheres A, Margulies DS, Kelly AM, Uddin LQ, Shehzad Z, Biswal B, Walters JR, Castellanos FX, Milham MP (2008) Functional connectivity of human striatum: a resting state FMRI study. Cereb Cortex 18:2735-2747.

Donner TH, Sagi D, Bonneh YS, Heeger DJ (2008) Opposite neural signatures of motion-induced blindness in human dorsal and ventral visual cortex. J Neurosci 28:10298-10310.

Doria V, Beckmann CF, Rees G, Nunes RG, Merchant N, Counsell S, Edwards D (2008) Spontaneous brain activity in infants from 33 weeks gestational age. Abstract at Society for Neuroscience: 787.13.

Dougherty RF, Koch VM, Brewer AA, Fischer B, Modersitzki J, Wandell BA (2003) Visual field representations and locations of visual areas V1/2/3 in human visual cortex. J Vision 3:586-598.

Drake CT, Iadecola C (2006) The role of neuronal signaling in controlling cerebral blood flow. Brain Lang 102:141-152.

Eckert MA, Kamdar NV, Chang CE, Beckmann CF, Greicius MD, Menon V (2008) A cross-modal system linking primary auditory and visual cortices: evidence from intrinsic fMRI connectivity analysis. Hum Brain Mapp 29:848-857.

Eichele T, Debener S, Calhoun VD, Specht K, Engel AK, Hugdahl K, Von Cramon DY, Ullsperger M (2008) Prediction of human errors by maladaptive changes in event-related brain networks. Proc Natl Acad Sci USA 105:6173-6178.

Engel AK, Fries P, Singer W (2001) Dynamic predictions: oscillations and synchrony in top-down processing. Nat Rev Neurosci 2:704-716.

Fang F, Kersten D, Murray SO (2008) Perceptual grouping and inverse fMRI activity patterns in human visual cortex. J Vision 8:2.1-2.9.

Faraci FM, Breese KR (1993) Nitric oxide mediates vasodilatation in response to activation of N-methyl-D-aspartate receptors in brain. Circ Res 72:476-480.

Farrell S, Wagenmakers EJ, Ratcliff R (2006) 1/f noise in human cognition: is it ubiquitous, and what does it mean? Psychon Bull Rev 13:737-741.

Fiser J, Chiu C, Weliky M (2004) Small modulation of ongoing cortical dynamics by sensory input during natural vision. Nature 431:573-578.

Fishman YI, Reser DH, Arezzo JC, Steinschneider M (2001) Neural correlates of auditory stream segregation in primary auditory cortex of the awake monkey. Hear Res 151:167-187.

Foster DJ, Wilson MA (2006) Reverse replay of behavioural sequences in hippocampal place cells during the awake state. Nature 440:680-683.

Fox MD, Corbetta M, Snyder AZ, Vincent JL, Raichle ME (2006a) Spontaneous neuronal activity distinguishes human dorsal and ventral attention systems. Proc Natl Acad Sci USA 103:10046-10051.

Fox MD, Raichle ME (2007) Spontaneous fluctuations in brain activity observed with functional magnetic resonance imaging. Nat Rev Neurosci 8:700-711.

Fox MD, Snyder AZ, Vincent JL, Corbetta M, Van Essen D, Raichle ME (2005) The human brain is intrinsically organized into dynamic, anticorrelated functional networks. Proc Natl Acad Sci USA 102:9673-9678.

Fox MD, Snyder AZ, Vincent JL, Raichle ME (2007) Intrinsic fluctuations within cortical systems account for intertrial variability in human behavior. Neuron 56:171-184.

Fox MD, Snyder AZ, Zacks JM, Raichle ME (2006b) Coherent spontaneous activity accounts for trial-to-trial variability in human evoked brain responses. Nat Neurosci 9:23-25.

Fox MD, Zhang D, Snyder AZ, Raichle ME (2009) The global signal and observed anticorrelated resting state brain networks. J Neurophysiol 101:3270-3283.

Fox PT, Raichle ME, Mintun MA, Dence C (1988) Nonoxidative glucose consumption during focal physiologic neural activity. Science 241:462-464.

Fransson P (2005) Spontaneous low-frequency BOLD signal fluctuations: an fMRI investigation of the resting-state default mode of brain function hypothesis. Hum Brain Mapp 26:15-29.

Fries P, Neuenschwander S, Engel AK, Goebel R, Singer W (2001a) Rapid feature selective neuronal synchronization through correlated latency shifting. Nat Neurosci 4:194-200.

Fries P, Reynolds JH, Rorie AE, Desimone R (2001b) Modulation of oscillatory neuronal synchronization by selective visual attention. Science 291:1560-1563.

Friston KJ, Frith CD, Liddle PF, Frackowiak RSJ (1993) Functional connectivity: the principal-component analysis of large (PET) data sets. J Cereb Blood Flow Metab 13:5-14.

Gandhi SP, Heeger DJ, Boynton GM (1999) Spatial attention affects brain activity in human primary visual cortex. Proc Natl Acad Sci USA 96:3314-3319.

Gavrilescu M, Shaw ME, Stuart GW, Eckersley P, Svalbe ID, Egan GF (2002) Simulation of the effects of global normalization procedures in functional MRI. Neuroimage 17:532-542.

Gerstein GL (1960) Analysis of firing patterns in single neurons. Science 131:1811-1812.

Gilden DL, Thornton T, Mallon MW (1995) 1/f noise in human cognition. Science 267:1837-1839.

Gjedde A, Marrett S, Vafaee M (2009) Oxidative and nonoxidative metabolism of excited neurons and astrocytes. J Cereb Blood Flow Metab 22:1-14.

Glover GH, Li TQ, Ress D (2000) Image-based method for retrospective correction of physiological motion artifacts in fMRI: RETROICOR. Magn Res Med 44:162-167.

Goldman RI, Stern JM, Engel JJ, Cohen MS (2002) Simultaneous EEG and fMRI of the alpha rhythm. NeuroReport 13:2487-2492.

Graf EW, Adams WJ, Lages M (2002) Modulating motion-induced blindness with depth-ordering and surface completion. Vis Research 42:2731-2735.

Gray CM, König P, Engel AK, Singer W (1989) Oscillatory responses in cat visual cortex exhibit inter-columnar synchronization which reflects global stimulus properties. Nature 338:334-337.

Greicius MD, Krasnow B, Reiss AL, Menon V (2003) Functional connectivity in the resting brain: a network analysis of the default mode hypothesis. Proc Natl Acad Sci USA 100:253-258.

Gutschalk AM, Micheyl C, Melcher JR, Rupp A, Scherg M, Oxenham AJ (2005) Neuromagnetic correlates of streaming in human auditory cortex. J Neurosci 25:5382-5388.

Hagmann P, Cammoun L, Gigandet X, Meuli R, Honey CJ, Wedeen VJ, Sporns O (2008) Mapping the structural core of human cerebral cortex. PLoS Biol 6:1479-1493.

HaiYan G, QianLan S, YunFeng L, Shan X, Ying Z (2007) Attentional modulation of motion-induced blindness. Chin Sci Bulletin 52:1001-6538.

Hampson M, Peterson BS, Skudlarski P, Gatenby JC, Gore JC (2002) Detection of functional connectivity using temporal correlations in MR images. Hum Brain Mapp 15:247-262.

Han F, Caporale N, Dan Y (2008) Reverberation of recent visual experience in spontaneous cortical waves. Neuron 60:321-327.

Haynes JD, Deichmann R, Rees G (2005) Eye-specific effects of binocular rivalry in the human lateral geniculate nucleus. Nature 438:496-499.

Haynes JD, Rees G (2005) Predicting the stream of consciousness from activity in human visual cortex. Curr Biol 15:1301-1307.

He BJ, Snyder AZ, Zempel JM, Smyth MD, Raichle ME (2008) Electrophysiological correlates of the brain's intrinsic large-scale functional architecture. Proc Natl Acad Sci USA 105:16039-16044.

Hegner YL, Saur R, Veit R, Butts R, Leiberg S, Grodd W, Braun C (2007) BOLD adaptation in vibrotactile stimulation: neuronal networks involved in frequency discrimination. J Neurophysiol 97:264-271.

Hesselmann G, Kell CA, Eger E, Kleinschmidt A (2008a) Spontaneous local variations in ongoing neural activity bias perceptual decisions. Proc Natl Acad Sci USA 105:10984-10989.

Hesselmann G, Kell CA, Kleinschmidt A (2008b) Ongoing activity fluctuations in hMT+ bias the perception of coherent visual motion. J Neurosci 28:14481-14485.

Hol K, Koene A, Van Ee R (2003) Attention-biased multi-stable surface perception in three-dimensional structure-from-motion. J Vision 3:486-498.

Honey CJ, Sporns O, Cammoun L, Gigandet X, Thiran J, Meuli R, Hagmann P (2009) Predicting human resting-state functional connectivity from structural connectivity. Proc Natl Acad Sci USA 106:2035-2040.

Horovitz SG, Fukunaga M, De Zwart JA, Van Gelderen P, Fulton SC, Bakin TJ, Duyn JH (2008) Low frequency BOLD fluctuations during resting wakefulness and light sleep: a simultaneous EEG-fMRI study. Hum Brain Mapp 29:671-682.

Horwitz B (2003) The elusive concept of brain connectivity. Neuroimage 19:466-470.

Hsieh P, Tse PU (2009) Microsaccade rate varies with subjective visibility during motion-induced blindness. PLoS One 4:1-9.

Hsu LC, Yeh SL, Kramer P (2004) Linking motion-induced blindness to perceptual filling-in. Vis Research 44:2857-2866.

Hsu LC, Yeh SL, Kramer P (2006) A common mechanism for perceptual filling-in and motion-induced blindness. Vis Research 46:1973-1981.

Hubel DH, Wiesel TN (1998) Early exploration of the visual cortex. Neuron 20:401-412.

Huk AC, Shadlen MN (2005) Neural activity in macaque parietal cortex reflects temporal integration of visual motion signals during perceptual decision making. J Neurosci 26:10420-10436.

Izumi A (2002) Auditory stream segregation in Japanese monkeys. Cognition 82:113-122.

Jeannerod M, Arbib MA, Rizzolatti G, Sakata H (1995) Grasping objects: the cortical mechanisms of visuomotor transformation. Trends Neurosci 18:314-320.

Johnston JM, Vaishnavi SN, Smyth MD, Zhang D, He BJ, Zempel JM, Shimony JS, Snyder AZ, Raichle ME (2008) Loss of resting interhemispheric functional connectivity after complete section of the corpus callosum. J Neurosci 28:6453-6458.

Juergens E, Guettler A, Eckhorn R (1999) Visual stimulation elicits locked and induced gamma oscillations in monkey intracortical- and EEG-potentials, but not in human EEG. Exp Brain Res 129:247-259.

Kandel ER, Schwartz JH, Jessell TM (2000) Principles of neural science. United States of America: McGraw-Hill Companies.

Kapadia MK, Ito M, Gilbert CD, Westheimer G (1995) Improvement in visual sensitivity by changes in local context: parallel studies in human observers and in V1 of alert monkeys. Neuron 15:843-856.

Kaplan IT, Metlay W (1964) Light intensity and binocular rivalry. J Exp Psychol 67:22-26.

Kasischke KA, Vishwasrao HD, Fisher PJ, Zipfel WR, Webb WW (2004) Neural activity triggers neuronal oxidative metabolism followed by astrocytic glycolysis. Science 305:99-103.

Kastner S, De Weerd P, Desimone R, Ungerleider LG (1998) Mechanisms of directed attention in the human extrastriate cortex as revealed by functional MRI. Science 282:108-111.

Kastner S, Pinsk MA, De Weerd P, Desimone R, Ungerleider LG (1999) Increased activity in human visual cortex during directed attention in the absence of visual stimulation. Neuron 22:751-761.

Kastner S, Ungerleider LG (2000) Mechanisms of visual attention in the human cortex. Ann Rev Neurosci 23:315-341.

Katzner S, Nauhaus I, Benucci A, Bonin V, Ringach DL, Carandini M (2009) Local origin of field potentials in visual cortex. Neuron 61:35-41.

Kenet T, Bibitchkov D, Tsodyks M, Grinvald A, Arieli A (2003) Spontaneously emerging cortical representations of visual attributes. Nature 425:954-956.

Keysers C, Perrett DI (2002) Visual masking and RSVP reveal neural competition. Trends Cogn Sci 6:120-125.

Kim JN, Shadlen MN (1999) Neural correlates of a decision in the dorsolateral prefrontal cortex of the macaque. Nat Neurosci 2:176-185.

Kiviniemi V, Kantola JH, Jauhiainen J, Hyvarinen A, Tervonen O (2003) Independent component analysis of nondeterministic fMRI signal sources. Neuroimage 19:253-260.

Kleinschmidt A, Büchel C, Zeki S, Frackowiak RSJ (1998) Human brain activity during spontaneously reversing perception of ambiguous figures. Proc Biol Sci 265:2427-2433.

Kohler A, Haddad L, Singer W, Muckli L (2008) Deciding what to see: The role of intention and attention in the perception of apparent motion. Vis Research 48:1096-1106.

Konings MK, Bartels LW, Smits HF, Bakker CJ (2000) Heating around intravascular guidewires by resonating RF waves. Magn Res Imag 12:79-85.

Lamotte RH, Mountcastle VB (1975) Capacities of humans and monkeys to discriminate vibratory stimuli of different frequency and amplitude: a correlation between neural events and psychological measurements. J Neurophysiol 38:539-559.

Laufs H, Daunizeau J, Carmichael DW, Kleinschmidt A (2008) Recent advances in recording electrophysiological data simultaneously with magnetic resonance imaging. Neuroimage 40:515-528.

Laufs H, Duncan JS (2007) Electroencephalography/functional MRI in human epilepsy: what it currently can and cannot do. Curr Opin Neurol 20:417-423.

Laufs H, Krakow K, Sterzer P, Eger E, Beyerle A, Salek-Haddadi A, Kleinschmidt A (2003) Electroencephalographic signatures of attentional and cognitive default modes in spontaneous brain activity fluctuations at rest. Proc Natl Acad Sci USA 100:11053-11058.

Laufs H, Walker MC, Lundt TE (2007) 'Brain activation and hypothalamic functional connectivity during human non-rapid eye movement sleep: an EEG/fMRI study'--its limitations and an alternative approach. Brain 130:e75.

Lavie N (1995) Perceptual load as a necessary condition for selective attention. J Exp Psychol 21:451-468.

Lavie N (2005) Distracted and confused?: selective attention under load. Trends Cogn Sci 9:75-82.

Lavie N, Hirst A, De Fockert JW, Viding E (2004) Load theory of selective attention and cognitive control. J Exp Psychol Gen 133:339-354.

Lee SH, Blake R, Heeger DJ (2005) Traveling waves of activity in primary visual cortex during binocular rivalry. Nat Neurosci 8:22-23.

Lee SH, Blake R, Heeger DJ (2007) Hierarchy of cortical responses underlying binocular rivalry. Nat Neurosci 10:1048-1054.

Lee TS, Nguyen M (2001) Dynamics of subjective contour formation in the early visual cortex. Proc Natl Acad Sci USA 98:1907-1911.

Leite FP, Tsao DY, Vanduffel W, Fize D, Sasaki Y, Wald LL, Dale AM, Kwong KK, Orban GA, Rosen BR (2002) Repeated fMRI using iron oxide contrast agent in awake, behaving macaques at 3 Tesla. Neuroimage 16:283-294.

Leopold DA, Logothetis NK (1999) Multistable phenomena: changing views in perception. Trends Cogn Sci 3:254-264.

Leopold DA, Murayama Y, Logothetis NK (2003) Very slow activity fluctuations in monkey visual cortex: implications for functional brain imaging. Cereb Cortex 13:422-433.

Libedinsky C, Savage T, Livingstone M (2009) Perceptual and physiological evidence for a role for early visual areas in motion-induced blindness. J Vision 9:14.1-14.10.

Logothetis NK (2003) The underpinnings of the BOLD functional magnetic resonance imaging signal. J Neurosci 23:3963-3971.

Logothetis NK, Pauls J, Augath M, Trinath T, Oeltermann A (2001) Neurophysiological investigation of the basis of the fMRI signal. Nature 412:150-157.

Lou L (1999) Selective peripheral fading: evidence for inhibitory sensory effect of attention. Perception 28:519-526.

Lowe MJ, Mock BJ, Sorenson JA (1998) Functional connectivity in single and multislice echoplanar imaging using resting-state fluctuations. Neuroimage 7:119-132.

Lu H, Zuo Y, Gu H, Waltz JA, Zhan W, Scholl CA, Rea W, Yang Y, Stein EA (2007) Synchronized delta oscillations correlate with the resting-state functional MRI signal. Proc Natl Acad Sci USA 104:18265-18269.

Luck SJ, Chelazzi L, Hillyard SA, Desimone R (1997) Neural mechanisms of spatial selective attention in areas V1, V2, and V4 of macaque visual cortex. J Neurophysiol 77:24-42.

Lumer ED, Friston K, Rees G (1998) Neural correlates of perceptual rivalry in the human brain. Science 280:1930-1934.

Macey PM, Macey KE, Kumar R, Harper RM (2004) A method for the removal of global effects from fMRI time series. Neuroimage 22:360-366.

Macmillan NA, Creelman CD (2005) Detection Theory: A User's Guide. Mahwah, New Jersey: Lawrence Erlbaum Associates.

Maier A, Wilke M, Aura C, Zhu C, Ye FQ, Leopold DA (2008) Divergence of fMRI and neural signals in V1 during perceptual suppression in the awake monkey. Nat Neurosci 11:1200.

Maldjian JA, Gottschalk A, Patel RS, Pincus D, Detre JA, Alsop DC (1999) Mapping of secondary somatosensory cortex activation induced by vibrational stimulation: an fMRI study. Brain Res 824:291-295.

Malonek D, Grinvald A (1996) Interactions between electrical activity and cortical microcirculation revealed by imaging spectroscopy: implications for functional brain mapping. Science 272:551-554.

Mantini D, Perrucci MG, Del Gratta C, Romani GL, Corbetta M (2007) Electrophysiological signatures of resting state networks in the human brain. Proc Natl Acad Sci USA 104:13170-13175.

Martinez-Conde S, Macknik SL, Troncoso XG, Dyar TA (2006) Microsaccades counteract visual fading during fixation. Neuron 49:297-305.

Mason MF, Norton MI, Van Horn JD, Wegner DM, Grafton ST, Macrae CN (2007) Wandering minds: the default mode network and stimulus independent thought. Science 315:393-395.

Mathewson KE, Gratton G, Fabiani M, Beck DM, Ro T (2009) To see or not to see: prestimulus alpha phase predicts visual awareness. J Neurosci 29:2725-2732.

McAvoy MP, Larson-Prior LJ, Nolan TS, Vaishnavi SN, Raichle ME, D'Avossa G (2008) Resting states affect spontaneous BOLD oscillations in sensory and paralimbic cortex. J Neurophysiol 100:922-931.

McKeefry DJ, Watson JDG, Frackowiak RSJ, Fong K, Zeki S (1997) The activity in human areas V1/V2, V3, and V5 during the perception of coherent and incoherent motion. Neuroimage 5:1-12.

McKeefry DJ, Zeki S (1997) The position and topography of the human colour centre as revealed by functional magnetic resonance imaging. Brain 120:2229-2242.

Mendola JD, Conner IP, Sharma S, Bahekar A, Lemieux S (2006) fMRI measures of perceptual filling-in in the human visual cortex. J Cogn Neurosci 18:363-375.

Meng M, Remus DA, Tong F (2005) Filling-in of visual phantoms in the human brain. Nat Neurosci 8:1248-1254.

Meng M, Tong F (2004) Can attention selectively bias bistable perception? Differences between binocular rivalry and ambiguous figures. J Vision 4:539-551.

Micheyl C, Tian B, Carlyon RP, Rauschecker JP (2005) Perceptual organization of tone sequences in the auditory cortex of awake macaques. Neuron 48:139-148.

Mitzdorf U (1985) Current source-density method and application in cat cerebral cortex: investigation of evoked potentials and EEG phenomena. Physiol Rev 65:37-100.

Mitzdorf U (1987) Properties of the evoked potential generators: current source-density analysis of visually evoked potentials in the cat cortex. Int J Neurosci 33:33-59.

Moeller S, Nallasamy N, Tsao DY, Freiwald WA (2009) Functional connectivity of the macaque brain across stimulus and arousal states. J Neurosci 29:5897-5909.

Monto S, Palva S, Voipio J, Palva JM (2009) Very slow EEG fluctuations predict the dynamics of stimulus detection and oscillation amplitudes in humans. J Neurosci 28:8268-8272.

Moosmann M, Ritter P, Krastel I, Brink A, Thees S, Blankenburg F, Taskin B, Obrig H, Villringer A (2003) Correlates of alpha rhythm in functional magnetic resonance imaging and near infrared spectroscopy. Neuroimage 20:145-158.

Morrone MC, Tosetti M, Montanaro D, Fiorentini A, Cioni G, Burr DC (2000) A cortical area that responds specifically to optic flow, revealed by fMRI. Nat Neurosci 3:1322-1328.

Mountcastle VB, Talbot WH, Darian-Smith I, Kornhuber HH (1967) Neural basis of the sense of flutter-vibration. Science 155:597-600.

Mueller TJ, Blake R (1989) A fresh look at the temporal dynamics of binocular rivalry. Biol Cybern 61:223-232.

Murphy K, Birn RM, Handwerker DA, Jones TB, Bandettini PA (2009) The impact of global signal regression on resting state correlations: are anti-correlated networks introduced? Neuroimage 44:893-905.

Niazy RK, Beckmann CF, Iannetti GJ, Brady JM, Smith SM (2005) Removal of FMRI environment artifacts from EEG data using optimal basis sets. Neuroimage 28:720-737.

Niessing J, Ebisch B, Schmidt KE, Niessing M, Singer W, Galuske RA (2005) Hemodynamic signals correlate tightly with synchronized gamma oscillations. Science 309:948-951.

Nir Y, Fisch L, Mukamel R, Gelbard-Sagiv H, Arieli A, Fried I, Malach R (2007) Coupling between neuronal firing rate, gamma LFP, and BOLD fMRI is related to interneuronal correlations. Curr Biol 17:1275-1285.

Nir Y, Hasson U, Levy I, Yeshurun Y, Malach R (2006) Widespread functional connectivity and fMRI fluctuations in human visual cortex in the absence of visual stimulation. Neuroimage 30:1313-1324.

Nir Y, Mukamel R, Dinstein I, Privman E, Harel M, Fisch L, Gelbard-Sagiv H, Kipervasser S, Andelman F, Neufeld MY, Kramer U, Arieli A, Fried I, Malach R (2008) Interhemispheric correlations of slow spontaneous neuronal fluctuations revealed in human sensory cortex. Nat Neurosci 11:1100-1108.

O'Reilly JX, Beckmann CF, Tomassini V, Ramnani N, Johansen-Berg H (2009) Distinct and overlapping functional zones in the cerebellum defined by resting state functional connectivity. Cereb Cortex epub.

Paffen CLE, Alais D, Verstraten FAJ (2006) Attention speeds binocular rivalry. Psych Sci 17:752-756.

Pastukhov A, Braun J (2007) Perceptual reversals need no prompting by attention. J Vision 7:5.1-5.17.

Pessoa L, Gutierrez E, Bandettini PA, Ungerleider LG (2002) Neural correlates of visual working memory: fMRI amplitude predicts task performance. Neuron 35:975-987.

Pessoa L, Kastner S, Ungerleider LG (2003) Neuroimaging studies of attention: from modulation of sensory processing to top-down control. J Neurosci 23:3990-3998.

Pessoa L, Padmala S (2005) Quantitative prediction of perceptual decisions during near-threshold fear detection. Proc Natl Acad Sci USA 102:5612-5617.

Phillips ML, Young AW, Senior C, Brammer M, Andrew C, Calder AJ, Bullmore ET, Perrett DI, Rowland D, Williams SC, Gray JA, David AS (1997) A specific neural substrate for perceiving facial expressions of disgust. Nature 389:495-498.

Pitts MA, Gavin WJ, Nerger JL (2008) Early top-down influences on bistable perception revealed by event-related potentials. Brain Cogn 67:11-24.

Polonsky A, Blake R, Braun J, Heeger DJ (2000) Neuronal activity in human primary visual cortex correlates with perception during binocular rivalry. Nat Neurosci 3:1153-1159.

Posner MI (1980) Orienting of attention. Q J Exp Psychol 32:3-25.

Pouget A, Dayan P, Zemel RS (2003) Inference and computation with population codes. Ann Rev Neurosci 26:381-410.

Raichle ME, MacLeod AM, Snyder AZ, Powers WJ, Gusnard DA, Shulman GL (2001) A default mode of brain function. Proc Natl Acad Sci USA 98:676-682.

Raichle ME, Mintun MA (2006) Brain work and brain imaging. Ann Rev Neurosci 29:449-476.

Ramachandran VS, Gregory RL (1991) Perceptual filling in of artificially induced scotomas in human vision. Nature 350:699-702.

Rees G, Friston K, Koch C (2000) A direct quantitative relationship between the functional properties of human and macaque V5. Nat Neurosci 3:716-723.

Rees G, Frith CD, Lavie N (1997) Modulating irrelevant motion perception by varying attentional load in an unrelated task. Science 278:1616-1619.

Rees G, Russell C, Frith CD, Driver J (1999) Inattentional blindness versus inattentional amnesia for fixated but ignored words. Science 286:2504-2507.

Ress D, Backus BT, Heeger DJ (2000) Activity in primary visual cortex predicts performance in a visual detection task. Nat Neurosci 3:940-945.

Ress D, Heeger DJ (2003) Neuronal correlates of perception in early visual cortex. Nat Neurosci 6:414-420.

Reynolds JH, Chelazzi L (2004) Attentional modulation of visual processing. Ann Rev Neurosci 27:611-647.

Rombouts SARB, Stam CJ, Kuijer JP, Scheltens P, Barkhof F (2003) Identifying confounds to increase specificity during a 'no task condition'. Evidence for hippocampal connectivity using fMRI. Neuroimage 20:1236-1245.

Romei V, Brodbeck V, Michel C, Amedi A, Pascual-Leone A, Thut G (2008) Spontaneous fluctuations in posterior alpha-band EEG activity reflect variability in excitability of human visual areas. Cereb Cortex 18:2010-2018.

Romo R, Hernandez A, Zainos A (2004) Neuronal correlates of a perceptual decision in ventral premotor cortex. Neuron 41:165-173.

Romo R, Hernandez A, Zainos A, Lemus L, Brody CD (2002) Neuronal correlates of decision-making in secondary somatosensory cortex. Nat Neurosci 5:1217-1225.

Romo R, Hernandez A, Zainos A, Salinas E (2003) Correlated neuronal discharges that increase coding efficiency during perceptual discrimination. Neuron 38:649-657.

Salek-Haddadi A, Friston K, Lemieux L, Fish DR (2003) Studying spontaneous EEG activity with fMRI. Brain Res Rev 43:110-133.

Salinas E, Sejnowski T (2001) Correlated neuronal activity and the flow of neural information. Nat Rev Neurosci 2:539-550.

Sapir A, D'Avossa G, McAvoy MP, Shulman GL, Corbetta M (2005) Brain signals for spatial attention predict performance in a motion discrimination task. Proc Natl Acad Sci USA 102:17810-17815.

Schneider KA, Bavelier D (2003) Components of visual prior entry. Cogn Psych 47:333-366.

Schwartz S, Vuilleumier P, Hutton C, Maravita A, Dolan RJ, Driver J (2005) Attentional load and sensory competition in human vision: modulation of fMRI responses by load at fixation during task-irrelevant stimulation in the peripheral visual field. Cereb Cortex 15:770-786.

Seeley WW, Menon V, Schatzberg AF, Keller J, Glover GH, Kenna H, Reiss AL, Greicius MD (2007) Dissociable intrinsic connectivity networks for salience processing and executive control. J Neurosci 27:2349-2356.

Sereno MI, Dale AM, Reppas JB, Kwong KK, Belliveau JW, Brady TJ, Rosen BR, Tootell RB (1995) Borders of multiple visual areas in humans revealed by functional magnetic resonance imaging. Science 268:889-893.

Sergent C, Baillet S, Dehaene S (2005) Timing of the brain events underlying access to consciousness during the attentional blink. Nat Neurosci 8:1391-1400.

Shatz CJ (1996) Emergence of order in visual system development. Proc Natl Acad Sci USA 93:602-608.

Shmuel A, Augath M, Oeltermann A, Logothetis NK (2006) Negative functional MRI response correlates with decreases in neuronal activity in monkey visual area V1. Nat Neurosci 9:569-577.

Shmuel A, Leopold DA (2008) Neuronal correlates of spontaneous fluctuations in fMRI signals in monkey visual cortex: Implications for functional connectivity at rest. Hum Brain Mapp 29:751-761.

Shmueli K, Van Gelderen P, De Zwart JA, Horovitz SG, Fukunaga M, Jansma JM, Duyn JH (2007) Low-frequency fluctuations in the cardiac rate as a source of variance in the resting-state fMRI BOLD signal. Neuroimage 38:306-320.

Shtoyerman E, Arieli A, Slovin H, Vanzetta I, Grinvald A (2000) Long-term optical imaging and spectroscopy reveal mechanisms underlying the intrinsic signal and stability of cortical maps in V1 of behaving monkeys. J Neurosci 20:8111-8121.

Sirotin YB, Das A (2009) Anticipatory haemodynamic signals in sensory cortex not predicted by local neuronal activity. Nature 457:475-479.

Slotnick SD, Yantis S (2005) Common neural substrates for the control and effects of visual attention and perceptual bistability. Cogn Brain Res 24:97-108.

Snowden RJ, Treue S, Andersen RA (1992) The response of neurons in areas V1 and MT of the alert rhesus monkey to moving random dot patterns. Exp Brain Res 88:389-400.

Sokoloff L, Mangold R, Wechsler R, Kennedy C, Kety SS (1955) The effect of mental arithmetic on cerebral circulation and metabolism. J Clin Invest 34:1101-1108.

Somers DC, Dale AM, Seiffert AE, Tootell RB (1999) Functional MRI reveals spatially specific attentional modulation in human primary visual cortex. Proc Natl Acad Sci USA 96:1663-1668.

Stefanovich B, Schwindt W, Hoehn M, Silva AC (2007) Functional uncoupling of hemodynamic from neuronal response by inhibition of neuronal nitric oxide synthase. J Cereb Blood Flow Metab 27:741-754.

Steriade M, McCormick DA, Sejnowski T (1993) Thalamocortical oscillations in the sleeping and aroused brain. Science 262:679-685.

Steriade M, Timofeev I (2003) Neuronal plasticity in thalamocortical networks during sleep and waking oscillations. Neuron 37:563-576.

Sterzer P, Eger E, Kleinschmidt A (2003) Responses of extrastriate cortex to switching perception of ambiguous visual motion stimuli. NeuroReport 14:2337-2341.

Sterzer P, Kleinschmidt A (2007) A neural basis for inference in perceptual ambiguity. Proc Natl Acad Sci USA 104:323-328.

Sterzer P, Kleinschmidt A, Rees G (2009) The neural bases of multistable perception. Trends Cogn Sci 13:310-318.

Stettler DD, Das A, Bennett J, Gilbert CD (2002) Lateral connectivity and contextual interactions in macaque primary visual cortex. Neuron 36:739-750.

Summerfield C, Egner T, Greene M, Koechlin E, Mangels J, Hirsch J (2006) Predictive codes for forthcoming perception in the frontal cortex. Science 314:1311-1314.

Super H, Van der Togt C, Spekreijse H, Lamme VAF (2003) Internal state of monkey primary visual cortex (V1) predicts figure-ground perception. J Neurosci 23:3407-3414.

Takano T, Tian GF, Peng W, Lou N, Han X, Nedergaard M (2006) Astrocyte-mediated control of cerebral blood flow. Nat Neurosci 9:260-267.

Teo PC, Sapiro G, Wandell BA (1997) Creating connected representations of cortical gray matter for functional MRI visualization. IEEE Trans Med Imaging 16:852-863.

Thut G, Nietzel A, Brandt SA, Pascual-Leone A (2006) Alpha-band electroencephalographic activity over occipital cortex indexes visuospatial attention bias and predicts visual target detection. J Neurosci 26:9494-9502.

Tong F, Engel SA (2001) Interocular rivalry revealed in the human cortical blind-spot representation. Nature 411:195-199.

Troxler D (1804) Über das Verschwinden gegebener Gegenstände innerhalb unseres Gesichtskreises. In: Opthalmische Bibliothek (Himly K, Schmidt JA, eds), pp 51-53. Frommann, Jena.

Tsodyks M, Kenet T, Grinvald A, Arieli A (1999) Linking spontaneous activity of single cortical neurons and the underlying functional architecture. Science 286:1943-1946.

Van de Ven VG, Formisano E, Prvulovic D, Roeder CH, Linden DEJ (2004) Functional connectivity as revealed by spatial independent component analysis of fMRI measurements during rest. Hum Brain Mapp 22:165-178.

Van Ee R, Van Dam LCJ, Brouwer GJ (2005) Voluntary control and the dynamics of perceptual bi-stability. Vis Research 45:41-55.

Van Essen D, Maunsell JHR, Bixby JL (1981) The middle temporal visual area in the macaque: myeloarchitecture, connections, functional properties and topographic organization. J Comp Neurol 199:293-326.

Vincent JL, Patel GH, Fox MD, Snyder AZ, Baker JT, Van Essen D, Zempel JM, Snyder LH, Corbetta M, Raichle ME (2007) Intrinsic functional architecture in the anaethestized monkey brain. Nature 447:83-86.

Viswanathan A, Freeman RD (2007) Neurometabolic coupling in cerebral cortex reflects synaptic more than spiking activity. Nat Neurosci 10:1308-1312.

Vogels R, Spileers W, Orban GA (1989) The response variability of striate cortical neurons in the behaving monkey. Exp Brain Res 77:432-436.

Von Stein A, Chiang C, König P (2000) Top-down processing mediated by interareal synchronization. Proc Natl Acad Sci USA 97:14748-14753.

Wagner AD, Schacter DL, Rotte M, Koutstaal W, Maril A, Dale AM, Rosen BR, Buckner RL (1998) Building memories: remembering and forgetting of verbal experiences as predicted by brain activity. Science1188-1191.

Wallis TSA, Arnold DH (2009) Motion-induced blindness and motion streak suppression. Curr Biol 19:325-329.

Wandell BA, Chial S, Backus BT (2000) Visualization and measurement of the cortical surface. J Cogn Neurosci 12:739-752.

Wang K, Jiang T, Yu C, Tian L, Li J, Liu Y, Zhou Y, Xu L, Song M, Li K (2008) Spontaneous activity associated with primary visual cortex: a resting-state fMRI study. Cereb Cortex 18:697-704.

Weil RS, Kilner JM, Haynes JD, Rees G (2007) Neural correlates of perceptual filling-in of an artificial scotoma in humans. Proc Natl Acad Sci USA 104:5211-5216.

Weil RS, Watkins S, Rees G (2008) Neural correlates of perceptual completion of an artificial scotoma in human visual cortex measured using functional MRI. Neuroimage 42:1518-1528.

Wilke M, Logothetis NK, Leopold DA (2006) Local field potential reflects perceptual suppression in monkey visual cortex. Proc Natl Acad Sci USA 103:17507-17512.

Wilson EC, Melcher JR, Micheyl C, Gutschalk AM, Oxenham AJ (2007) Cortical fMRI activation to sequences of tones alternating in frequency: Relationship to perceived rate and streaming. J Neurophysiol 97:2230-2238.

Windmann S, Wehrmann M, Calabrese P, Güntürkün O (2006) Role of the prefrontal cortex in attentional control over bistable vision. J Cogn Neurosci 18:456-471.

Wise RJS, Ide K, Poulin MJ, Tracey I (2004) Resting state fluctuations in arterial carbon dioxide induce significant low frequency variations in BOLD signal. Neuroimage 21:1652-1664.

Wunderlich K, Schneider KA, Kastner S (2005) Neural correlates of binocular rivalry in the human lateral geniculate nucleus. Nat Neurosci 8:1595-1602.

Wyart V, Tallon-Baudry C (2009) How ongoing fluctuations in human visual cortex predict perceptual awareness: baseline shift versus decision bias. J Neurosci 29:8715-8725.

Xiong J, Parsons LM, Gao JH, Fox PT (1998) Interregional connectivity to primary motor cortex revealed using MRI resting state images. Hum Brain Mapp 8:151-156.

Yacoub E, Harel N, Ugurbil K (2008) High-field fMRI unveils orientation columns in humans. Proc Natl Acad Sci USA 105:10607-10612.

Yang H, Long XY, Yang Y, Yan H, Zhu CZ, Zhou XP, Zang YF, Gong QY (2007) Amplitude of low frequency fluctuation within visual areas revealed by resting-state functional MRI. Neuroimage 36:144-152.

Zarahn E, Aguirre GK, D'Esposito M (1997) Empirical analyses of BOLD fMRI statistics. I. Spatially unsmoothed data collected under null-hypothesis conditions. Neuroimage 5:179-197.

Zeki SM, Watson JDG, Lueck CJ, Friston K, Kennard C, Frackowiak RSJ (1991) A direct demonstration of functional specialization in human visual cortex. J Neurosci 11:641-649.

Zhan Y, Guo S, Kendrick KM, Feng J (2009) Filtering noise for synchronised activity in multi-trial electrophysiology data using Wiener and Kalman filters. Biosystems 96:1-13.

Zhang D, Snyder AZ, Fox MD, Sansbury MW, Shimony JS, Raichle ME (2008) Intrinsic functional relations between human cerebral cortex and thalamus. J Neurophysiol 100:1740-1748.

Zonta M, Angulo MC, Gobbo S, Rosengarten B, Hossmann KA, Pozzan T, Carmignoto G (2003) Neuron-to-astrocyte signaling is central to the dynamic control of brain microcirculation. Nat Neurosci 6:43-50.